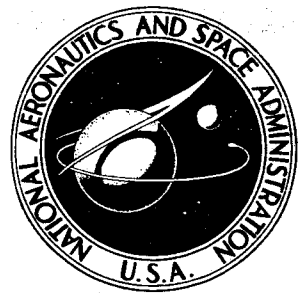


NASA CONTRACTOR
REPORT



NASA CR-148

NASA CR-148

FACILITY FORM 602

N 65 14849
(ACCESSION NUMBER)
141
(PAGES)
CR-148
(NASA CR OR TMA OR AD NUMBER)

(THRU)
1
(CODE)
29
(CATEGORY)

GPO PRICE \$ _____
OTS PRICE(S) \$ 5.70

Hard copy (HC) _____
Microfiche (MF) 1.25

COSMIC RAY COLLISIONS IN SPACE

PART I — THE ENERGY SPECTRA OF
ELECTRONS FROM PION-MUON-ELECTRON
DECAYS IN INTERSTELLAR SPACE

by Joseph H. Scanlon and S. N. Milford

Prepared under Contract No. NASw-699 by
GRUMMAN AIRCRAFT ENGINEERING CORPORATION
Bethpage, N. Y.
for

NATIONAL AERONAUTICS AND SPACE ADMINISTRATION • WASHINGTON, D. C. • JANUARY 1965

COSMIC RAY COLLISIONS IN SPACE

PART I - THE ENERGY SPECTRA OF ELECTRONS
FROM PION-MUON-ELECTRON DECAYS IN INTERSTELLAR SPACE

By Joseph H. Scanlon and S. N. Milford

Distribution of this report is provided in the interest of information exchange. Responsibility for the contents resides in the author or organization that prepared it.

Prepared under Contract No. NASw-699 by
GRUMMAN AIRCRAFT ENGINEERING CORPORATION
Bethpage, N. Y.

for

NATIONAL AERONAUTICS AND SPACE ADMINISTRATION

For sale by the Office of Technical Services, Department of Commerce,
Washington, D.C. 20230 -- Price \$5.00

FOREWORD

This document comprises Part I of the final report on Contract No. NASw-699, Cosmic Ray Collisions in Space. The complete report describes in detail the research carried out on this contract by the Geo-Astrophysics Section of the Research Department of Grumman Aircraft Engineering Corporation between July 3, 1963 and November 3, 1964. This work was performed under the technical cognizance of Drs. L. J. Cahill, J. W. Freeman, and A. W. Schardt of the Office of Space Sciences, NASA.

The final report is presented in four separately-bound parts:

Part I - The Energy Spectra of Electrons from Pion-Muon-Electron Decays in Interstellar Space;

Part II - High Energy Gamma Rays from Cosmic Ray Collisions in Space;

Part III - Low Energy Protons from Cosmic Ray Collisions in Space;

Part IV - Cosmic Ray Hazards in the Solar System.

SUMMARY

For the success and safety of future manned and unmanned space missions, it is necessary to acquire as much information as possible about the types and energies of particles in interplanetary space. Though some information is available about cosmic rays in the vicinity of earth, no satellite or space probe measurements have as yet been made in the more distant regions of the solar system.

Reliable theoretical estimates of cosmic ray intensities in space would, therefore, be extremely useful. A program has been undertaken to calculate the distribution of stable secondary particles resulting from high energy collisions of cosmic rays with the interstellar gas. As part of this effort, the energy spectra of electrons from charged pion decays in interstellar space have been determined. These electron energy spectra are presented in this report.

The predominant $\pi\text{-}\mu\text{-}e$ mode is considered. The analysis starts with the known distribution of electrons from muon decay in the muon rest frame. After Lorentz

transformation to the pion rest frame, the muon distribution from pion decay is introduced. All directions are related to a fixed set of axes. The muon momentum and angular dependence is then integrated out. A second relativistic transformation yields the electron energy and angular distribution in the system in which the pion decays in flight. Integration over the electron direction then gives the energy spectra of the electrons.

It is found that as a direct consequence of the relativistic transformation kinematics, the distribution function assumes a different mathematical form in four well-defined regions of pi meson energy. Within three of these pion ranges, four regions of electron energy must be separately considered; in the highest pion energy region, there are three electron energy regions. The normalization requirement yields a useful check on the distribution in the pion rest and moving frames.

Numerical values of the electron energy spectra were computed on an IBM 7094 for twenty-six pion kinetic energy values covering a range from 3 mev to about 110 bev. The peak of the distribution is found to decrease monotonically from 0.31×10^{-1} mev⁻¹ at $\gamma_{\pi} = 1.02$ to 0.20×10^{-4} mev⁻¹ at $\gamma_{\pi} = 800$.

The assumptions of μ CMS isotropy and large pion lab energies have been avoided. Use of the anisotropic μ CMS electron distribution improves the $N_{\pi\mu e}$ values as much as 15 per cent near the distribution maximum and 80 per cent at the higher electron energies.

Since the final expressions for the electron spectra are in closed form, they offer the possibility of analytical solutions in problems involving $\pi-\mu-e$ decay.

TABLE OF CONTENTS

Chapter	Page
Introduction	xix
I Electron Distribution from Muon Decay	1
II Electron Distribution in Pion Rest System	9
III Electron Distribution in Laboratory Frame	23
IV Computations	36
V Discussion	134
Appendix A	138
Appendix B	147
Appendix C	155
Appendix D	167
Bibliography	172

LIST OF TABLES

Table	Page
I Limits on Electron Direction	31
II Electron Distribution Function (Per Mev) ($\xi = 1$): $\gamma_{\pi} = 1.02, 1.07$	44
III Electron Distribution Function (Per Mev) ($\xi = 1$): $\gamma_{\pi} = 1.15, 1.3$	47
IV Electron Distribution Function (Per Mev) ($\xi = 1$): $\gamma_{\pi} = 1.45, 1.6$	49
V Electron Distribution Function (Per Mev) ($\xi = 1$): $\gamma_{\pi} = 1.7, 2.4$	51
VI Electron Distribution Function (Per Mev) ($\xi = 1$): $\gamma_{\pi} = 3.9, 5.3$	53
VII Electron Distribution Function (Per Mev) ($\xi = 1$): $\gamma_{\pi} = 6.7, 8.2$	55
VIII Electron Distribution Function (Per Mev) ($\xi = 1$): $\gamma_{\pi} = 15, 30$	57
IX Electron Distribution Function (Per Mev) ($\xi = 1$): $\gamma_{\pi} = 40, 45$	59
X Electron Distribution Function (Per Mev) ($\xi = 1$): $\gamma_{\pi} = 60, 72$	61
XI Electron Distribution Function (Per Mev) ($\xi = 1$): $\gamma_{\pi} = 100, 145$	64
XII Electron Distribution Function (Per Mev) ($\xi = 1$): $\gamma_{\pi} = 200, 290$	67

Table		Page
XIII Electron Distribution Function (Per Mev) ($\xi = 1$): $\gamma_{\pi} = 430, 570 \dots$		70
XIV Electron Distribution Function (Per Mev) ($\xi = 1$): $\gamma_{\pi} = 720, 800 \dots$		73
XV Electron Distribution Function (Per Mev) ($\xi = 0$): $\gamma_{\pi} = 1.02, 1.07 \dots$		76
XVI Electron Distribution Function (Per Mev) ($\xi = 0$): $\gamma_{\pi} = 1.15, 1.3 \dots$		78
XVII Electron Distribution Function (Per Mev) ($\xi = 0$): $\gamma_{\pi} = 1.7, 2.4 \dots$		80
XVIII Electron Distribution Function (Per Mev) ($\xi = 0$): $\gamma_{\pi} = 3.9, 5.3 \dots$		82
XIX Electron Distribution Function (Per Mev) ($\xi = 0$): $\gamma_{\pi} = 40, 100 \dots$		84
XX Electron Distribution Function (Per Mev) ($\xi = 0$): $\gamma_{\pi} = 200, 800 \dots$		87
B-I Allowed Sin λ Roots		149

LIST OF FIGURES

Figure	Page
1 Lorentz Transformation in μ^- Decay	4
2 Lorentz Transformation in μ^+ Decay	8
3 The Transformation $xyz \rightarrow \xi\eta\zeta$	10
4 The Transformation $\xi\eta\zeta \rightarrow x'y'z'$	10
5 The Transformation $x'y'z' \rightarrow x''y''z''$	10
6 Rotation in $x''z''$ Plane	10
7 Decay Axes	10
8 Momentum Directions	10
9 Region of Muon Angular Integration for $\lambda_e < \pi/2$. .	19
10 Region of Muon Angular Integration for $\lambda_e > \pi/2$. .	19
A1 Lorentz Transformation	142
A2 Momentum Ellipse for $\tilde{p}_e > p$	142
A3 Momentum Ellipse for $\tilde{p}_e < p$	142
A4 Nest of Momentum Ellipses for $\tilde{p}_{e \max} > p$	143
A5 Nest of Momentum Ellipses for $\tilde{p}_{e \max} < p$	143
B1 Definition of C	153
B2 $s \cot C$ for $s > 0$	153
B3 z_+ Derivative for $s, \delta_e > 0$	153

Figure	Page
B4 z - Derivative for s, $\delta_e > 0$	153
D1 Momentum Ellipses for $\gamma_\pi \geq \bar{w}$	170
D2 Momentum Ellipses for $\bar{w} \geq \gamma_\pi \geq \bar{\gamma}_{e_t}$	170
D3 Momentum Ellipses for $\bar{\gamma}_{e_t} \geq \gamma_\pi \geq \gamma_\mu$	171
D4 Momentum Ellipses for $\gamma_\mu \geq \gamma_\pi$	171

LIST OF GRAPHS

Graph		Page
1 Electron Distribution Function ($\xi = 1$):		
$\gamma_{\pi} = 1.02 \dots$		91
2 Electron Distribution Function ($\xi = 1$):		
$\gamma_{\pi} = 1.07 \dots$		92
3 Electron Distribution Function ($\xi = 1$):		
$\gamma_{\pi} = 1.15 \dots$		93
4 Electron Distribution Function ($\xi = 1$):		
$\gamma_{\pi} = 1.3 \dots$		94
5 Electron Distribution Function ($\xi = 1$):		
$\gamma_{\pi} = 1.45 \dots$		95
6 Electron Distribution Function ($\xi = 1$):		
$\gamma_{\pi} = 1.6 \dots$		96
7 Electron Distribution Function ($\xi = 1$):		
$\gamma_{\pi} = 1.7 \dots$		97
8 Electron Distribution Function ($\xi = 1$):		
$\gamma_{\pi} = 2.4 \dots$		98
9 Electron Distribution Function ($\xi = 1$):		
$\gamma_{\pi} = 3.9 \dots$		99
10 Electron Distribution Function ($\xi = 1$):		
$\gamma_{\pi} = 5.3 \dots$		100
11 Electron Distribution Function ($\xi = 1$):		
$\gamma_{\pi} = 6.7 \dots$		101

Graph	Page
12 Electron Distribution Function ($\xi = 1$): $\gamma_{\pi} = 8.2 \dots$	102
13 Electron Distribution Function ($\xi = 1$): $\gamma_{\pi} = 15 \dots$	103
14 Electron Distribution Function ($\xi = 1$): $\gamma_{\pi} = 30 \dots$	104
15 Electron Distribution Function ($\xi = 1$): $\gamma_{\pi} = 40 \dots$	105
16 Electron Distribution Function ($\xi = 1$): $\gamma_{\pi} = 45 \dots$	106
17 Electron Distribution Function ($\xi = 1$): $\gamma_{\pi} = 60 \dots$	107
18 Electron Distribution Function ($\xi = 1$): $\gamma_{\pi} = 72 \dots$	108
19 Electron Distribution Function ($\xi = 1$): $\gamma_{\pi} = 100 \dots$	109
20 Electron Distribution Function ($\xi = 1$): $\gamma_{\pi} = 145 \dots$	110
21 Electron Distribution Function ($\xi = 1$): $\gamma_{\pi} = 200 \dots$	111
22 Electron Distribution Function ($\xi = 1$): $\gamma_{\pi} = 290 \dots$	112
23 Electron Distribution Function ($\xi = 1$): $\gamma_{\pi} = 430 \dots$	113
24 Electron Distribution Function ($\xi = 1$): $\gamma_{\pi} = 570 \dots$	114
25 Electron Distribution Function ($\xi = 1$): $\gamma_{\pi} = 720 \dots$	115

Graph	Page
26 Electron Distribution Function ($\xi = 1$): $\gamma_{\pi} = 800 \dots$	116
27 Electron Distribution Function ($\xi = 1$): $\gamma_{\pi} = 1.02, 1.07, 1.15, 1.3, 1.45, 1.6, 1.7, 2.4 \dots$	117
28 Electron Distribution Function ($\xi = 1$): $\gamma_{\pi} = 2.4, 3.9, 5.3, 6.7, 8.2, 15, 30 \dots$	118
29 Electron Distribution Function ($\xi = 1$): $\gamma_{\pi} = 30, 40, 45, 60, 72, 100, 145, 200 \dots$	119
30 Electron Distribution Function ($\xi = 1$): $\gamma_{\pi} = 200, 290, 430, 570, 720, 800 \dots$	120
31 Electron Distribution Function ($\xi = 1, 0$): $\gamma_{\pi} = 1.02 \dots$	121
32 Electron Distribution Function ($\xi = 1, 0$): $\gamma_{\pi} = 1.07 \dots$	122
33 Electron Distribution Function ($\xi = 1, 0$): $\gamma_{\pi} = 1.15 \dots$	123
34 Electron Distribution Function ($\xi = 1, 0$): $\gamma_{\pi} = 1.3 \dots$	124
35 Electron Distribution Function ($\xi = 1, 0$): $\gamma_{\pi} = 1.7 \dots$	125
36 Electron Distribution Function ($\xi = 1, 0$): $\gamma_{\pi} = 2.4 \dots$	126
37 Electron Distribution Function ($\xi = 1, 0$): $\gamma_{\pi} = 3.9 \dots$	127
38 Electron Distribution Function ($\xi = 1, 0$): $\gamma_{\pi} = 5.3 \dots$	128
39 Electron Distribution Function ($\xi = 1, 0$): $\gamma_{\pi} = 40 \dots$	129

INTRODUCTION

As cosmic rays journey through the interstellar gas they collide with the atoms and molecules of the gas. Since both the cosmic rays and the interstellar gas are comprised largely of protons, proton-proton events are expected to be of greatest importance. When the collision energy is sufficiently above the threshold for production of additional particles, charged pi mesons are produced in abundance. The charged pions rapidly decay, chiefly into mu mesons and neutrinos. The muons are likewise unstable, and disintegrate immediately into electrons and neutrinos.

It is the purpose of this work to determine the energy spectra of electrons resulting from the decay of charged pions via the $\pi\rightarrow\mu\rightarrow e$ mode in interstellar space. Since the lifetime of both pions and muons is very much smaller than the mean time between collisions in interstellar space, decays in flight must be considered.

Previous investigators estimating the equilibrium energy distribution of electrons in space have had to deal with $\pi\rightarrow\mu\rightarrow e$ decay. The most recent attempts are those of

Hayakawa and Okuda (1962), Jones (1963), and Ginzburg and Syrovat-skii (1964). In each of these papers, to simplify the mathematical formulation the authors assumed: (1) an isotropic angular distribution of electrons in the muon rest system, and (2) sufficiently large values of the pion energy that the muon travels at the same speed as the pion.

Numerical values of the electron energy distribution from pion decay are presented by none of these authors; in each case the expression representing the $\pi\text{-}\mu\text{-}e$ process is directly combined with the distribution of charged pions from cosmic ray collisions to obtain the production spectrum of electrons from these collisions.

Our analysis of the $\pi\text{-}\mu\text{-}e$ decay makes neither of the two common assumptions. The treatment starts with the known asymmetric distribution of electrons from muon decay in the muon rest system. A Lorentz transformation to the pion rest frame is performed, after which the muon distribution from pion decay is introduced. A second relativistic transformation is then made to the frame in which the pion is moving.

Calculations of the electron energy spectra have been made on an IBM 7094 computer for values of the pion kinetic energy between 3 mev and 110 bev.

For comparison with the present results, the electron spectra resulting from an isotropic muon-rest-frame distribution have also been computed at a number of pion energies.

We wish to thank Drs. James Joseph, Melvin Ferentz, Frank R. Pomilla, and S. P. Shen for their helpful discussions.

This report contains substantial parts of a doctoral dissertation submitted to St. John's University, New York, by J. H. Scanlon.

CHAPTER I

ELECTRON DISTRIBUTION FROM MUON DECAY

The known asymmetric distribution of electrons from muon decay in the muon rest frame is taken as the starting point for the analysis.

Muon Rest Frame

Consider the decay $\mu^- \rightarrow e^- + \bar{\nu} + \nu$. The energy and angular distribution of electrons in the muon center-of-mass system (μ CMS) due to a fully polarized muon is given by (Bouchiat and Michel [1957], Lee and Yang [1957a], Vaisenberg [1960])

$$\begin{aligned}\tilde{N}(\tilde{E}_e, \tilde{\theta}_e) d\tilde{E}_e d\tilde{\Omega}_e &= C \tilde{P}_e [(3W - 2\tilde{E}_e) \tilde{E}_e \\ &+ (W - 2\tilde{E}_e) \tilde{P}_e \xi \cos \tilde{\theta}_e + O(\eta)] d\tilde{E}_e d\tilde{\Omega}_e\end{aligned}\quad (1)$$

where

$\tilde{\theta}_e$ = the angle between the electron momentum \tilde{P}_e

and the spin of the μ^-

W = the maximum value of the electron (total) energy \tilde{E}_e in this frame

ξ = a parameter that depends on the interaction

C = the normalization constant.

The velocity of light is taken as unity throughout.

Since the parameter η could be determined only at very low energy, its value is not known. The η -dependent terms contribute only at small momenta, and because of the form of the distribution in Eq. (1), have very little effect on the over-all spectrum (Vaisenberg [1960]). Therefore this contribution is ignored.

Equation (1) could be improved by the inclusion of radiative corrections. The first order corrections are quite complicated. They are found to be small, however, and affect the over-all spectrum only slightly (Kinoshita and Sirlin [1957b]), Berman [1958]), so they are neglected.

Normalizing the distribution to unity

$$\int_{m_e}^W d\tilde{E}_e \int_0^\pi \int_0^{2\pi} d\tilde{\Omega}_e \tilde{N}(\tilde{E}_e, \tilde{\theta}_e) = 1 \quad (2)$$

gives

$$\frac{1}{C} = 2\pi w m_e^4 \left[v^3 - \frac{1}{2} v + \frac{1}{2w} \ln(w+v) \right] \quad (3)$$

in which

$$w = W/m_e \quad (4)$$

$$v = \sqrt{w^2 - 1} \quad (5)$$

where m_e is the electron mass.

One can show that the (nondimensionalized) maximum energy (4) and momentum (5) of the electron in the muon rest frame are given by (Baldin et al. [1961])

$$w = \frac{1}{2} \left[\frac{m_\mu}{m_e} + \frac{m_e}{m_\mu} \right] \quad (6)$$

$$v = \frac{1}{2} \left[\frac{m_\mu}{m_e} - \frac{m_e}{m_\mu} \right]. \quad (7)$$

The normalization constant can be approximated (to within 0.02%) by

$$\frac{1}{C} = 2\pi w^4. \quad (8)$$

Pion Rest Frame

The spin of the μ^- in the pion center-of-mass system (π CMS) is known to be fully polarized in the direction of its momentum (Vaisenbergs [1960], Backenstoss et al. [1961], Rainwater [1957]). Under Lorentz transformation to

the μ CMS the muon spin S_μ remains parallel to the transformation axis (Ascoli [1958], Wigner [1957], Williams [1961]). Thus the angles that the electron momentum makes with the muon spin direction and with the axis of Lorentz transformation from the π CMS are identical. See Fig. 1.

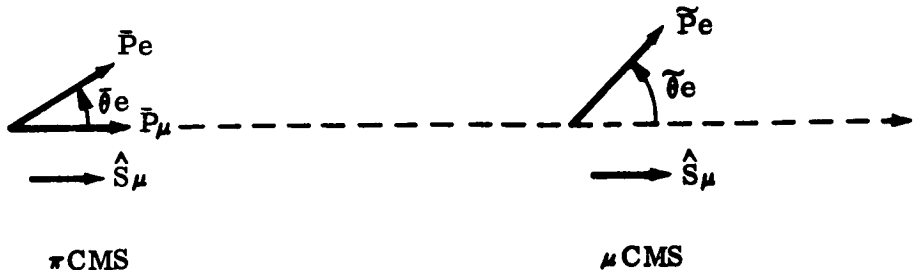


Fig. 1 Lorentz Transformation in μ^- Decay

The energy distribution N in any frame is related to the corresponding momentum distribution M by

$$M(P, \theta) = \frac{P}{E} N(E, \theta) . \quad (9)$$

We now transform from the μ CMS to a system moving in the $-S_\mu$ direction (we shall later specify the π CMS).

The electron momentum distribution in the new system is related to that in the μ CMS by

$$\begin{aligned} \bar{M}(\bar{P}_e, \bar{\theta}_e) d\bar{P}_e d\bar{\Omega}_e &= \tilde{M}(\tilde{P}_e, \tilde{\theta}_e) \tilde{d}P_e \tilde{d}\Omega_e \\ &= JM(\tilde{P}_e[\bar{P}_e, \bar{\theta}_e], \tilde{\theta}_e[\bar{P}_e, \bar{\theta}_e]) d\bar{P}_e d\bar{\Omega}_e \end{aligned} \quad (10)$$

where the Jacobian for the transformation is (Baldin et al. [1961])

$$J = \frac{\partial(\tilde{P}_e, \tilde{\theta}_e)}{\partial(\bar{P}_e, \bar{\theta}_e)} = \frac{\bar{P}_e^2 \tilde{E}_e}{\tilde{P}_e^2 \bar{E}_e}. \quad (11)$$

With the introduction of the Lorentz transformation equations

$$\tilde{E}_e = \gamma_\mu \bar{E}_e - p_\mu \bar{P}_e \cos \bar{\theta}_e \quad (12)$$

$$\tilde{P}_e \cos \tilde{\theta}_e = \gamma_\mu \bar{P}_e \cos \bar{\theta}_e - p_\mu \bar{E}_e \quad (13)$$

where γ and p are the energy and momentum of a particle in units of its own mass

$$\begin{aligned} \gamma &= E/m \\ p &= P/m, \end{aligned} \quad (14)$$

the distribution takes the form

$$\begin{aligned} \bar{M}_{\mu e}(\bar{P}_e, \bar{\theta}_e) d\bar{P}_e d\bar{\Omega}_e &= C \frac{\bar{P}_e^2}{\bar{E}_e} \left[a_1 \bar{E}_e + a_2 \bar{E}_e^2 \right. \\ &\quad \left. + (a_3 + a_4 \bar{E}_e) \bar{P}_e \cos \bar{\theta}_e + a_5 \bar{P}_e^2 \cos^2 \bar{\theta}_e \right] d\bar{P}_e d\bar{\Omega}_e \end{aligned} \quad (15)$$

with

$$\begin{aligned}
 a_1 &= w(3\gamma_\mu - \xi p_\mu) \\
 a_2 &= 2(\xi\gamma_\mu - p_\mu - \gamma_\mu^2) \\
 a_3 &= w(\xi\gamma_\mu - 3p_\mu) \\
 a_4 &= 2(2\gamma_\mu p_\mu - \xi\gamma_u^2 - \xi p_\mu^2) \\
 a_5 &= 2(\xi\gamma_\mu p_\mu - p_\mu^2) .
 \end{aligned} \tag{16}$$

It will be noticed that the bars denoting the π CMS have been omitted on γ_μ and p_μ for convenience.

In the new system the range of allowed directions $\bar{\theta}_e$ of electron emission relative to the muon direction is dependent upon the electron momentum \bar{P}_e . It is shown in Appendix A that for the case $w > \gamma_\mu$, with which we shall be concerned, that the range is given by

$$\bar{\theta}_{e \min} = 0 \tag{17}$$

$$\bar{y}_m = \begin{cases} -1 , & \bar{P}_e \leq \bar{P}_{et} \\ \bar{y}_p , & \bar{P}_e \geq \bar{P}_{et} \end{cases} \tag{18}$$

where

$$\bar{y}_m = \cos(\bar{\theta}_{e \max}) \tag{19}$$

$$\bar{y}_p = \frac{\gamma_\mu \bar{E}_e - w}{p_\mu p_e} \quad (20)$$

$$\begin{aligned}\bar{E}_{et} &= \gamma_\mu w - p_\mu v \\ \bar{P}_{et} &= \gamma_\mu v - p_\mu w\end{aligned} \quad (21)$$

$$v = v m_e . \quad (22)$$

The range of permissible \bar{E}_e values is γ_μ -dependent. In Appendix A it is also shown that

$$\begin{aligned}\bar{E}_{e \max} &= \gamma_\mu w + p_\mu v \\ \bar{P}_{e \max} &= \gamma_\mu v + p_\mu w\end{aligned} \quad (23)$$

and, for $w \geq \gamma_\mu$

$$\begin{aligned}\bar{E}_{e \min} &= m_e \\ \bar{P}_{e \min} &= 0 .\end{aligned} \quad (24)$$

To this point only the μ^- decay has been mentioned. For the μ^+ decay, Eq. (1) holds with the substitution of $-\xi$ for ξ . The helicity of the μ^+ in the π CMS is -1, so that the angle the electron momentum \tilde{P}_e

makes with the muon spin is the supplement of the angle it makes with the axis of Lorentz transformation from the π CMS. Thus the e^+ from μ^+ decay will also obey Eq. (1), where $\tilde{\theta}_e$ is now the angle between \tilde{P}_e and the (indicated) direction of the Lorentz transformation axis. See Fig. 2. Consequently, all our results will be equally applicable to μ^+ decay.

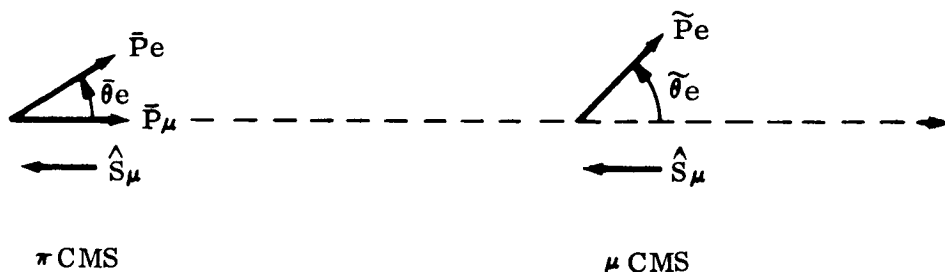


Fig. 2 Lorentz Transformation in μ^+ Decay

CHAPTER II

ELECTRON DISTRIBUTION IN PION REST SYSTEM

$\bar{M}_{\mu e}$ in Eq. (15) is the electron distribution in the π CMS relative to the direction of the parent decay muon. Each individual muon will in general have some direction with respect to a given fixed set of axes in the π CMS system. We wish to relate the electron direction to such a set of axes.

Fixed Set of Axes

Define a fixed system xyz in the π CMS. Consider a set of Eulerian rotations (Figs. 3 - 8):

- (1) Rotate clockwise an angle $\pi/2-\mu$ about the z axis. Call the new axes $\xi\eta\zeta$.
- (2) Rotate clockwise by λ about the ξ axis; call the new axes $x'y'z'$.
- (3) Rotate counterclockwise φ about the z' axis; call the new axes $x''y''z''$.
- (4) In the $x''z''$ plane, the angle θ is defined by a counterclockwise rotation from z''

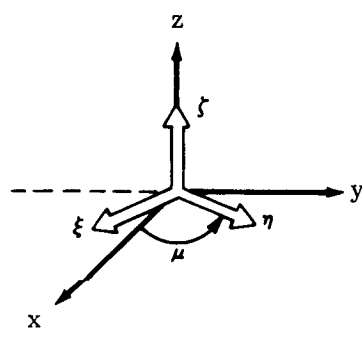


Fig. 3 The Transformation
 $xyz \rightarrow \xi\eta\zeta$

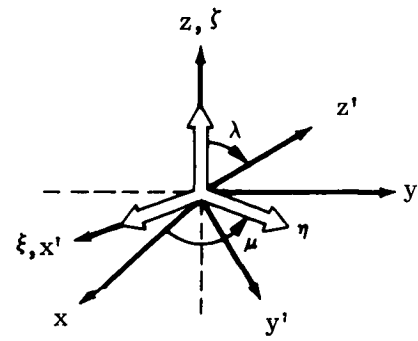


Fig. 4 The Transformation
 $\xi\eta\zeta \rightarrow x'y'z'$

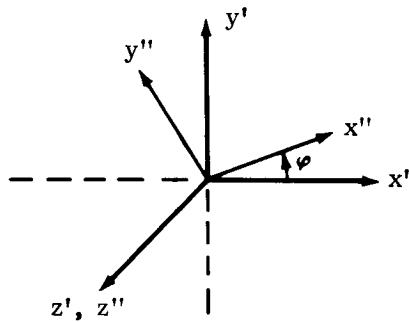


Fig. 5 The Transformation
 $x'y'z' \rightarrow x''y''z''$

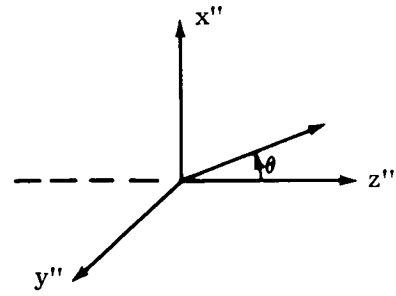


Fig. 6 Rotation in $x''z''$ Plane

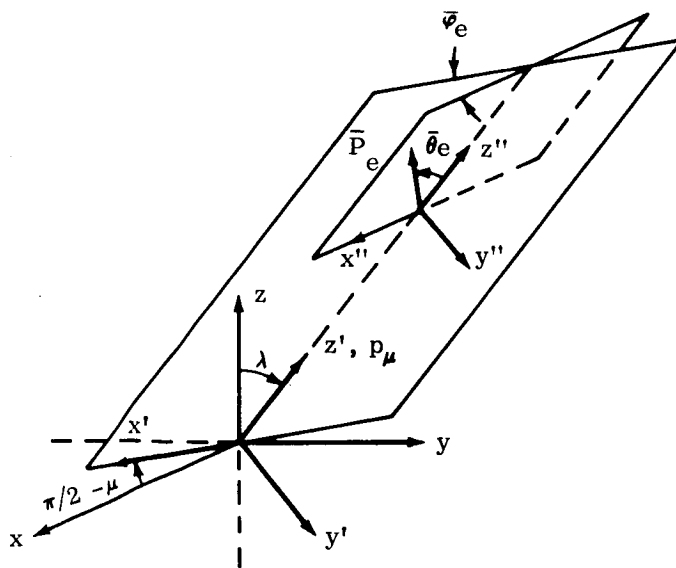


Fig. 7 Decay Axes

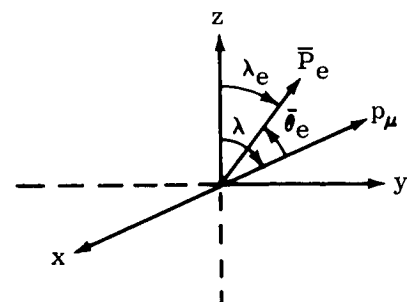


Fig. 8 Momentum Directions

about the y'' axis.

We shall take z' as the direction of the muon and the $x''z''$ plane as the plane in which the electron is emitted. The angles λ and μ without subscript will refer to the muon.

The transformation between the $x''y''z''$ system and the xyz system is found to be

$$(\bar{P}_e'') = F(\bar{P}_e) \quad (25)$$

where

$$F = \begin{bmatrix} \sin\mu \cos\bar{\phi}_e & -\cos\mu \cos\bar{\phi}_e & -\sin\lambda \sin\bar{\phi}_e \\ +\cos\lambda \cos\mu \sin\bar{\phi}_e & +\cos\lambda \sin\mu \sin\bar{\phi}_e & \\ -\sin\mu \sin\bar{\phi}_e & \cos\mu \sin\bar{\phi}_e & -\sin\lambda \cos\bar{\phi}_e \\ +\cos\lambda \cos\mu \cos\bar{\phi}_e & +\cos\lambda \sin\mu \cos\bar{\phi}_e & \\ \sin\lambda \cos\mu & \sin\lambda \sin\mu & \cos\lambda \end{bmatrix} \quad (26)$$

$$(\bar{P}_e'') = \begin{bmatrix} \bar{P}_{e_x}'' \\ \bar{P}_{e_y}'' \\ \bar{P}_{e_z}'' \end{bmatrix} = \bar{P}_e \begin{bmatrix} \sin \bar{\theta}_e \\ 0 \\ \cos \bar{\theta}_e \end{bmatrix} \quad (27)$$

$$(\bar{P}_e) = \bar{P}_e \begin{bmatrix} \alpha_e \\ \beta_e \\ \delta_e \end{bmatrix}. \quad (28)$$

The α_e , β_e , and δ_e are the direction cosines of the electron.

$$\alpha_e = \sin \lambda_e \cos \mu_e$$

$$\beta_e = \sin \lambda_e \sin \mu_e \quad (29)$$

$$\delta_e = \cos \lambda_e .$$

The distribution (\bar{M}_λ) relative to the new coordinate system is related to that in the old (\bar{M}_θ) by

$$\begin{aligned} \bar{M}_\lambda(\bar{P}_e, \lambda_e, \mu_e) d\bar{\Omega}_\lambda &= \bar{M}_\theta(\bar{P}_e, \bar{\theta}_e, \bar{\varphi}_e) d\bar{\Omega}_\theta \\ &= J \bar{M}_\theta(\bar{P}_e, \bar{\theta}_e[\lambda_e, \mu_e], \bar{\varphi}_e[\lambda_e, \mu_e]) d\bar{\Omega}_\lambda \end{aligned} \quad (30)$$

with

$$J = \frac{\partial(\cos \bar{\theta}_e, \bar{\varphi}_e)}{\partial(\cos \lambda_e, \mu_e)} . \quad (31)$$

This is a transformation between two polar coordinate systems; one finds the Jacobian $J = 1$ as might be expected. The λ subscript notation on \bar{M} and $\bar{\Omega}$ can now be dropped.

Muon Distribution

Define $\bar{M}_{\pi\mu}(p_\mu, \Omega) dp_\mu d\Omega$ as the number of muons produced in the range p_μ to $p_\mu + dp_\mu$, Ω to $\Omega + d\Omega$, by a pion in the π CMS. $\bar{M}_{\mu e}(p_\mu, \Omega; \bar{P}_e, \bar{\Omega}_e) d\bar{P}_e d\bar{\Omega}_e$ is the number of electrons produced in the range \bar{P}_e to $\bar{P}_e + d\bar{P}_e$, $\bar{\Omega}_e$ to $\bar{\Omega}_e + d\bar{\Omega}_e$, by a muon of momentum p_μ and direction Ω .

The $\bar{M}_{\mu e}$ in Eq. (15) is the electron spectrum from the decay of a single muon. Since we wish to obtain $\bar{M}_{\pi\mu e}$, the distribution of electrons resulting from the decay of a single pion, we must integrate over all possible muon momenta and directions:

$$\bar{M}_{\pi\mu e} d\bar{P}_e d\bar{\Omega}_e = d\bar{P}_e d\bar{\Omega}_e \left[\int \left[\bar{M}_{\pi\mu}(p_\mu, \Omega) \cdot \bar{M}_{\mu e}(p_\mu, \Omega; \bar{P}_e, \bar{\Omega}_e) \right] dp_\mu d\Omega \right]. \quad (32)$$

The muon momentum distribution in the π CMS from pion decay ($\pi \rightarrow \mu + \nu$) is regarded as isotropic by most investigators (Vaisenberg et al. [1962]).

$$\bar{M}_{\pi\mu} dp_\mu d\Omega = \frac{1}{4\pi} \delta(p_\mu - \bar{p}_\mu) dp_\mu d\Omega. \quad (33)$$

The dimensionless energy $\bar{\gamma}_\mu$ and momentum \bar{p}_μ of the muon

in the π CMS are given by (Baldin et al. [1961])

$$\bar{\gamma}_\mu = \frac{1}{2} \left[\frac{m_\pi}{m_\mu} + \frac{m_\mu}{m_\pi} \right] \quad (34)$$

$$\bar{p}_\mu = \frac{1}{2} \left[\frac{m_\pi}{m_\mu} - \frac{m_\mu}{m_\pi} \right]. \quad (35)$$

Therefore,

$$\bar{M}_{\pi\mu e}(\bar{P}_e, \bar{\Omega}_e) = \frac{1}{4\pi} \int \bar{M}_{\mu e}(p_\mu, \Omega; \bar{P}_e, \bar{\Omega}_e) d\Omega \quad (36)$$

where again the bar has been dropped on p_μ for convenience.

The relation between $\bar{\theta}_e$ and the new angles λ_e and μ_e is found from Eq. (25).

$$\cos \bar{\theta}_e = \sin \lambda \sin \lambda_e \cos U + \cos \lambda \cos \lambda_e \quad (37)$$

where

$$U = \mu - \mu_e. \quad (38)$$

Thus it turns out that the integration in Eq. (36) depends on μ and μ_e only through their difference U . This must be so, for it is simply the statement that the electron distribution from a pion decay has azimuthal symmetry about the z axis. Physically the z axis means nothing as yet, since we are in the π CMS, so there should be spherical

symmetry, not just azimuthal symmetry. It will be seen subsequently that the formulas do in fact yield this result.

The Jacobian of the transformation $(\lambda, \mu) \rightarrow (\lambda, U)$ is unity, so that $d\Omega$ in Eq. (36) can simply be identified with $\sin \lambda d\lambda dU$. With the aid of Eq. (15) the electron distribution can then be written in the form

$$\begin{aligned} \bar{M}_{\pi\mu e}(\bar{P}_e, \lambda_e) = & \frac{C}{4\pi} \frac{\bar{P}_e^2}{\bar{E}_e} \left[(a_1 \bar{E}_e + a_2 \bar{E}_e^2) L_1 \right. \\ & + (a_3 \bar{P}_e + a_4 \bar{E}_e \bar{P}_e) (L_2 \sin \lambda_e + L_3 \cos \lambda_e) \\ & + a_5 \bar{P}_e^2 (L_4 \sin^2 \lambda_e + L_5 \cos^2 \lambda_e \\ & \left. + 2L_6 \sin \lambda_e \cos \lambda_e) \right] \end{aligned} \quad (39)$$

where

$$\begin{aligned} L_1 &= \int \int d\Omega \\ L_2 &= \int \int \sin \lambda \cos U d\Omega \\ L_3 &= \int \int \cos \lambda d\Omega \end{aligned} \quad (40)$$

$$L_4 = \int \int \sin^2 \lambda \cos^2 U d\Omega$$

$$L_5 = \int \int \cos^2 \lambda d\Omega$$

$$L_6 = \int \int \sin \lambda \cos \lambda \cos U d\Omega .$$

Muon Integrations

To evaluate the L_i , one must determine the region of integration (λ, U) as a function of the momentum (\bar{P}_e) and direction (λ_e) of the electron. From Fig. 8 it can be seen that for each $\bar{\theta}_e$ the geometry restricts the combinations of (λ, U) that can contribute to a particular λ_e . To determine the actual limits of the (λ, U) integration in Eq. (40), one must therefore take into account the range of $\bar{\theta}_e$ values given by Eq. (18).

We choose to integrate over the muon polar angle first. Solving Eq. (37) yields λ as a function of U

$$z_{\pm} = \cos \lambda_{\pm} = \frac{v_e \bar{y} \mp s \sqrt{A^2 - \bar{y}^2}}{A^2} \quad (41)$$

$$x_{\pm} = \sin \lambda_{\pm} = \frac{s \bar{y} \pm \delta_e \sqrt{A^2 - \bar{y}^2}}{A^2} \quad (42)$$

where

$$\bar{y} = \cos \bar{\theta}_e \quad (43)$$

$$s = \sin \lambda_e \cos U \quad (44)$$

$$A^2 = s^2 + \delta_e^2. \quad (45)$$

The juxtaposition of the \pm and \mp signs in Eqs. (41) and (42) is intentional; the identity $\sin^2 \lambda + \cos^2 \lambda = 1$ requires the \mp signs between the two terms in $\cos \lambda$ to correspond to the \pm signs in $\sin \lambda$.

At this point the known physical and mathematical restrictions are imposed on the expressions for λ . In this manner it is possible to determine which of the roots z_{\pm} apply for particular combinations of λ_e , $\bar{\theta}_e$ and $|U|$. Diagrams showing the variation of λ vs. U with $\bar{\theta}_e$ as a parameter can then be constructed for this transformation. The details of this procedure are presented in Appendix B.

The areas of muon angular integration are found to differ for $\lambda_e < \pi/2$ and $\lambda_e > \pi/2$. Figs. 9 and 10

picture the two cases. The curves shown are drawn with arbitrary curvature since there is no need to determine their exact shape. Whether $2\zeta_e^2 - 1$ is positive or negative depends on the particular λ_e value. The shaded area in Fig. 9 corresponds to z_- , the unshaded area to z_+ . The reverse is true for Fig. 10.

The regions between $U = 0$ and $U = -\pi$ mirror those between $U = 0$ and $U = \pi$. Since all the L_i integrals are even in U , one can treat positive U alone and double the result.

We have made no systematic investigation of all the symmetries involved. It became evident in this and later considerations that they do exist, however, and in certain instances we have found it convenient to make use of them.

Consider now the L_i integrations. It is necessary to take into account the fact that $\bar{\theta}_{e \max}$ is \bar{P}_e - dependent as given by Eq. (18). For $\bar{P}_e \leq \bar{P}_{et}$, $\bar{y}_m = -1$, and one finds for all λ_e values that

$$L_1 = 4\pi$$

$$L_2 = L_3 = L_6 = 0 \quad (46)$$

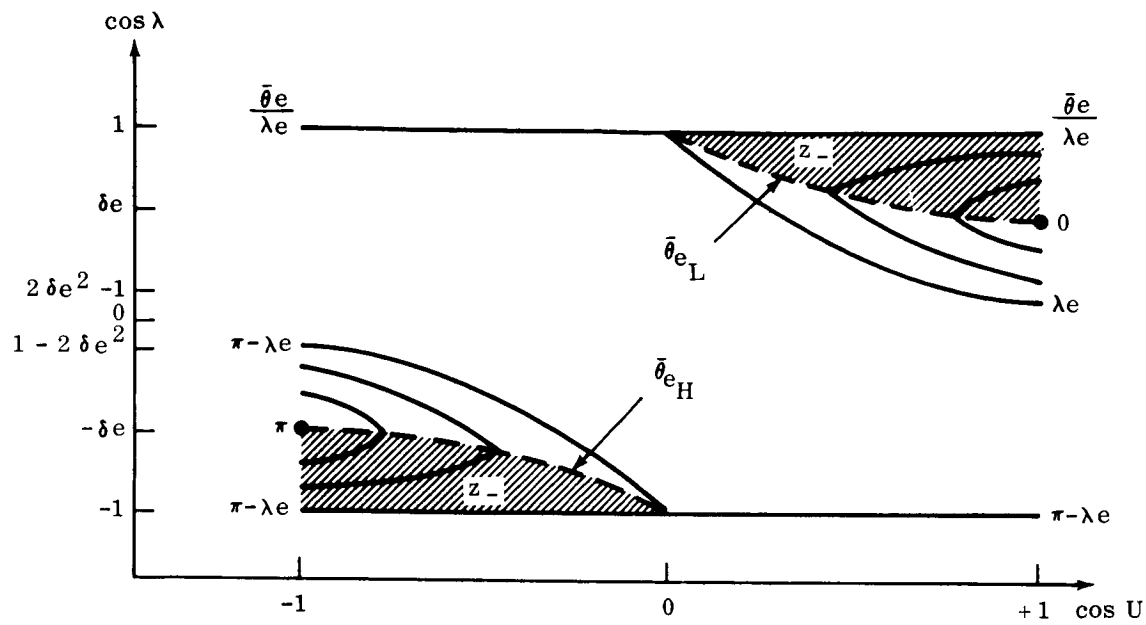


Fig. 9 Region of Muon Angular Integration for $\lambda e < \pi/2$

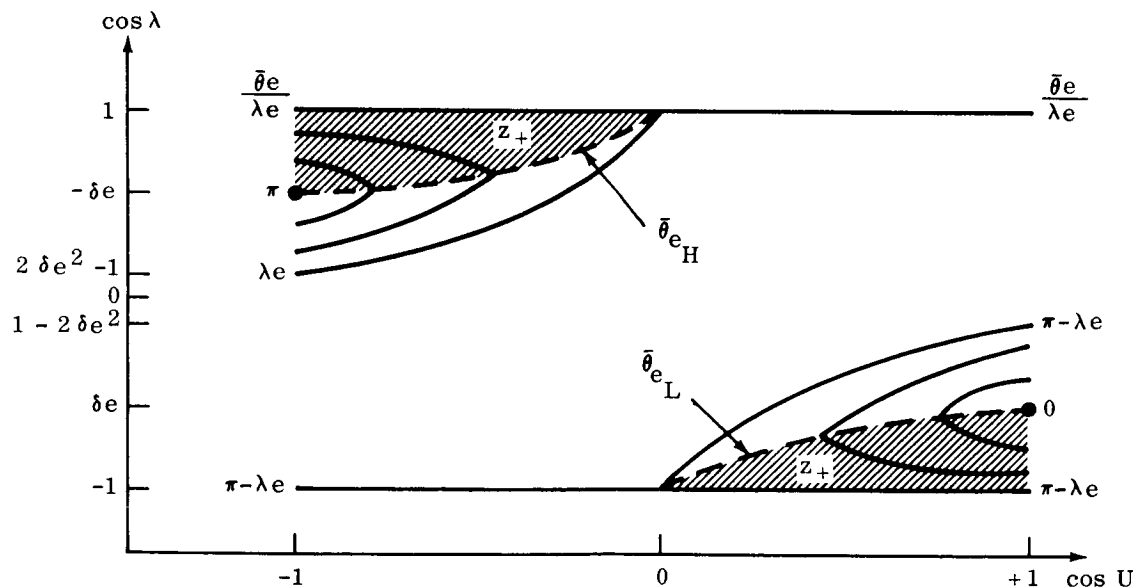


Fig. 10 Region of Muon Angular Integration for $\lambda e > \pi/2$

$$L_4 = L_5 = 4\pi/3 , \quad \bar{P}_e \leq \bar{P}_{et} .$$

For $\bar{P}_e \geq \bar{P}_{et}$, $\bar{y}_m = \bar{y}_p(\bar{P}_e)$, so the situation is considerably more complicated. It can be seen from the diagrams that it is necessary to consider six separate cases:

$$\lambda_e < \pi/2 \quad \bar{\theta}_{e \max} < \lambda_e$$

$$\lambda_e < \bar{\theta}_{e \ max} < \pi - \lambda_e$$

$$\pi - \lambda_e < \bar{\theta}_{e \ max}$$

$$\lambda_e > \pi/2 \quad \bar{\theta}_{e \ max} < \pi - \lambda_e$$

$$\pi - \lambda_e < \bar{\theta}_{e \ max} < \lambda_e$$

$$\lambda_e < \bar{\theta}_{e \ max} .$$

The treatment of the integrations is lengthy; in Appendix C is indicated a method of solution. In each of the six cases (fortunately), the identical set of L_i are obtained.

$$L_1 = 2\pi (1 - \bar{y}_m)$$

$$L_2 = \pi (1 - \bar{y}_m^2) \sin \lambda_e$$

$$L_3 = \pi (1 - \bar{y}_m^2) \cos \lambda_e \quad (47)$$

$$L_4 = \frac{\pi}{3} (1 - \bar{y}_m) \left[2 + \bar{y}_m (1 + \bar{y}_m) (2 - 3 \delta_e^2) \right]$$

$$L_5 = \frac{\pi}{3} (1 - \bar{y}_m) \left[2 + \bar{y}_m (1 + \bar{y}_m) (3 \delta_e^2 - 1) \right]$$

$$L_6 = \pi \bar{y}_m (1 - \bar{y}_m^2) \sin \lambda_e \cos \lambda_e \quad , \quad \bar{P}_e \geq \bar{P}_{e_t} .$$

In the limit $\bar{\theta}_{e \max} = \pi$ these reduce to Eqs. (46).

So the electron momentum and angular distribution in the π CMS assumes the form

$$\begin{aligned} \bar{M}_{\pi\mu e} = & \frac{C}{12} \frac{\bar{P}_e^2}{\bar{E}_e} \left[\begin{aligned} & 6(1 - \bar{y}_m) (a_1 \bar{E}_e + a_2 \bar{E}_e^2) \\ & + 3(1 - \bar{y}_m^2) (a_3 \bar{P}_e + a_4 \bar{E}_e \bar{P}_e) \\ & + 2(1 - \bar{y}_m^3) a_5 \bar{P}_e^2 \end{aligned} \right] . \end{aligned} \quad (48)$$

This is independent not only of μ_e but also of λ_e . As noted earlier this is to be expected, since we have assumed isotropic muon emission and azimuthally symmetric electron emission relative to muon direction.

As a check on the correctness of Eq. (48) one can

integrate over the electron direction and energy in the π CMS to verify that the normalization is still unity.

Consider

$$\int_{\bar{E}_e \text{ min}}^{\bar{E}_e \text{ max}} \bar{N}_{\pi\mu e} d\bar{E}_e d\Omega_e = 4\pi \int_{\bar{E}_e \text{ min}}^{\bar{E}_{e_t}} \bar{N}_{\pi u e} (\bar{y}_m = -1) d\bar{E}_e$$

$$+ 4\pi \int_{\bar{E}_{e_t}}^{\bar{E}_e \text{ max}} \bar{N}_{\pi\mu e} (\bar{y}_m = \bar{y}_p) d\bar{E}_e . \quad (49)$$

It is possible to demonstrate after a very considerable volume of detail that the expression (49) does in fact reduce to unity.

CHAPTER III

ELECTRON DISTRIBUTION IN LABORATORY FRAME

Equation (48) represents the distribution of electrons in momentum and direction in the π CMS. The next step then is to effect the final transformation to the pion laboratory system (π LS).

Transformation to Laboratory Frame

We choose the direction of the pion in the π LS as the polar axis. As in Eqs. (10) and (11), we find the distribution $M_{\pi\mu e}$ in the π LS is given by

$$M(P_e, \theta_e) dP_e d\Omega_e = J \bar{M} (\bar{P}_e [P_e, \theta_e], \bar{\theta}_e [P_e, \theta_e]) dP_e d\Omega_e \quad (50)$$

with

$$J = \frac{P_e^2 \bar{E}_e}{\bar{P}_e^2 E_e} . \quad (51)$$

The energy distribution N is related to the momentum distribution M by Eq. (9).

The electron energy in the π CMS is eliminated via the transformation equation

$$\bar{E}_e = \gamma_\pi E_e - p_\pi p_e y \quad (52)$$

where

$$y = \cos \theta_e . \quad (53)$$

In transforming the distribution (48), one must take into account the two possible \bar{y}_m cases given by Eq. (18). Let N^1 designate the first of these ($\bar{y}_m = -1$) and N^2 the other ($\bar{y}_m = \bar{y}_p$). The differential spectra can be shown to be

$$N_{\pi\mu e}^1 (E_e, \theta_e) = \frac{C_m^3}{36} p_e (b_1 + 2b_2 y + 3b_3 y^3) \quad (54)$$

where

$$\begin{aligned} b_1 &= 36 \frac{a_1}{m_e} \gamma_\pi \gamma_e - 12 a_5 + 12 a_6 \gamma_\pi^2 \gamma_e^2 \\ b_2 &= -12 a_6 \gamma_\pi p_\pi \gamma_e p_e - 18 \frac{a_1}{m_e} p_\pi p_e \\ b_3 &= 4 a_6 p_\pi^2 p_e^2 \end{aligned} \quad (55)$$

$$a_6 = 3 a_2 + a_5 \quad (56)$$

and

$$N_{\pi\mu e}^2 = N_{\pi\mu e}^{2a} + N_{\pi\mu e}^{2b} \quad (57)$$

$$N_{\pi\mu e}^{2a} (E_e, \theta_e) = \frac{1}{2} N_{\pi\mu e}^1 (E_e, \theta_e) \quad (58)$$

$$\begin{aligned} N_{\pi\mu e}^{2b} (E_e, \theta_e) &= \frac{C_m e^3}{12} p_e (k_1 \bar{\gamma}_e \bar{p}_e \\ &+ k_2 \bar{p}_e + k_3 \frac{1}{\bar{p}_e} + k_4 \frac{\bar{\gamma}_e}{\bar{p}_e} + k_5 \frac{\bar{\gamma}_e^2}{\bar{p}_e} + k_6 \frac{\bar{\gamma}_e^3}{\bar{p}_e}) \end{aligned} \quad (59)$$

with

$$\bar{p}_e = \sqrt{\bar{\gamma}_e^2 - 1} \quad (60)$$

$$k_1 = 3 a_4$$

$$k_2 = 3 \frac{a_3}{m_e}$$

$$k_3 = 2 a_5 \frac{w^3}{p_\mu^3} - 3 \frac{a_3}{m_e} \frac{w^2}{p_\mu^2} \quad (61)$$

$$k_4 = 6 \frac{a_1}{m_e} \frac{w}{p_\mu} + 6 \frac{a_3}{m_e} w \frac{\gamma_\mu}{p_\mu^2} - 3 a_4 \frac{w^2}{p_\mu^2} - 6 a_5 w^2 \frac{\gamma_\mu}{p_\mu^3}$$

$$k_5 = 6 a_2 \frac{w}{p_\mu} + 6 a_5 w \frac{\gamma_\mu^2}{p_\mu^3} - 6 \frac{a_1}{m_e} \frac{\gamma_\mu}{p_\mu} - 3 \frac{a_3}{m_e} \frac{\gamma_\mu^2}{p_\mu^2} + 6 a_4 w \frac{\gamma_\mu}{p_\mu^2}$$

$$k_6 = -6 a_2 \frac{\gamma_\mu}{p_\mu} - 3 a_4 \frac{\gamma_\mu^2}{p_\mu^2} - 2 a_5 \frac{\gamma_\mu^3}{p_\mu^3} .$$

We are specifically interested in the energy spectrum alone, so we now integrate out the angular dependence. Call

$$N_{\pi\mu e}(E_e) = \int N_{\pi\mu e}(E_e, \theta_e) d\Omega_e . \quad (62)$$

After integration and manipulation it is found that

$$N_{\pi\mu e}^1(E_e) = B p_e \sum_{i=1}^3 b_i R_i \quad (63)$$

$$B = \frac{\pi C_m e^3}{18} \quad (64)$$

$$R_i = y_3^i - y_2^i \quad (65)$$

and

$$N_{\pi\mu e}^{2a}(E_e) = B p_e \sum_{i=1}^3 b_i S_i \quad (66)$$

$$S_i = \frac{1}{2} (y_2^i - y_1^i) \quad (67)$$

where the b_i are given by Eqs. (55). Also

$$N_{\pi\mu e}^{2b}(E_e) = \frac{B}{p_\pi} \sum_{i=1}^4 c_i T_i \quad (68)$$

$$c_1 = -18\xi\gamma_\mu^2 + 6\xi \frac{\gamma_\mu^4}{p_\mu^2} + 12 \frac{\gamma_\mu^3}{p_\mu}$$

$$c_2 = \frac{w}{2} (27\xi\gamma_\mu^2 - 9\xi \frac{\gamma_\mu^3}{p_\mu^2} - 27 \frac{\gamma_\mu^2}{p_\mu}) \quad (69)$$

$$c_3 = -18\xi\gamma_\mu^2 + 6\xi + 2\xi \frac{\gamma_\mu^4}{p_\mu^2} + 12 \frac{\gamma_\mu^3}{p_\mu} + 4 \frac{\gamma_\mu^3}{p_\mu}$$

$$c_4 = \frac{w}{2} (-9\xi \frac{\gamma_\mu^3}{p_\mu^2} - 27 \frac{1}{p_\mu}) + w^3 (3\xi \frac{\gamma_\mu^3}{p_\mu^2} + \frac{15}{p_\mu})$$

$$T_1 = \left[\sqrt{t^2 - 1} \right]_{t_2}^{t_1}$$

$$T_2 = \left[t \sqrt{t^2 - 1} \right]_{t_2}^{t_1} \quad (70)$$

$$T_3 = \left[(t^2 - 1)^{3/2} \right]_{t_2}^{t_1}$$

$$T_4 = \left[\ln \left(t + \sqrt{t^2 - 1} \right) \right]_{t_2}^{t_1}$$

where

$$t = \gamma_\pi \gamma_e - p_\pi p_e y . \quad (71)$$

The limits will be explained shortly.

After transformation from the π CMS to the π LS the range of permissible directions for a given electron momentum p_e is again restricted. It is proved in Appendix A that

$$\theta_{e \min} = 0 \quad (72)$$

$$\gamma_\pi \leq \bar{w}, \quad y_m = \begin{cases} -1 & , p_e \leq p_{et} \\ y_x & , p_e \geq p_{et} \end{cases} \quad (73)$$

$$\gamma_\pi \geq \bar{w}, \quad y_m = y_x$$

where

$$y_x = \frac{\gamma_\pi \gamma_e - \bar{w}}{p_\pi p_e} \quad (74)$$

and

$$\gamma_{e_t} = \gamma_\pi \bar{w} - p_\pi \bar{v}$$

(75a)

$$p_{e_t} = \gamma_\pi \bar{v} - p_\pi \bar{w}$$

$$\bar{w} = \bar{\gamma}_{e \max}$$

(76a)

$$\bar{v} = \bar{p}_{e \max}.$$

Likewise, the range of γ_e is dependent upon γ_π . It is also shown in Appendix A that

$$\gamma_{e \max} = \gamma_\pi \bar{w} + p_\pi \bar{v}$$

(77)

$$p_{e \max} = \gamma_\pi \bar{v} + p_\pi \bar{w}$$

(78)

$$\gamma_{e \min} = \begin{cases} 1 & , \gamma_\pi \leq \bar{w} \\ \gamma_\pi \bar{w} - p_\pi \bar{v} & , \gamma_\pi \geq \bar{w} . \end{cases}$$

(79a)

It is necessary to determine, in terms of π LS quantities, the circumstances under which either N^1 or N^2 is required, with the appropriate angle limits.

Appendix D contains an analysis of the problem by means of the properties of momentum ellipses. Table I summarizes the results of these considerations. It is found that one must treat four well-defined ranges of pi meson energy.

Each γ_π interval is further subdivided into three or four regions of electron energy.

The new quantities used in Table I are defined by

$$\gamma_{e_s} = \gamma_\pi \bar{\gamma}_{e_t} - p_\pi \bar{p}_{e_t} \quad (80a)$$

$$\gamma_{e_r} = \gamma_\pi \bar{\gamma}_{e_t} + p_\pi \bar{p}_{e_t} \quad (81)$$

$$y_t = \frac{\gamma_\pi \gamma_e - \bar{\gamma}_{e_t}}{p_\pi p_e} . \quad (82)$$

Equations (34), (23), and (21) give γ_μ , $\bar{E}_{e \text{ max}}$, and \bar{E}_{e_t} , respectively.

Alternate Equation Forms

For calculational purposes it is convenient to recast some of the equations. Accordingly, we rewrite

$$\bar{w} = \frac{1}{2} \left[\frac{m_\pi}{m_e} + \frac{m_e}{m_\pi} \right] \quad (76b)$$

$$\bar{v} = \frac{1}{2} \left[\frac{m_\pi}{m_e} - \frac{m_e}{m_\pi} \right]$$

$$\bar{\gamma}_{e_t} = \frac{1}{2} \left[\frac{m_\mu^2}{m_\pi m_e} + \frac{m_\pi m_e}{m_\mu^2} \right] \quad (83)$$

TABLE I
LIMITS ON ELECTRON DIRECTION

γ_π Range	γ_e Range	y_1	y_2	y_3
	$\gamma_e \text{ min} \rightarrow \gamma_{e_s}$	y_x	+1	
$\gamma_\pi \geq \bar{w}$	$\gamma_{e_s} \rightarrow \gamma_{e_r}$	y_x	y_t	+1
	$\gamma_{e_r} \rightarrow \gamma_e \text{ max}$	y_x	+1	
	$+1 \rightarrow \gamma_{e_s}$	-1	+1	
	$\gamma_{e_s} \rightarrow \gamma_{e_t}$	-1	y_t	+1
$\bar{w} \geq \gamma_\pi \geq \bar{\gamma}_{e_t}$	$\gamma_{e_t} \rightarrow \gamma_{e_r}$	y_x	y_t	+1
	$\gamma_{e_r} \rightarrow \gamma_e \text{ max}$	y_x	+1	
	$+1 \rightarrow \gamma_{e_s}$	-1	+1	
	$\gamma_{e_s} \rightarrow \gamma_{e_t}$	-1	y_t	+1
$\bar{\gamma}_{e_t} \geq \gamma_\pi \geq \gamma_\mu$	$\gamma_{e_t} \rightarrow \gamma_{e_r}$	y_x	y_t	+1
	$\gamma_{e_r} \rightarrow \gamma_e \text{ max}$	y_x	+1	

TABLE I (CONTINUED)

γ_π Range	γ_e Range	y_1	y_2	y_3
	$+1 \rightarrow \gamma_{e_s}$		-1	+1
	$\gamma_{e_s} \rightarrow \gamma_{e_r}$	-1	y_t	+1
$\gamma_\mu \geq \gamma_\pi$	$\gamma_{e_r} \rightarrow \gamma_{e_t}$	-1	+1	
	$\gamma_{e_t} \rightarrow \gamma_{e \text{ max}}$	y_x	+1	

$$\bar{p}_{e_t} = \frac{1}{2} \left[\frac{\frac{m_\mu^2}{m_\pi m_e}}{\frac{m_\pi}{m_\mu}} - \frac{\frac{m_\pi m_e}{2}}{\frac{m_\mu}{m_\pi}} \right] . \quad (83)$$

Define

$$f_e = \gamma_e - p_e . \quad (84)$$

For large values of γ_e this can be computed most accurately by a Taylor expansion

$$f_e = \frac{1}{2\gamma_e} \left\{ 1 + \frac{1}{4} \gamma_e^{-2} [1 + \frac{1}{2} \gamma_e^{-2} (1 + \frac{5}{8} \gamma_e^{-2} \left\{ 1 + \frac{7}{10} \gamma_e^{-2} [1 + \frac{3}{4} \gamma_e^{-2} (1 + \frac{11}{14} \gamma_e^{-2} \left\{ 1 + \frac{13}{16} \gamma_e^{-2} \right\})] \right\})] \right\}. \quad (85)$$

A similar expression is useful for f_π . Because strong cancellation occurs in $\gamma_{e \min}$, γ_{e_s} , and γ_{e_t} for large γ_π values, it is desirable to rewrite these as

$$\gamma_{e \min} = f_\pi \bar{v} + \frac{m_e}{m_\pi} \gamma_\pi, \quad \gamma_\pi \geq \bar{w} \quad (79b)$$

$$\gamma_{e_s} = f_\pi \bar{p}_{e_t} + \frac{\frac{m_\pi}{m_e}}{\frac{m_\mu}{2}} \gamma_\pi \quad (80b)$$

$$\gamma_{e_t} = f_\pi \bar{v} + \frac{m_e}{m_\pi} \gamma_\pi, \quad \gamma_\pi \leq \bar{w}. \quad (75b)$$

The cancellation becomes quite severe in R_i and S_i also as γ_π increases, especially for the larger γ_e values. It is found helpful to use

$$y_x = 1 - r_x \quad (86)$$

$$y_t = 1 - r_t \quad (87)$$

where

$$r_x = \frac{\bar{w} - g}{p_{\pi} p_e} \quad (88)$$

$$r_t = \frac{\bar{\gamma}_{et} - g}{p_{\pi} p_e} \quad (89)$$

and

$$g = \gamma_{\pi} \gamma_e - p_{\pi} p_e = f_{\pi} \gamma_e + f_e \gamma_{\pi} - f_{\pi} f_e . \quad (90)$$

For the case $y_3 = 1$, $y_2 = y_t$, the R_i take the form

$$R_1 = r_t$$

$$R_2 = r_t (2 - r_t) \quad (91)$$

$$R_3 = r_t (3 - 3r_t + r_t^2) .$$

For $y_2 = y_x$ instead of $y_2 = y_t$, r_x merely replaces r_t . For the S_i a factor of $1/2$ appears in each R_i expression. For the case $y_2 = y_t$, $y_1 = y_x$, the S_i are instead

$$S_1 = \frac{\bar{w} - \bar{\gamma}_{et}}{2 p_{\pi} p_e}$$

$$S_2 = S_1 [2 - (r_x + r_t)] \quad (92)$$

$$S_3 = S_1 [3 - 3(r_x + r_t) + r_t^2 + r_x^2 + r_x r_t] .$$

Formula Checks

One can again use normalization, this time in the π LS, as a check on the final formulas and limits. For the highest energy case, $\gamma_\pi \geq \bar{w}$, this has been done analytically. The detail here is even more immense and complicated than in the π CMS. Consequently this would appear to constitute a rather good check on the numerous expressions and limits involved.

A numerical check on the normalization was incorporated into the computer program for calculating $N_{\pi\mu e}$. This will be discussed in a later section.

It can be shown analytically that $N_{\pi\mu e}$ vanishes for all four cases in Table I at both $\gamma_e \text{ max}$ and $\gamma_e \text{ min}$. This is a natural consequence of the fact that the muon distribution in the π LS from pion decay falls to zero in a step function at the upper and lower muon energy limits.

It is also possible to prove, after considerable manipulation, that the $N_{\pi\mu e}$ expression reduces, as p_π goes to zero, to the correct $N_{\pi\mu e}$ expression in the π CMS.

CHAPTER IV

COMPUTATIONS

Extensive use was made of the IBM 7094 computers at Grumman Aircraft to obtain numerical results. Eight separate programs of varying size, several of which are discussed below, were written and used by the authors in the course of the work.

Electron Distribution Function

The first and largest program computes the electron distribution function $N_{\pi\mu e}$ for the desired pion energies entered as machine input. For each γ_π , $N_{\pi\mu e}$ is found for a large number of electron energies according to a systematic pattern. It appeared from earlier considerations that a logarithmic γ_e scale would be advantageous for present uses, so the pattern of γ_e values to be used was chosen on this basis. In addition, a provision is incorporated whereby the rate of change of $N_{\pi\mu e}$ between each two adjacent points of the pattern is ascertained and, if the rate exceeds a pre-selected input value, $N_{\pi\mu e}$ is

calculated at the median γ_e point.

Because hand calculations had indicated possible cancellation problems, double-precision is employed in the instructions leading to $N_{\pi\mu e}$.

After the electron distribution function is calculated for the complete group of γ_e values, the normalization is computed to check how closely it approximates unity. This is accomplished by numerical integration of the $N_{\pi\mu e} - \gamma_e$ points using a parabolic approximation method that allows for the unequal γ_e increments.

The program generates for each γ_π , in addition to the extensive printed results, a deck of punched cards containing the $N_{\pi\mu e}$ values, with one card allotted to each γ_e and the corresponding $N_{\pi\mu e}$ value. The output decks were extremely useful in later programs to be discussed below, and are expected to be used also in the future applications of the electron distribution from pion decay.

Calculations on the 7094 computer were performed for twenty-six γ_π values corresponding roughly, in pion kinetic energy, to 3, 10, 20, 40, 60, 80, 100, 200, 400, 600, and 800 mev, and 1, 2, 4, 5, 6, 8, 10, 15, 20, 30, 40, 60, 80, 100, and 110 bev. This range embraces γ_π values in all four of the regions of Table I. According to the Landau hydrodynamical model (Milford et al. [1964]), 100 mev

pions would be produced in proton-proton collisions having a collision energy of the order of 10 bev. This corresponds to the energy region in which cosmic ray protons are most abundant (1 - 10 bev).

Experimental results (Bardon et al. [1959], Plano [1960], Ali-Zade et al. [1961]) confirm the theoretical prediction (Lee and Yang [1957b]) that the value of ξ in Eq. (1) is quite close to unity; consequently we have adopted $\xi = 1$ in all our computations.

A third, very convenient form of output that is incorporated into the program is a machine-generated graph of the results. Basic Calcomp (plotting) routines available were utilized to write a routine which creates a variable-length logarithmic scale for γ_e . The reader should take care to observe that the ordinate $N_{\pi\mu e}$ will be plotted to one of three possible scales, and with a variable power-of-ten scale factor, computed for the particular γ_π . The program selects the $N_{\pi\mu e}$ scale which permits optimum use of the ordinate.

The values of the distribution function are plotted in Graphs 1 to 26 and listed in Tables II to XIV. It will be seen that a large number of γ_e values are used for each pion energy. This is done explicitly (1) to obtain as smooth a curve as possible, since it is generated by

vectors drawn between adjacent points, and (2) to secure a reasonably accurate numerical check on the normalization.

Quite clearly, except for a few regions where rapid changes occur, the curves are very smooth.

The plotting routine in the $N_{\pi\mu e}$ program was modified somewhat and then incorporated into a program which provides for up to ten curves to be drawn on the same graph. The punch output of the $N_{\pi\mu e}$ program serves as input for the composite graphing routine. Graphs 27 to 30 were generated in this way to allow easy comparison of the variation in the electron energy spectra with pion energy.

A program was also written to tabulate the values of the electron distribution, using the punch output of the $N_{\pi\mu e}$ program as input. Tables II to XIV were prepared in this manner.

Normalization

The numerical checks on the normalization from the $N_{\pi\mu e}$ program are quite good. Of the 26 values of γ_e , only one had a normalization constant that differed by more than 1% from unity (1.4%), and in 20 cases the disparity was less than 0.5%.

It was desired to see if the inclusion of additional γ_e values would have any significant effect upon

the normalization, particularly the higher γ_e values, which provide the dominant contribution to the normalization, and γ_e values in regions where $N_{\pi\mu e}$ undergoes rapid change. The $N_{\pi\mu e}$ program has the useful option that the distribution function can also be computed for individual pre-selected γ_e values, instead of the logarithmic pattern. A simple change of input data accomplishes this.

Additional $N_{\pi\mu e}$ values were calculated for four different pion energies (one in each γ_π region): 11 for $\gamma_\pi = 1.02$, 8 for $\gamma_\pi = 1.07$, 6 for $\gamma_\pi = 100$, and 4 for $\gamma_\pi = 800$. The resulting output cards were inserted into the output deck from the initial run, and the new deck then served as the input to a program for recalculating the normalization. This latter program is similar in form to the previous normalization routine.

The results are impressive. The difference in the normalization from unity decreases in all four cases by factors ranging from 6.6 to 25. The new normalization difference is less than 0.025% in three of the cases, and less than 0.08% in the fourth. It is felt that this constitutes a good check on the equations derived and used.

Computation Accuracy

As γ_π increases the calculational accuracy in

N^1 and N^{2a} deteriorates, particularly for the larger γ_e values. In the region of 100 bev pion energy, the cancellation of the $b_i R_i$ and $b_i S_i$ is very severe, in spite of the recast equations (91) and (92). It is possible to expand the R_i , and rearrange the sum $\sum b_i R_i$ in another form which seems to be satisfactory in this pion energy range. This formula is expected to extend the computations to higher γ_π .

We have adopted the mass values of Snow and Shapiro (1961): $m_\pi = 139.59$ mev, $m_\mu = 105.66$ mev, and $m_e = 0.51098$ mev. In view of the cancellation problem, it was decided to perform a series of calculations with values of the particle masses changed by at least the amount of the estimated experimental error in order to see the effect upon $N_{\pi\mu e}$. For the increased pion mass, 139.64 mev was used. For the muon, the extremes 105.67 and 105.63 mev were adopted, and for the electron, 0.51100 and 0.51097 mev. If an increased mass is designated by \uparrow and a decreased mass by \downarrow , then the combinations (m_π, m_μ, m_e) that were tested may be signified by $(\uparrow\uparrow\uparrow)$, $(\uparrow\uparrow\downarrow)$, $(\uparrow\downarrow\downarrow)$, and $(\downarrow\downarrow\uparrow)$. Computations were carried out for γ_π values of 1.02, 40, 100, 720, and 800 (at least one in each pion energy region). The results for the electron distribution

function were not substantially different from before; it is estimated that $N_{\pi\mu e}$ is consistent to about three digits at $\gamma_\pi = 800$.

Check Calculations

To verify the $N_{\pi\mu e}$ program results, extensive calculations were performed on a desk calculator. Check runs were made for $\gamma_\pi = 1.02, 1.07, 100$, and 200 (one for each γ_π region); for each of these cases $N_{\pi\mu e}$ was calculated at one γ_e in each electron energy range.

Before the present mathematical formulation of the problem, which covers all γ_π values, was attempted, another approach was used whereby one transforms directly from the μ CMS to the π LS. The derivations involve an assumption which is expected to be valid only for small pion energies. The treatment is not very much different in complication from that reported here. A 7094 program, checked out by even more extensive hand calculations than here, was written and run.

The results of the low p_π approximation were checked for $\gamma_\pi = 1.07$ against the present more general results. The difference in $N_{\pi\mu e}$ was found to be never greater than 20%, and was actually less than 5% for 14 of the 22 values of γ_e .

Effect of μ CMS Anisotropy

It has been assumed in previous approximate treatments of the $\pi\mu e$ process that the electrons from muon decay are emitted isotropically in the μ CMS (Hayakawa and Okuda [1962], Jones [1963], and Ginzburg and Syrovatskii [1964]). The present treatment is based on the known anisotropic distribution in the μ CMS. Since neither numerical values nor closed-form expressions are provided for $N_{\pi\mu e}$ in the earlier papers, it is difficult to make a direct comparison with the present results.

It is possible, however, to assess the effect of the anisotropy within the framework of our own treatment. The form of our derived expressions permits the symmetric distribution to be treated as a special limiting case of the asymmetric one by setting ξ , the asymmetry parameter, equal to zero. Computations were performed with $\xi = 0$ for twelve γ_π values between 3 mev and 110 bev. The values of the distribution function are listed in Tables XV to XX.

An additional plotting routine was prepared to allow comparison of spectra on a linear scale. Graphs 31 through 42 show the variation in $N_{\pi\mu e}$ resulting from μ CMS anisotropy. Ratios of the asymmetric to symmetric distributions are given in Graph 43.

TABLE II
ELECTRON DISTRIBUTION FUNCTION (PER MEV)
($\xi = 1$)

<u>GAMMAE</u> ($= \gamma_e$)	<u>GAMMAPI</u> ($= \gamma_{\pi}$)	
1.0200E 00	1.0200E 00	1.0700E 00
1.0000E 00	0.	0.
0.2000E 01	0.351E-04	0.368E-04
0.3000E 01	0.856E-04	0.897E-04
0.4000E 01	0.155E-03	0.163E-03
0.5000E 01	0.244E-03	0.256E-03
0.6000E 01	0.352E-03	0.369E-03
0.7000E 01	0.479E-03	0.501E-03
0.8000E 01	0.624E-03	0.652E-03
0.9000E 01	0.787E-03	0.822E-03
1.0000E 01	0.967E-03	0.101E-02
0.1500E 02	0.213E-02	0.221E-02
0.2000E 02	0.368E-02	0.382E-02
0.2500E 02	0.559E-02	0.580E-02
0.3000E 02	0.782E-02	0.808E-02
0.3500E 02	0.103E-01	0.106E-01

TABLE II (CONTINUED)

ELECTRON DISTRIBUTION FUNCTION (PER MEV)
 $(\xi = 1)$

GAMMAE	GAMMAPI	GAMMAPI
1.0200E 00		1.0700E 00
0.4000E 02	0.131E-01	0.134E-01
0.4500E 02	0.160E-01	0.164E-01
0.5000E 02	0.191E-01	0.195E-01
0.5500E 02	0.224E-01	0.227E-01
0.6000E 02	0.257E-01	0.250E-01
0.6500E 02	0.290E-01	
0.7000E 02	0.311E-01	0.264E-01
0.8000E 02	0.306E-01	0.248E-01
0.8600E 02	0.279E-01	
0.9000E 02	0.254E-01	0.214E-01
0.9500E 02	0.216E-01	
1.0000E 02	0.175E-01	0.174E-01
0.1050E 03	0.138E-01	
0.1070E 03		0.144E-01
0.1130E 03	0.898E-02	

TABLE II (CONTINUED)

ELECTRON DISTRIBUTION FUNCTION (PER MEV)
($\xi = 1$)

GAMMAE	GAMMAPI
	1.0200E 00
0.1150E 03	0.109E-01
0.1170E 03	0.705E-02
0.1200E 03	0.581E-02
0.1250E 03	0.410E-02
0.1290E 03	0.300E-02
0.1340E 03	0.194E-02
0.1370E 03	0.145E-02
0.1390E 03	0.117E-02
0.1420E 03	0.826E-03
0.1460E 03	0.483E-03
0.1500E 03	0.253E-03
0.1668E 03	0.
0.1700E 03	0.380E-03
0.1800E 03	0.100E-03
0.1981E 03	0.

TABLE III

ELECTRON DISTRIBUTION FUNCTION (PER MEV)
 $(\xi = 1)$

GAMMAE	GAMMAPI
	1.1500E 00 1.3000E 00
1.0000E 00	0.
0.2000E 01	0.395E-04 0.446E-04
0.3000E 01	0.962E-04 0.108E-03
0.4000E 01	0.175E-03 0.196E-03
0.5000E 01	0.274E-03 0.308E-03
0.6000E 01	0.395E-03 0.443E-03
0.7000E 01	0.536E-03 0.601E-03
0.8000E 01	0.698E-03 0.781E-03
0.9000E 01	0.879E-03 0.983E-03
1.0000E 01	0.108E-02 0.121E-02
0.1500E 02	0.236E-02 0.261E-02
0.2000E 02	0.405E-02 0.446E-02
0.2500E 02	0.668E-02
0.3000E 02	0.849E-02 0.920E-02
0.3500E 02	0.111E-01 0.119E-01
0.4000E 02	0.140E-01 0.146E-01
0.4500E 02	0.170E-01
0.5000E 02	0.196E-01 0.169E-01

TABLE III(CONTINUED)

ELECTRON DISTRIBUTION FUNCTION (PER MEV)

(ξ = 1)

GAMMAE	GAMMAPI
	1.1500E 00
	1.3000E 00
<u>0.6000E 02</u>	<u>0.218E-01</u>
<u>0.7000E 02</u>	<u>0.214E-01</u>
<u>0.8000E 02</u>	<u>0.198E-01</u>
<u>0.9000E 02</u>	<u>0.179E-01</u>
<u>1.0000E 02</u>	<u>0.158E-01</u>
<u>0.1250E 03</u>	<u>0.101E-01</u>
<u>0.1500E 03</u>	<u>0.453E-02</u>
<u>0.1650E 03</u>	<u>0.245E-02</u>
<u>0.1750E 03</u>	<u>0.425E-02</u>
<u>0.1830E 03</u>	<u>0.973E-03</u>
<u>0.2000E 03</u>	<u>0.287E-03</u>
<u>0.2160E 03</u>	<u>0.438E-04</u>
<u>0.2190E 03</u>	<u>0.955E-03</u>
<u>0.2346E 03</u>	<u>0.</u>
<u>0.2480E 03</u>	<u>0.197E-03</u>
<u>0.2680E 03</u>	<u>0.296E-04</u>
<u>0.2910E 03</u>	<u>0.</u>

TABLE IV
ELECTRON DISTRIBUTION FUNCTION (PER MEV)
($\xi = 1$)

GAMMAE	1.4500E 00	1.6000E 00
1.0000E 00	0.	0.
0.2000E 01	0.496E-04	0.546E-04
0.3000E 01	0.120E-03	0.133E-03
0.4000E 01	0.218E-03	0.240E-03
0.5000E 01	0.342E-03	0.375E-03
0.6000E 01	0.491E-03	0.538E-03
0.7000E 01	0.665E-03	0.728E-03
0.8000E 01	0.863E-03	0.943E-03
0.9000E 01	0.108E-02	0.118E-02
1.0000E 01	0.133E-02	0.145E-02
0.1500E 02	0.286E-02	0.310E-02
0.2000E 02	0.485E-02	0.521E-02
0.2500E 02	0.720E-02	0.768E-02
0.3000E 02	0.983E-02	0.102E-01
0.3500E 02	0.122E-01	

TABLE IV (CONTINUED)
 ELECTRON DISTRIBUTION FUNCTION (PER MEV)
 $(\xi = 1)$

GAMMAE	GAMMAPI
	1.4500E 00
0.4000E 02	0.136E-01
0.5000E 02	0.142E-01
0.6000E 02	0.138E-01
0.7000E 02	0.134E-01
0.8000E 02	0.129E-01
0.9000E 02	0.124E-01
1.0000E 02	0.118E-01
0.1250E 03	0.101E-01
0.1500E 03	0.818E-02
0.1750E 03	0.606E-02
0.2000E 03	0.380E-02
0.2500E 03	0.965E-03
0.3000E 03	0.857E-04
0.3415E 03	0.
0.3891E 03	0.

TABLE V
ELECTRON DISTRIBUTION FUNCTION (PER MEV)
($\xi = 1$)

GAMMAE	GAMMAPI	
	1.7000E 00	2.4000E 00
1.0000E 00	0.	0.
0.2000E 01	0.580E-04	0.811E-04
0.3000E 01	0.141E-03	0.195E-03
0.4000E 01	0.254E-03	0.351E-03
0.5000E 01	0.397E-03	0.546E-03
0.6000E 01	0.569E-03	0.779E-03
0.7000E 01	0.769E-03	0.105E-02
0.8000E 01	0.996E-03	0.135E-02
0.9000E 01	0.125E-02	0.168E-02
1.0000E 01	0.153E-02	0.204E-02
0.1250E 02		0.305E-02
0.1500E 02	0.325E-02	0.420E-02
0.1750E 02		0.543E-02
0.2000E 02	0.544E-02	0.636E-02
0.2500E 02	0.797E-02	
0.3000E 02	0.100E-01	0.722E-02
0.4000E 02	0.112E-01	0.718E-02
0.5000E 02	0.111E-01	0.714E-02
0.6000E 02	0.109E-01	0.708E-02
0.7000E 02	0.107E-01	0.701E-02
0.8000E 02	0.104E-01	0.694E-02
0.9000E 02	0.101E-01	0.685E-02

TABLE V (CONTINUED)

ELECTRON DISTRIBUTION FUNCTION (PER MEV)
($\xi = 1$)

GAMMAPI		
GAMMAE	1.7000E 00	2.4000E 00
1.0000E 02	0.981E-02	0.676E-02
0.1500E 03	0.788E-02	0.617E-02
0.2000E 03	0.545E-02	0.539E-02
0.2500E 03	0.269E-02	0.445E-02
0.2940E 03	0.105E-02	
0.3000E 03	0.900E-03	0.339E-02
0.3040E 03	0.810E-03	
0.3150E 03	0.595E-03	
0.3250E 03	0.437E-03	
0.3360E 03	0.299E-03	
0.3460E 03	0.203E-03	
0.3500E 03		0.222E-02
0.3560E 03	0.130E-03	
0.3670E 03	0.734E-04	
0.3780E 03	0.362E-04	
0.4000E 03	0.385E-05	0.118E-02
0.4200E 03	0.	
0.4380E 03		0.661E-03
0.5000E 03		0.192E-03
0.5250E 03		0.974E-04
0.6000E 03		0.158E-05
0.6258E 03		0.

TABLE VI

ELECTRON DISTRIBUTION FUNCTION (PER MEV)
 $(\xi = 1)$

GAMMAE	GAMMAPI	GAMMAPI
1.0000E 00	3.9000E 00	5.3000E 00
1.0000E 00	0.	0.
0.2000E 01	0.129E-03	0.172E-03
0.3000E 01	0.308E-03	0.406E-03
0.4000E 01	0.547E-03	0.713E-03
0.5000E 01	0.840E-03	0.108E-02
0.6000E 01	0.118E-02	0.150E-02
0.7000E 01	0.157E-02	0.197E-02
0.8000E 01	0.199E-02	0.243E-02
0.9000E 01	0.245E-02	0.274E-02
1.0000E 01	0.293E-02	0.292E-02
0.1250E 02	0.383E-02	
0.1500E 02	0.415E-02	0.305E-02
0.2000E 02	0.420E-02	0.305E-02
0.3000E 02	0.420E-02	0.304E-02
0.4000E 02	0.419E-02	0.304E-02
0.5000E 02	0.418E-02	0.304E-02
0.6000E 02	0.417E-02	0.303E-02
0.7000E 02	0.415E-02	0.303E-02

TABLE VI (CONTINUED)

ELECTRON DISTRIBUTION FUNCTION (PER MEV)

(ξ = 1)

GAMMAE	3.9000E 00	5.3000E 00
0.8000E 02	0.414E-02	0.302E-02
0.9000E 02	0.412E-02	0.301E-02
1.0000E 02	0.410E-02	0.300E-02
0.1500E 03	0.397E-02	0.295E-02
0.2000E 03	0.379E-02	0.288E-02
0.3000E 03	0.332E-02	0.269E-02
0.4000E 03	0.270E-02	0.243E-02
0.5000E 03	0.198E-02	0.212E-02
0.6000E 03	0.117E-02	0.177E-02
0.7000E 03	0.524E-03	0.137E-02
0.8000E 03	0.182E-03	0.943E-03
0.9000E 03	0.375E-04	0.548E-03
1.0000E 03	0.122E-05	0.286E-03
0.1048E 04	0.	
0.1120E 04		0.105E-03
0.1220E 04		0.327E-04
0.1320E 04		0.489E-05
0.1435E 04		0.

TABLE VII
ELECTRON DISTRIBUTION FUNCTION (PER MEV)
($\xi = 1$)

GAMMAE	6.7000E 00	8.2000E 00
1.0000E 00	0.	0.
0.2000E 01	0.214E-03	0.257E-03
0.3000E 01	0.499E-03	0.590E-03
0.4000E 01	0.864E-03	0.101E-02
0.5000E 01	0.129E-02	0.148E-02
0.6000E 01	0.177E-02	0.179E-02
0.7000E 01	0.213E-02	0.192E-02
0.8000E 01	0.231E-02	0.195E-02
0.9000E 01	0.238E-02	0.195E-02
1.0000E 01	0.239E-02	0.195E-02
0.1500E 02	0.239E-02	0.195E-02
0.2000E 02	0.239E-02	0.195E-02
0.3000E 02	0.239E-02	0.195E-02
0.4000E 02	0.239E-02	0.195E-02
0.5000E 02	0.239E-02	0.195E-02
0.6000E 02	0.239E-02	0.194E-02
0.7000E 02	0.238E-02	0.194E-02
0.8000E 02	0.238E-02	0.194E-02

TABLE VII (CONTINUED)
 ELECTRON DISTRIBUTION FUNCTION (PER MEV)
 $(\xi = 1)$

GAMMAE	6.7000E 00	8.2000E 00
0.9000E 02	0.238E-02	0.194E-02
1.0000E 02	0.237E-02	0.194E-02
0.1500E 03	0.235E-02	0.192E-02
0.2000E 03	0.231E-02	0.190E-02
0.3000E 03	0.222E-02	0.185E-02
0.4000E 03	0.209E-02	0.178E-02
0.5000E 03	0.193E-02	0.169E-02
0.6000E 03	0.174E-02	0.158E-02
0.7000E 03	0.153E-02	0.146E-02
0.8000E 03	0.129E-02	0.133E-02
0.9000E 03	0.105E-02	0.118E-02
1.0000E 03	0.781E-03	0.102E-02
0.1250E 04	0.249E-03	0.593E-03
0.1500E 04	0.419E-04	0.234E-03
0.1820E 04	0.	
0.2000E 04		0.687E-05
0.2232E 04		0.

TABLE VIII
ELECTRON DISTRIBUTION FUNCTION (PER MEV)
($\xi = 1$)

GAMMAE	1.5000E 01	3.0000E 01
1.0000E 00	0.	0.
0.1500E 01	0.220E-03	0.374E-03
0.2000E 01	0.426E-03	0.514E-03
0.2500E 01	0.661E-03	
0.3000E 01	0.887E-03	0.527E-03
0.4000E 01	0.105E-02	0.528E-03
0.5000E 01	0.106E-02	0.528E-03
0.6000E 01	0.106E-02	0.528E-03
0.7000E 01	0.106E-02	0.528E-03
0.8000E 01	0.106E-02	0.529E-03
0.9000E 01	0.106E-02	0.529E-03
1.0000E 01	0.106E-02	0.529E-03
0.1500E 02	0.106E-02	0.529E-03
0.2000E 02	0.106E-02	0.529E-03
0.3000E 02	0.106E-02	0.529E-03
0.4000E 02	0.106E-02	0.529E-03
0.5000E 02	0.106E-02	0.529E-03
0.6000E 02	0.106E-02	0.529E-03
0.7000E 02	0.106E-02	0.529E-03
0.8000E 02	0.106E-02	0.529E-03
0.9000E 02	0.106E-02	0.529E-03
1.0000E 02	0.106E-02	0.529E-03

TABLE VIII (CONTINUED)
 ELECTRON DISTRIBUTION FUNCTION (PER MEV)
 $(\xi = 1)$

GAMMAE	1.5000E 01	3.0000E 01
0.1500E 03	0.106E-02	0.528E-03
0.2000E 03	0.105E-02	0.528E-03
0.3000E 03	0.104E-02	0.527E-03
0.4000E 03	0.103E-02	0.525E-03
0.5000E 03	0.102E-02	0.523E-03
0.6000E 03	0.997E-03	0.521E-03
0.7000E 03	0.975E-03	0.518E-03
0.8000E 03	0.950E-03	0.515E-03
0.9000E 03	0.923E-03	0.511E-03
1.0000E 03	0.893E-03	0.507E-03
0.1500E 04	0.708E-03	0.481E-03
0.2000E 04	0.475E-03	0.446E-03
0.2500E 04	0.219E-03	
0.3000E 04	0.671E-04	0.354E-03
0.4000E 04	0.385E-07	0.237E-03
0.4093E 04	0.	
0.5000E 04		0.110E-03
0.6000E 04		0.337E-04
0.7000E 04		0.521E-05
0.8000E 04		0.214E-07
0.8193E 04		0.

TABLE IX
ELECTRON DISTRIBUTION FUNCTION (PER MEV)
($\xi = 1$)

GAMMAE	4.0000E 01	4.5000E 01
1.0000E 00	0.	0.
0.1500E 01	0.366E-03	0.334E-03
0.2000E 01	0.390E-03	0.345E-03
0.3000E 01	0.394E-03	0.349E-03
0.4000E 01	0.395E-03	0.351E-03
0.5000E 01	0.396E-03	0.351E-03
0.6000E 01	0.396E-03	0.352E-03
0.7000E 01	0.396E-03	0.352E-03
0.8000E 01	0.396E-03	0.352E-03
0.9000E 01	0.396E-03	0.352E-03
1.0000E 01	0.396E-03	0.352E-03
0.1500E 02	0.396E-03	0.352E-03
0.2000E 02	0.397E-03	0.352E-03
0.3000E 02	0.397E-03	0.352E-03
0.4000E 02	0.397E-03	0.352E-03
0.5000E 02	0.397E-03	0.352E-03
0.6000E 02	0.397E-03	0.352E-03
0.7000E 02	0.397E-03	0.352E-03
0.8000E 02	0.397E-03	0.352E-03
0.9000E 02	0.396E-03	0.352E-03
1.0000E 02	0.396E-03	0.352E-03
0.1500E 03	0.396E-03	0.352E-03

TABLE IX (CONTINUED)
 ELECTRON DISTRIBUTION FUNCTION (PER MEV)
 $(\xi = 1)$

GAMMAE	GAMMAPI	GAMMAPI
4.0000E 01		4.5000E 01
0.2000E 03	0.396E-03	0.352E-03
0.3000E 03	0.396E-03	0.352E-03
0.4000E 03	0.395E-03	0.351E-03
0.5000E 03	0.394E-03	0.351E-03
0.6000E 03	0.393E-03	0.350E-03
0.7000E 03	0.392E-03	0.349E-03
0.8000E 03	0.390E-03	0.348E-03
0.9000E 03	0.389E-03	0.347E-03
1.0000E 03	0.387E-03	0.346E-03
0.1500E 04	0.376E-03	0.338E-03
0.2000E 04	0.361E-03	0.327E-03
0.3000E 04	0.319E-03	0.297E-03
0.4000E 04	0.265E-03	0.258E-03
0.5000E 04	0.201E-03	0.211E-03
0.6000E 04	0.130E-03	0.158E-03
0.7000E 04	0.635E-04	0.100E-03
0.8000E 04	0.253E-04	0.515E-04
0.9000E 04	0.699E-05	0.225E-04
1.0000E 04	0.755E-06	0.738E-05
0.1093E 05	0.	
0.1229E 05		0.

TABLE X
ELECTRON DISTRIBUTION FUNCTION (PER MEV)
($\xi = 1$)

GAMMAE	6.0000E 01	7.2000E 01	GAMMAPI
1.0000E 00	0.	0.	
0.1500E 01	0.244E-03	0.196E-03	
0.2000E 01	0.254E-03	0.208E-03	
0.3000E 01	0.260E-03	0.215E-03	
0.4000E 01	0.262E-03	0.217E-03	
0.5000E 01	0.263E-03	0.218E-03	
0.6000E 01	0.263E-03	0.219E-03	
0.7000E 01	0.264E-03	0.219E-03	
0.8000E 01	0.264E-03	0.220E-03	
0.9000E 01	0.264E-03	0.220E-03	
1.0000E 01	0.264E-03	0.220E-03	
0.1500E 02	0.264E-03	0.220E-03	
0.2000E 02	0.264E-03	0.220E-03	
0.3000E 02	0.264E-03	0.220E-03	
0.4000E 02	0.264E-03	0.220E-03	

TABLE X (CONTINUED)
 ELECTRON DISTRIBUTION FUNCTION (PER MEV)
 $(\xi = 1)$

GAMMAE	GAMMAPI
6.0000E 01	7.2000E 01
0.5000E 02	0.264E-03
0.6000E 02	0.264E-03
0.7000E 02	0.264E-03
0.8000E 02	0.264E-03
0.9000E 02	0.264E-03
1.0000E 02	0.264E-03
0.1500E 03	0.264E-03
0.2000E 03	0.264E-03
0.3000E 03	0.264E-03
0.4000E 03	0.264E-03
0.5000E 03	0.264E-03
0.6000E 03	0.263E-03
0.7000E 03	0.263E-03
0.8000E 03	0.263E-03
0.9000E 03	0.262E-03

TABLE X (CONTINUED)
 ELECTRON DISTRIBUTION FUNCTION (PER MEV)
 $(\xi = 1)$

GAMMAE	6.0000E 01	7.2000E 01
1.0000E 03	0.262E-03	0.219E-03
0.1500E 04	0.258E-03	0.217E-03
0.2000E 04	0.253E-03	0.214E-03
0.3000E 04	0.240E-03	0.206E-03
0.4000E 04	0.223E-03	0.196E-03
0.5000E 04	0.202E-03	0.183E-03
0.6000E 04	0.177E-03	0.168E-03
0.7000E 04	0.149E-03	0.151E-03
0.8000E 04	0.119E-03	0.132E-03
0.9000E 04	0.864E-04	0.112E-03
1.0000E 04	0.548E-04	0.901E-04
0.1250E 05		0.369E-04
0.1500E 05	0.505E-06	0.968E-05
0.1639E 05	0.	
0.1967E 05		0.

TABLE XI
ELECTRON DISTRIBUTION FUNCTION (PER MEV)
($\xi = 1$)

GAMMAE	GAMMAPI	
	10.0000E 01	1.4500E 02
1.0000E 00	0.	
0.1002E 01		0.
0.1020E 01	0.352E-04	
0.1040E 01	0.508E-04	
0.1200E 01	0.989E-04	
0.1500E 01	0.127E-03	
0.1501E 01		0.659E-04
0.2000E 01	0.142E-03	0.865E-04
0.3000E 01	0.152E-03	0.995E-04
0.4000E 01	0.155E-03	0.104E-03
0.5000E 01	0.156E-03	0.106E-03
0.6000E 01	0.157E-03	0.107E-03
0.7000E 01	0.157E-03	0.108E-03
0.8000E 01	0.158E-03	0.108E-03
0.9000E 01	0.158E-03	0.108E-03
1.0000E 01	0.158E-03	0.108E-03
0.1500E 02	0.158E-03	0.109E-03
0.2000E 02	0.158E-03	0.109E-03
0.3000E 02	0.159E-03	0.109E-03
0.4000E 02	0.159E-03	0.109E-03

TABLE XI (CONTINUED)
 ELECTRON DISTRIBUTION FUNCTION (PER MEV)
 $(\xi = 1)$

GAMMAE	10.0000E 01	1.4500E 02
0.5000E 02	0.159E-03	0.109E-03
0.6000E 02	0.159E-03	0.109E-03
0.7000E 02	0.159E-03	0.109E-03
0.8000E 02	0.159E-03	0.109E-03
0.9000E 02	0.159E-03	0.109E-03
1.0000E 02	0.159E-03	0.109E-03
0.1500E 03	0.159E-03	0.109E-03
0.2000E 03	0.159E-03	0.109E-03
0.3000E 03	0.159E-03	0.109E-03
0.4000E 03	0.158E-03	0.109E-03
0.5000E 03	0.158E-03	0.109E-03
0.6000E 03	0.158E-03	0.109E-03
0.7000E 03	0.158E-03	0.109E-03
0.8000E 03	0.158E-03	0.109E-03
0.9000E 03	0.158E-03	0.109E-03
1.0000E 03	0.158E-03	0.109E-03
0.1500E 04	0.157E-03	0.109E-03
0.2000E 04	0.156E-03	0.109E-03
0.3000E 04	0.153E-03	0.108E-03
0.4000E 04	0.149E-03	0.106E-03

TABLE XI (CONTINUED)
 ELECTRON DISTRIBUTION FUNCTION (PER MEV)
 $(\xi = 1)$

GAMMAE	GAMMAP I	
10.0000E 01	1.4500E 02	
0.5000E 04	0.144E-03	0.105E-03
0.6000E 04	0.138E-03	0.102E-03
0.7000E 04	0.131E-03	0.100E-03
0.8000E 04	0.124E-03	0.974E-04
0.9000E 04	0.115E-03	0.944E-04
1.0000E 04	0.106E-03	0.911E-04
0.1100E 05	0.962E-04	
0.1250E 05	0.805E-04	
0.1400E 05	0.636E-04	
0.1500E 05	0.519E-04	0.709E-04
0.1650E 05	0.346E-04	
0.1750E 05	0.254E-04	
0.1900E 05	0.151E-04	
0.2000E 05	0.101E-04	0.455E-04
0.2200E 05	0.379E-05	
0.2400E 05	0.899E-06	
0.2500E 05		0.190E-04
0.2732E 05	0.	
0.3000E 05		0.514E-05
0.3961E 05		0.

TABLE XII
ELECTRON DISTRIBUTION FUNCTION (PER MEV)
($\xi = 1$)

GAMMAE	GAMMAPT	GAMMAPR
2.0000E 02		2.9000E 02
0.1074E 01	0.	
0.1200E 01	0.254E-05	
0.1297E 01		0.
0.1537E 01	0.272E-04	
0.1649E 01		0.412E-05
0.2000E 01	0.495E-04	0.156E-04
0.2500E 01		0.292E-04
0.3000E 01	0.662E-04	0.367E-04
0.4000E 01	0.719E-04	0.443E-04
0.5000E 01	0.745E-04	0.480E-04
0.6000E 01	0.759E-04	0.500E-04
0.7000E 01	0.768E-04	0.512E-04
0.8000E 01	0.774E-04	0.520E-04
0.9000E 01	0.778E-04	0.525E-04
1.0000E 01	0.781E-04	0.529E-04
0.1500E 02	0.787E-04	0.539E-04
0.2000E 02	0.790E-04	0.542E-04
0.3000E 02	0.792E-04	0.545E-04
0.4000E 02	0.792E-04	0.546E-04
0.5000E 02	0.792E-04	0.546E-04
0.6000E 02	0.793E-04	0.546E-04
0.7000E 02	0.793E-04	0.546E-04

TABLE XII (CONTINUED)
 ELECTRON DISTRIBUTION FUNCTION (PER MEV)
 ($\xi = 1$)

GAMMAE	2.0000E 02	2.9000E 02
0.8000E 02	0.793E-04	0.547E-04
0.9000E 02	0.793E-04	0.547E-04
1.0000E 02	0.793E-04	0.547E-04
0.1500E 03	0.793E-04	0.547E-04
0.2000E 03	0.793E-04	0.547E-04
0.3000E 03	0.793E-04	0.547E-04
0.4000E 03	0.793E-04	0.547E-04
0.5000E 03	0.793E-04	0.547E-04
0.6000E 03	0.793E-04	0.547E-04
0.7000E 03	0.793E-04	0.547E-04
0.8000E 03	0.792E-04	0.547E-04
0.9000E 03	0.792E-04	0.547E-04
1.0000E 03	0.792E-04	0.547E-04
0.1500E 04	0.791E-04	0.546E-04
0.2000E 04	0.790E-04	0.546E-04
0.3000E 04	0.786E-04	0.545E-04
0.4000E 04	0.781E-04	0.543E-04
0.5000E 04	0.774E-04	0.541E-04
0.6000E 04	0.766E-04	0.538E-04
0.7000E 04	0.757E-04	0.535E-04
0.8000E 04	0.746E-04	0.531E-04

TABLE XII (CONTINUED)

ELECTRON DISTRIBUTION FUNCTION (PER MEV)

 $(\xi = 1)$

GAMMAPI		
GAMMAE	2.0000E 02	2.9000E 02
0.9000E 04	0.734E-04	0.527E-04
1.0000E 04	0.721E-04	0.523E-04
0.1500E 05	0.638E-04	0.494E-04
0.2000E 05	0.530E-04	0.455E-04
0.2500E 05	0.402E-04	
0.3000E 05	0.259E-04	0.354E-04
0.3500E 05	0.127E-04	
0.3824E 05	0.720E-05	
0.4000E 05	0.507E-05	0.228E-04
0.4098E 05	0.409E-05	
0.4234E 05	0.296E-05	
0.4371E 05	0.206E-05	
0.4507E 05	0.137E-05	
0.4644E 05	0.854E-06	
0.4781E 05	0.491E-06	
0.4917E 05	0.249E-06	
0.5000E 05	0.152E-06	0.951E-05
0.5464E 05	0.	
0.6000E 05		0.257E-05
0.7000E 05		0.273E-06
0.7922E 05		0.

TABLE XIII
ELECTRON DISTRIBUTION FUNCTION (PER MEV)
($\xi = 1$)

GAMMAE	4.3000E 02	5.7000E 02
0.1733E 01	0.	
0.2000E 01	0.452E-06	
0.2206E 01		0.
0.2500E 01	0.510E-05	
0.3000E 01	0.127E-04	0.213E-05
0.3500E 01	0.186E-04	0.583E-05
0.4000E 01	0.226E-04	0.102E-04
0.5000E 01	0.274E-04	0.160E-04
0.6000E 01	0.302E-04	0.193E-04
0.7000E 01	0.319E-04	0.214E-04
0.8000E 01	0.330E-04	0.228E-04
0.9000E 01	0.338E-04	0.238E-04
1.0000E 01	0.344E-04	0.246E-04
0.1500E 02	0.357E-04	0.263E-04
0.2000E 02	0.362E-04	0.270E-04
0.3000E 02	0.366E-04	0.274E-04
0.4000E 02	0.367E-04	0.276E-04
0.5000E 02	0.368E-04	0.277E-04
0.6000E 02	0.368E-04	0.277E-04

TABLE XIII(continued)
 ELECTRON DISTRIBUTION FUNCTION (PER MEV)
 $(\xi = 1)$

GAMMAE	4.3000E 02	5.7000E 02
0.7000E 02	0.368E-04	0.277E-04
0.8000E 02	0.368E-04	0.278E-04
0.9000E 02	0.368E-04	0.278E-04
1.0000E 02	0.369E-04	0.278E-04
0.1500E 03	0.369E-04	0.278E-04
0.2000E 03	0.369E-04	0.278E-04
0.3000E 03	0.369E-04	0.278E-04
0.4000E 03	0.369E-04	0.278E-04
0.5000E 03	0.369E-04	0.278E-04
0.6000E 03	0.369E-04	0.278E-04
0.7000E 03	0.369E-04	0.278E-04
0.8000E 03	0.369E-04	0.278E-04
0.9000E 03	0.369E-04	0.278E-04
1.0000E 03	0.369E-04	0.278E-04
0.1500E 04	0.369E-04	0.278E-04
0.2000E 04	0.368E-04	0.278E-04
0.3000E 04	0.368E-04	0.278E-04
0.4000E 04	0.368E-04	0.278E-04
0.5000E 04	0.367E-04	0.277E-04

TABLE XIII (CONTINUED)
 ELECTRON DISTRIBUTION FUNCTION (PER MEV)
 $(\xi = 1)$

GAMMAE	GAMMAPI
	4.3000E 02
	5.7000E 02
0.6000E 04	0.366E-04
0.7000E 04	0.365E-04
0.8000E 04	0.364E-04
0.9000E 04	0.363E-04
1.0000E 04	0.361E-04
0.1500E 05	0.352E-04
0.2000E 05	0.340E-04
0.3000E 05	0.306E-04
0.4000E 05	0.262E-04
0.5000E 05	0.209E-04
0.6000E 05	0.149E-04
0.7000E 05	0.857E-05
0.8000E 05	0.406E-05
0.9000E 05	0.155E-05
1.0000E 05	0.386E-06
0.1175E 06	0.
0.1500E 06	0.427E-08
0.1557E 06	0.

TABLE XIV
ELECTRON DISTRIBUTION FUNCTION (PER MEV)
($\xi = 1$)

GAMMAE	GAMMAPI	GAMMAPI
	7.2000E 02	8.0000E 02
0.2730E 01	0.	
0.3000E 01	0.604E-07	
0.3014E 01		0.
0.4000E 01	0.271E-05	0.110E-05
0.5000E 01	0.795E-05	0.476E-05
0.6000E 01	0.118E-04	0.877E-05
0.7000E 01	0.143E-04	0.114E-04
0.8000E 01	0.160E-04	0.132E-04
0.9000E 01	0.171E-04	0.145E-04
1.0000E 01	0.180E-04	0.154E-04
0.1500E 02	0.202E-04	0.178E-04
0.2000E 02	0.210E-04	0.186E-04
0.3000E 02	0.215E-04	0.193E-04
0.4000E 02	0.218E-04	0.195E-04
0.5000E 02	0.218E-04	0.196E-04
0.6000E 02	0.219E-04	0.197E-04
0.7000E 02	0.219E-04	0.197E-04
0.8000E 02	0.220E-04	0.197E-04
0.9000E 02	0.220E-04	0.198E-04
1.0000E 02	0.220E-04	0.198E-04

TABLE XIV(CONTINUED)
 ELECTRON DISTRIBUTION FUNCTION (PER MEV)
 $(\xi = 1)$

GAMMAE	GAMMAPI	GAMMAPI
7.2000E 02	8.0000E 02	
0.1500E 03	0.220E-04	0.198E-04
0.2000E 03	0.220E-04	0.198E-04
0.3000E 03	0.220E-04	0.198E-04
0.4000E 03	0.220E-04	0.198E-04
0.5000E 03	0.220E-04	0.198E-04
0.6000E 03	0.220E-04	0.198E-04
0.7000E 03	0.220E-04	0.198E-04
0.8000E 03	0.220E-04	0.198E-04
0.9000E 03	0.220E-04	0.198E-04
1.0000E 03	0.220E-04	0.198E-04
0.1500E 04	0.220E-04	0.198E-04
0.2000E 04	0.220E-04	0.198E-04
0.3000E 04	0.220E-04	0.198E-04
0.4000E 04	0.220E-04	0.198E-04
0.5000E 04	0.220E-04	0.198E-04
0.6000E 04	0.220E-04	0.198E-04
0.7000E 04	0.219E-04	0.198E-04
0.8000E 04	0.219E-04	0.197E-04
0.9000E 04	0.219E-04	0.197E-04

TABLE XIV(CONTINUED)
 ELECTRON DISTRIBUTION FUNCTION (PER MEV)
 $(\xi = 1)$

GAMMAE	7.2000E 02	8.0000E 02
1.0000E 04	0.219E-04	0.197E-04
0.1500E 05	0.217E-04	0.196E-04
0.2000E 05	0.214E-04	0.194E-04
0.3000E 05	0.206E-04	0.188E-04
0.4000E 05	0.196E-04	0.180E-04
0.5000E 05	0.183E-04	0.171E-04
0.6000E 05	0.168E-04	0.159E-04
0.7000E 05	0.151E-04	0.147E-04
0.8000E 05	0.132E-04	0.133E-04
0.9000E 05	0.112E-04	0.117E-04
1.0000E 05	0.901E-05	0.101E-04
0.1150E 06		0.740E-05
0.1250E 06	0.368E-05	0.554E-05
0.1350E 06		0.386E-05
0.1500E 06	0.972E-06	0.207E-05
0.1650E 06		0.966E-06
0.1800E 06		0.347E-06
0.1967E 06	0.	
0.2185E 06		0.

TABLE XV

ELECTRON DISTRIBUTION FUNCTION (PER MEV)
 $(\xi = 0)$

GAMMAE	GAMMAPI	GAMMAPI
1.0000E 00	1.0200E 00	1.0700E 00
1.0000E 00	0.	0.
0.2000E 01	0.385E-04	0.403E-04
0.3000E 01	0.935E-04	0.979E-04
0.4000E 01	0.169E-03	0.177E-03
0.5000E 01	0.266E-03	0.278E-03
0.6000E 01	0.383E-03	0.400E-03
0.7000E 01	0.519E-03	0.542E-03
0.8000E 01	0.674E-03	0.704E-03
0.9000E 01	0.849E-03	0.885E-03
1.0000E 01	0.104E-02	0.109E-02
0.1500E 02	0.226E-02	0.235E-02
0.2000E 02	0.386E-02	0.400E-02
0.3000E 02	0.797E-02	0.818E-02
0.4000E 02	0.129E-01	0.131E-01
0.5000E 02	0.182E-01	0.182E-01
0.6000E 02	0.233E-01	0.225E-01
0.7000E 02	0.271E-01	0.240E-01

TABLE XV (CONTINUED)

ELECTRON DISTRIBUTION FUNCTION (PER MEV)

(ξ = 0)

GAMMAE	GAMMAPI	GAMMAPI
	1.0200E 00	1.0700E 00
<u>0.8000E 02</u>	<u>0.272E-01</u>	<u>0.233E-01</u>
<u>0.9000E 02</u>	<u>0.242E-01</u>	<u>0.208E-01</u>
<u>1.0000E 02</u>	<u>0.190E-01</u>	<u>0.173E-01</u>
<u>0.1150E 03</u>		<u>0.119E-01</u>
<u>0.1170E 03</u>	<u>0.100E-01</u>	
<u>0.1200E 03</u>	<u>0.869E-02</u>	
<u>0.1250E 03</u>	<u>0.672E-02</u>	<u>0.871E-02</u>
<u>0.1290E 03</u>	<u>0.536E-02</u>	
<u>0.1340E 03</u>	<u>0.392E-02</u>	
<u>0.1370E 03</u>	<u>0.318E-02</u>	<u>0.571E-02</u>
<u>0.1420E 03</u>	<u>0.214E-02</u>	
<u>0.1460E 03</u>	<u>0.147E-02</u>	
<u>0.1500E 03</u>	<u>0.933E-03</u>	<u>0.331E-02</u>
<u>0.1668E 03</u>	<u>0.</u>	
<u>0.1700E 03</u>		<u>0.102E-02</u>
<u>0.1800E 03</u>		<u>0.405E-03</u>
<u>0.1981E 03</u>		<u>0.</u>

TABLE XVI

ELECTRON DISTRIBUTION FUNCTION (PER MEV)

 $(\xi = 0)$

GAMMAE	GAMMAPI	GAMMAPI
1.0000E 00	0.	0.
0.2000E 01	0.432E-04	0.487E-04
0.3000E 01	0.105E-03	0.118E-03
0.4000E 01	0.190E-03	0.213E-03
0.5000E 01	0.298E-03	0.334E-03
0.6000E 01	0.428E-03	0.479E-03
0.7000E 01	0.579E-03	0.647E-03
0.8000E 01	0.751E-03	0.837E-03
0.9000E 01	0.943E-03	0.105E-02
1.0000E 01	0.116E-02	0.128E-02
0.1500E 02	0.249E-02	0.273E-02
0.2000E 02	0.421E-02	0.457E-02
0.2500E 02		0.669E-02
0.3000E 02	0.849E-02	0.898E-02
0.3500E 02		0.113E-01
0.4000E 02	0.134E-01	0.135E-01
0.5000E 02	0.179E-01	0.159E-01

TABLE XVI (CONTINUED)

ELECTRON DISTRIBUTION FUNCTION (PER MEV)
 $(\xi = 0)$

GAMMAE	GAMMAP1
	1.1500E 00
0.6000E 02	0.202E-01
0.7000E 02	0.204E-01
0.8000E 02	0.191E-01
0.9000E 02	0.173E-01
1.0000E 02	0.153E-01
0.1250E 03	0.103E-01
0.1500E 03	0.553E-02
0.1650E 03	0.350E-02
0.1750E 03	0.480E-02
0.1830E 03	0.178E-02
0.2000E 03	0.746E-03
0.2160E 03	0.202E-03
0.2190E 03	0.158E-02
0.2346E 03	0.
0.2480E 03	0.511E-03
0.2680E 03	0.137E-03
0.2910E 03	0.

TABLE XVII
ELECTRON DISTRIBUTION FUNCTION (PER MEV)
($\xi = 0$)

GAMMAPI		
GAMMAE	1.7000E 00	2.4000E 00
1.0000E 00	0.	0.
0.2000E 01	0.632E-04	0.881E-04
0.3000E 01	0.153E-03	0.211E-03
0.4000E 01	0.274E-03	0.376E-03
0.5000E 01	0.427E-03	0.581E-03
0.6000E 01	0.610E-03	0.823E-03
0.7000E 01	0.820E-03	0.110E-02
0.8000E 01	0.106E-02	0.140E-02
0.9000E 01	0.132E-02	0.173E-02
1.0000E 01	0.160E-02	0.208E-02
0.1250E 02		0.304E-02
0.1500E 02	0.332E-02	0.407E-02
0.1750E 02		0.512E-02
0.2000E 02	0.537E-02	0.595E-02
0.2500E 02	0.756E-02	
0.3000E 02	0.936E-02	0.708E-02
0.4000E 02	0.109E-01	0.704E-02
0.5000E 02	0.108E-01	0.699E-02
0.6000E 02	0.106E-01	0.693E-02
0.7000E 02	0.104E-01	0.686E-02
0.8000E 02	0.101E-01	0.678E-02
0.9000E 02	0.984E-02	0.669E-02

TABLE XVII (CONTINUED)

ELECTRON DISTRIBUTION FUNCTION (PER MEV)

 $(\xi = 0)$

GAMMAE	GAMMAPI
	1.7000E 00
	2.4000E 00
1.0000E 02	0.952E-02
0.1500E 03	0.762E-02
0.2000E 03	0.536E-02
0.2500E 03	0.301E-02
0.2940E 03	0.148E-02
0.3000E 03	0.132E-02
0.3040E 03	0.123E-02
0.3150E 03	0.978E-03
0.3250E 03	0.782E-03
0.3360E 03	0.595E-03
0.3460E 03	0.451E-03
0.3500E 03	0.234E-02
0.3560E 03	0.329E-03
0.3670E 03	0.220E-03
0.3780E 03	0.135E-03
0.4000E 03	0.290E-04
0.44E-02	0.144E-02
0.4200E 03	0.
0.4380E 03	0.935E-03
0.5000E 03	0.379E-03
0.5250E 03	0.234E-03
0.6000E 03	0.136E-04
0.6258E 03	0.

TABLE XVIII
ELECTRON DISTRIBUTION FUNCTION (PER MEV)
($\xi = 0$)

GAMMAE	GAMMAPI
3.9000E 00	5.3000E 00
<u>1.0000E 00</u>	<u>0.</u>
<u>0.2000E 01</u>	<u>0.139E-03</u>
<u>0.3000E 01</u>	<u>0.328E-03</u>
<u>0.4000E 01</u>	<u>0.575E-03</u>
<u>0.5000E 01</u>	<u>0.871E-03</u>
<u>0.6000E 01</u>	<u>0.121E-02</u>
<u>0.7000E 01</u>	<u>0.158E-02</u>
<u>0.8000E 01</u>	<u>0.197E-02</u>
<u>0.9000E 01</u>	<u>0.237E-02</u>
<u>1.0000E 01</u>	<u>0.278E-02</u>
<u>0.1250E 02</u>	<u>0.359E-02</u>
<u>0.1500E 02</u>	<u>0.400E-02</u>
<u>0.2000E 02</u>	<u>0.413E-02</u>
<u>0.3000E 02</u>	<u>0.412E-02</u>
<u>0.4000E 02</u>	<u>0.411E-02</u>
<u>0.5000E 02</u>	<u>0.410E-02</u>
<u>0.6000E 02</u>	<u>0.409E-02</u>
<u>0.7000E 02</u>	<u>0.407E-02</u>

TABLE XVIII (CONTINUED)

ELECTRON DISTRIBUTION FUNCTION (PER MEV)

 $(\xi = 0)$

GAMMAE	GAMMAPI
	3.9000E 00
	5.3000E 00
<u>0.8000E 02</u>	<u>0.405E-02</u>
<u>0.9000E 02</u>	<u>0.404E-02</u>
<u>1.0000E 02</u>	<u>0.401E-02</u>
<u>0.1500E 03</u>	<u>0.388E-02</u>
<u>0.2000E 03</u>	<u>0.369E-02</u>
<u>0.3000E 03</u>	<u>0.321E-02</u>
<u>0.4000E 03</u>	<u>0.261E-02</u>
<u>0.5000E 03</u>	<u>0.195E-02</u>
<u>0.6000E 03</u>	<u>0.125E-02</u>
<u>0.7000E 03</u>	<u>0.683E-03</u>
<u>0.8000E 03</u>	<u>0.314E-03</u>
<u>0.9000E 03</u>	<u>0.102E-03</u>
<u>1.0000E 03</u>	<u>0.961E-05</u>
<u>0.1048E 04</u>	<u>0.</u>
<u>0.1120E 04</u>	<u>0.193E-03</u>
<u>0.1220E 04</u>	<u>0.838E-04</u>
<u>0.1320E 04</u>	<u>0.224E-04</u>
<u>0.1435E 04</u>	<u>0.</u>

TABLE XIX
ELECTRON DISTRIBUTION FUNCTION (PER MEV)
($\xi = 0$)

GAMMAPI		
GAMMAE	4.0000E 01	10.0000E 01
<u>1.0000E 00</u>	<u>0.</u>	<u>0.</u>
<u>0.1500E 01</u>	<u>0.346E-03</u>	<u>0.122E-03</u>
<u>0.2000E 01</u>	<u>0.382E-03</u>	<u>0.138E-03</u>
<u>0.3000E 01</u>	<u>0.386E-03</u>	<u>0.148E-03</u>
<u>0.4000E 01</u>	<u>0.388E-03</u>	<u>0.152E-03</u>
<u>0.5000E 01</u>	<u>0.388E-03</u>	<u>0.153E-03</u>
<u>0.6000E 01</u>	<u>0.389E-03</u>	<u>0.154E-03</u>
<u>0.7000E 01</u>	<u>0.389E-03</u>	<u>0.154E-03</u>
<u>0.8000E 01</u>	<u>0.389E-03</u>	<u>0.155E-03</u>
<u>0.9000E 01</u>	<u>0.389E-03</u>	<u>0.155E-03</u>
<u>1.0000E 01</u>	<u>0.389E-03</u>	<u>0.155E-03</u>
<u>0.1500E 02</u>	<u>0.389E-03</u>	<u>0.155E-03</u>
<u>0.2000E 02</u>	<u>0.389E-03</u>	<u>0.156E-03</u>
<u>0.3000E 02</u>	<u>0.389E-03</u>	<u>0.156E-03</u>
<u>0.4000E 02</u>	<u>0.389E-03</u>	<u>0.156E-03</u>
<u>0.5000E 02</u>	<u>0.389E-03</u>	<u>0.156E-03</u>
<u>0.6000E 02</u>	<u>0.389E-03</u>	<u>0.156E-03</u>

TABLE XIX(CONTINUED)

ELECTRON DISTRIBUTION FUNCTION (PER MEV)
 $(\xi = 0)$

GAMMAE	GAMMAPI
4.0000E 01	10.0000E 01
0.7000E 02	0.389E-03
0.8000E 02	0.389E-03
0.9000E 02	0.389E-03
1.0000E 02	0.389E-03
0.1500E 03	0.389E-03
0.2000E 03	0.389E-03
0.3000E 03	0.388E-03
0.4000E 03	0.388E-03
0.5000E 03	0.387E-03
0.6000E 03	0.386E-03
0.7000E 03	0.384E-03
0.8000E 03	0.383E-03
0.9000E 03	0.381E-03
1.0000E 03	0.379E-03
0.1500E 04	0.367E-03
0.2000E 04	0.351E-03
0.3000E 04	0.309E-03

TABLE XIX (CONTINUED)

ELECTRON DISTRIBUTION FUNCTION (PER MEV)

 $(\xi = 0)$

GAMMAE	GAMMAPI
4.0000E 01	10.0000E 01
<u>0.4000E 04</u>	<u>0.256E-03</u>
<u>0.5000E 04</u>	<u>0.197E-03</u>
<u>0.6000E 04</u>	<u>0.134E-03</u>
<u>0.7000E 04</u>	<u>0.777E-04</u>
<u>0.8000E 04</u>	<u>0.393E-04</u>
<u>0.9000E 04</u>	<u>0.155E-04</u>
<u>1.0000E 04</u>	<u>0.327E-05</u>
<u>0.1093E 05</u>	<u>0.</u>
<u>0.1250E 05</u>	<u>0.787E-04</u>
<u>0.1500E 05</u>	<u>0.538E-04</u>
<u>0.1750E 05</u>	<u>0.311E-04</u>
<u>0.1900E 05</u>	<u>0.211E-04</u>
<u>0.2000E 05</u>	<u>0.157E-04</u>
<u>0.2200E 05</u>	<u>0.771E-05</u>
<u>0.2400E 05</u>	<u>0.279E-05</u>
<u>0.2732E 05</u>	<u>0.</u>

TABLE XX
ELECTRON DISTRIBUTION FUNCTION (PER MEV)
($\xi = 0$)

GAMMAE	2.0000E 02	8.0000E 02	GAMMAP1
<u>0.1074E 01</u>	<u>0.</u>		
<u>0.1537E 01</u>	<u>0.279E-04</u>		
<u>0.2000E 01</u>	<u>0.479E-04</u>		
<u>0.3000E 01</u>	<u>0.642E-04</u>		
<u>0.3014E 01</u>			<u>0.</u>
<u>0.4000E 01</u>	<u>0.700E-04</u>		<u>0.177E-05</u>
<u>0.5000E 01</u>	<u>0.727E-04</u>		<u>0.529E-05</u>
<u>0.6000E 01</u>	<u>0.743E-04</u>		<u>0.869E-05</u>
<u>0.7000E 01</u>	<u>0.752E-04</u>		<u>0.111E-04</u>
<u>0.8000E 01</u>	<u>0.758E-04</u>		<u>0.128E-04</u>
<u>0.9000E 01</u>	<u>0.762E-04</u>		<u>0.140E-04</u>
<u>1.0000E 01</u>	<u>0.765E-04</u>		<u>0.149E-04</u>
<u>0.1500E 02</u>	<u>0.773E-04</u>		<u>0.173E-04</u>
<u>0.2000E 02</u>	<u>0.775E-04</u>		<u>0.182E-04</u>
<u>0.3000E 02</u>	<u>0.777E-04</u>		<u>0.189E-04</u>
<u>0.4000E 02</u>	<u>0.778E-04</u>		<u>0.191E-04</u>
<u>0.5000E 02</u>	<u>0.778E-04</u>		<u>0.193E-04</u>

TABLE XX (CONTINUED)

ELECTRON DISTRIBUTION FUNCTION (PER MEV)

(ξ = 0)

GAMMAE	GAMMAPI
2.0000E 02	8.0000E 02
0.6000E 02	0.778E-04
0.7000E 02	0.778E-04
0.8000E 02	0.778E-04
0.9000E 02	0.778E-04
1.0000E 02	0.778E-04
0.1500E 03	0.778E-04
0.2000E 03	0.778E-04
0.3000E 03	0.778E-04
0.4000E 03	0.778E-04
0.5000E 03	0.778E-04
0.6000E 03	0.778E-04
0.7000E 03	0.778E-04
0.8000E 03	0.778E-04
0.9000E 03	0.778E-04
1.0000E 03	0.778E-04
0.1500E 04	0.777E-04
0.2000E 04	0.775E-04

TABLE XX (CONTINUED)
 ELECTRON DISTRIBUTION FUNCTION (PER MEV)
 $(\xi = 0)$

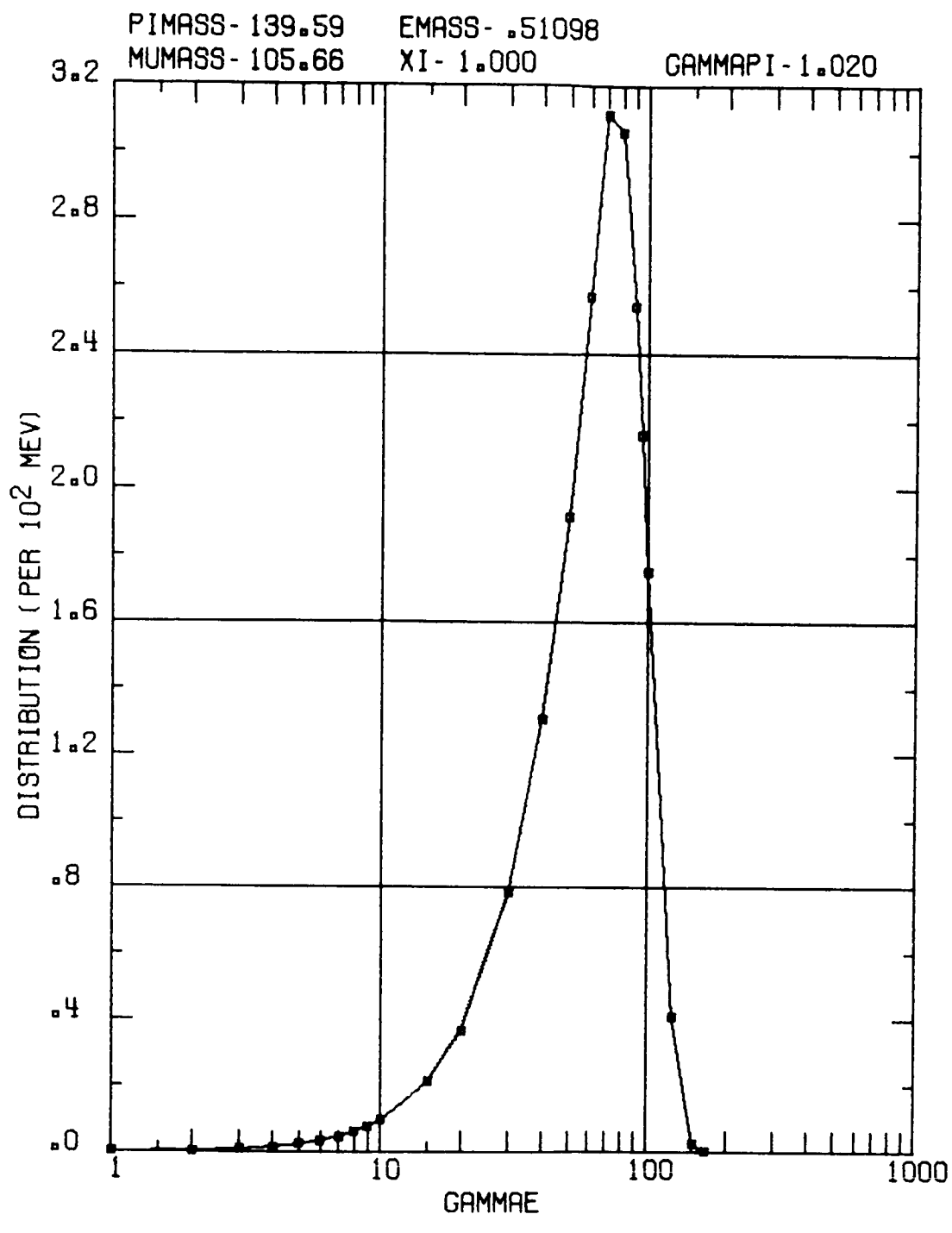
GAMMAE	2.0000E 02	8.0000E 02
<u>0.3000E 04</u>	<u>0.771E-04</u>	<u>0.195E-04</u>
<u>0.4000E 04</u>	<u>0.765E-04</u>	<u>0.194E-04</u>
<u>0.5000E 04</u>	<u>0.758E-04</u>	<u>0.194E-04</u>
<u>0.6000E 04</u>	<u>0.750E-04</u>	<u>0.194E-04</u>
<u>0.7000E 04</u>	<u>0.740E-04</u>	<u>0.194E-04</u>
<u>0.8000E 04</u>	<u>0.728E-04</u>	<u>0.194E-04</u>
<u>0.9000E 04</u>	<u>0.716E-04</u>	<u>0.194E-04</u>
<u>1.0000E 04</u>	<u>0.702E-04</u>	<u>0.193E-04</u>
<u>0.1500E 05</u>	<u>0.618E-04</u>	<u>0.192E-04</u>
<u>0.2000E 05</u>	<u>0.513E-04</u>	<u>0.190E-04</u>
<u>0.2500E 05</u>	<u>0.394E-04</u>	
<u>0.3000E 05</u>	<u>0.269E-04</u>	<u>0.184E-04</u>
<u>0.3824E 05</u>	<u>0.102E-04</u>	
<u>0.4000E 05</u>	<u>0.786E-05</u>	<u>0.176E-04</u>
<u>0.4098E 05</u>	<u>0.672E-05</u>	
<u>0.4234E 05</u>	<u>0.531E-05</u>	
<u>0.4371E 05</u>	<u>0.409E-05</u>	

TABLE XX (CONTINUED)

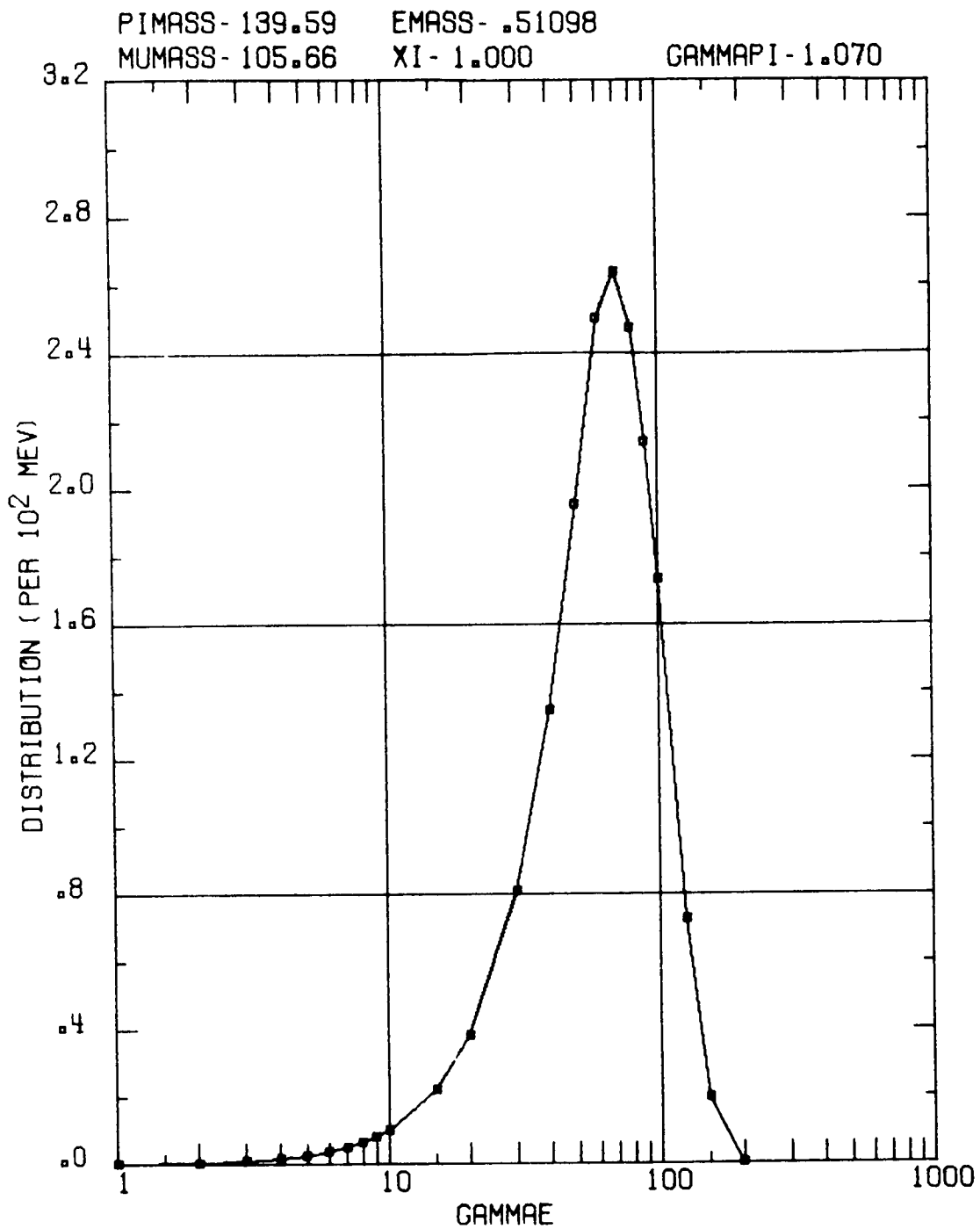
ELECTRON DISTRIBUTION FUNCTION (PER MEV)

 $(\xi = 0)$

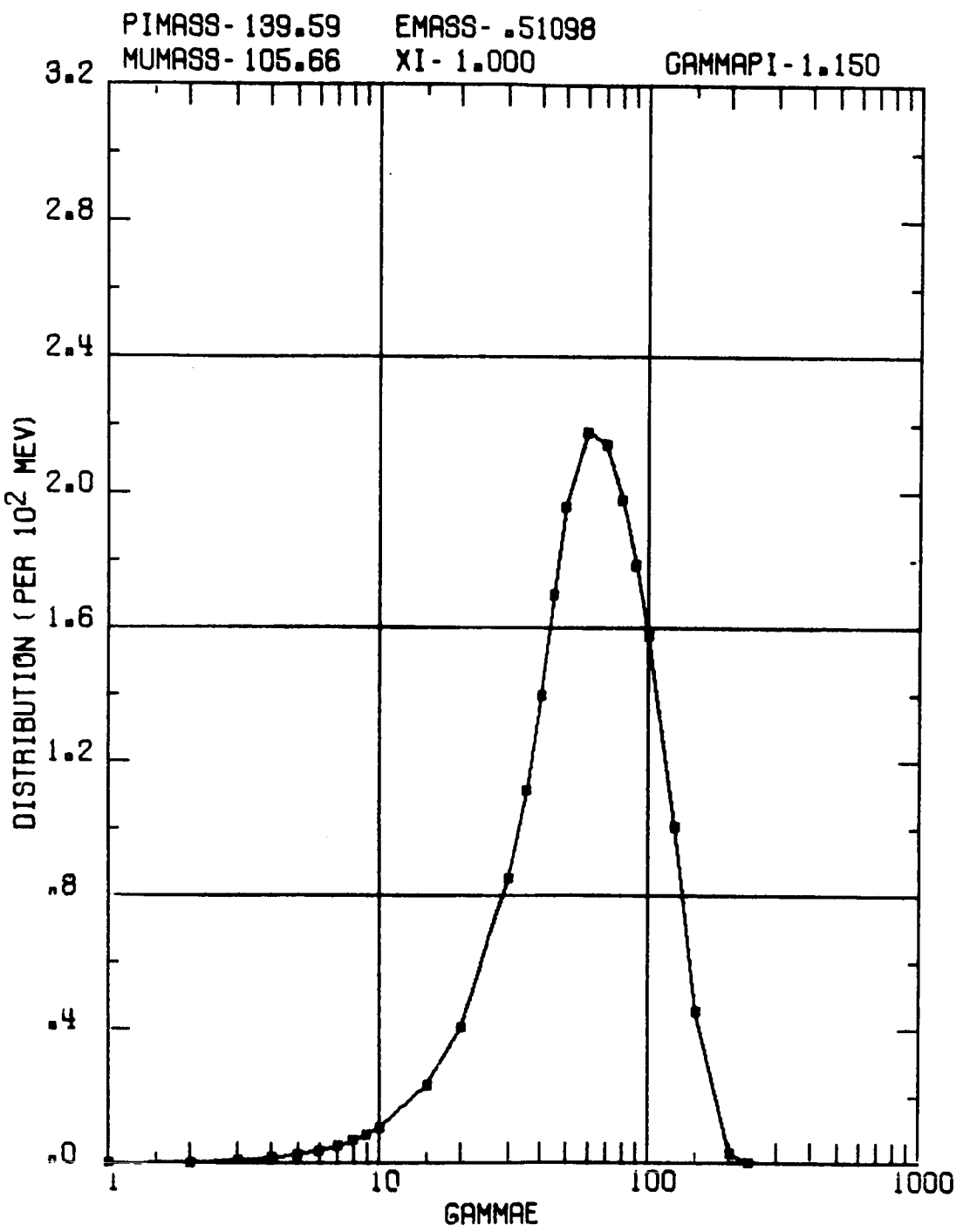
GAMMAE	GAMMAPI
2.0000E 02	8.0000E 02
<u>0.4507E 05</u>	<u>0.306E-05</u>
<u>0.4644E 05</u>	<u>0.219E-05</u>
<u>0.4781E 05</u>	<u>0.148E-05</u>
<u>0.4917E 05</u>	<u>0.926E-06</u>
<u>0.5000E 05</u>	<u>0.657E-06</u>
<u>0.5464E 05</u>	<u>0.</u>
<u>0.6000E 05</u>	<u>0.154E-04</u>
<u>0.7000E 05</u>	<u>0.142E-04</u>
<u>0.8000E 05</u>	<u>0.128E-04</u>
<u>0.9000E 05</u>	<u>0.114E-04</u>
<u>1.0000E 05</u>	<u>0.984E-05</u>
<u>0.1250E 06</u>	<u>0.594E-05</u>
<u>0.1350E 06</u>	<u>0.451E-05</u>
<u>0.1500E 06</u>	<u>0.283E-05</u>
<u>0.1650E 06</u>	<u>0.162E-05</u>
<u>0.1800E 06</u>	<u>0.769E-06</u>
<u>0.2185E 06</u>	<u>0.</u>



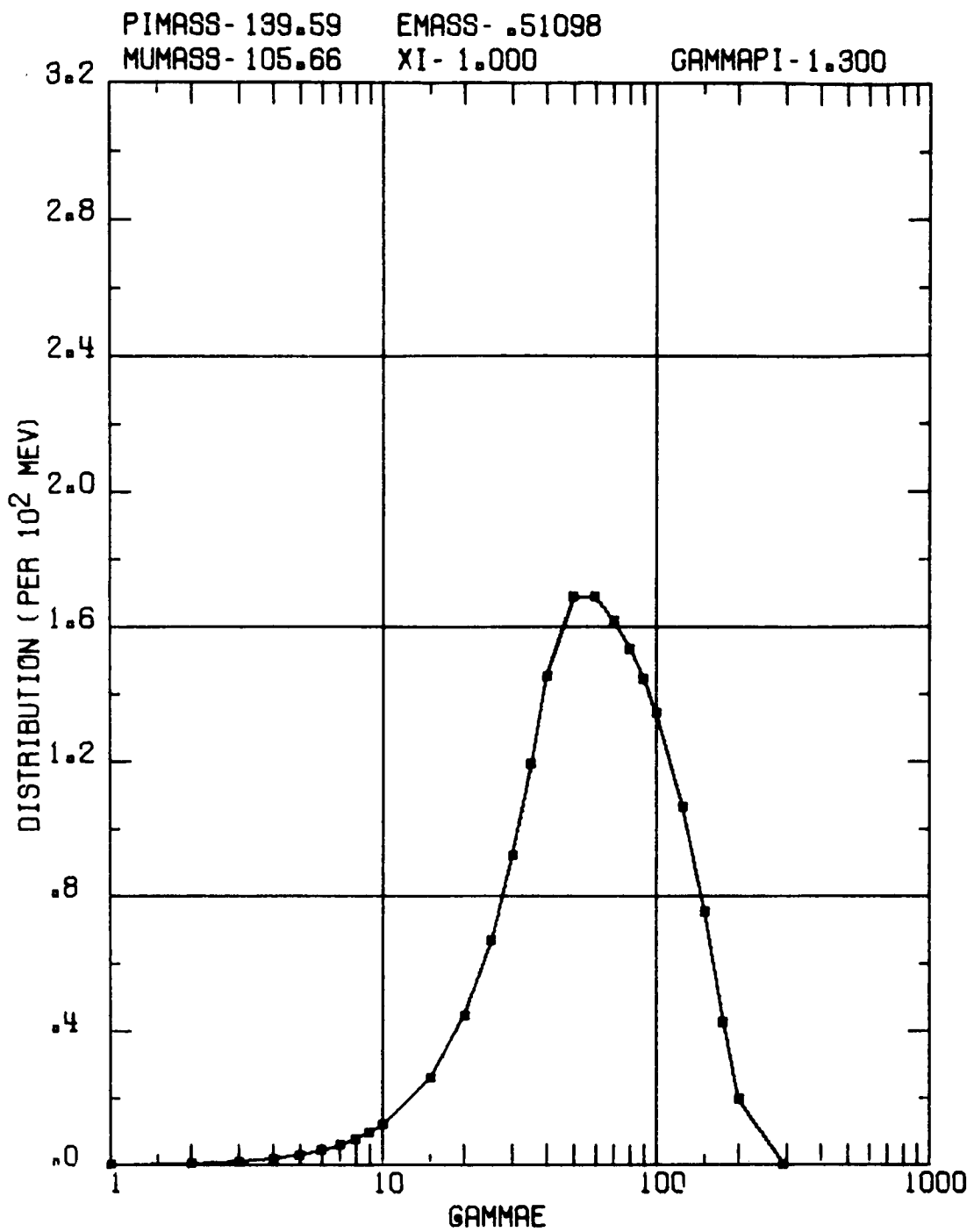
Graph 1. Electron Distribution Function ($\xi = 1$)



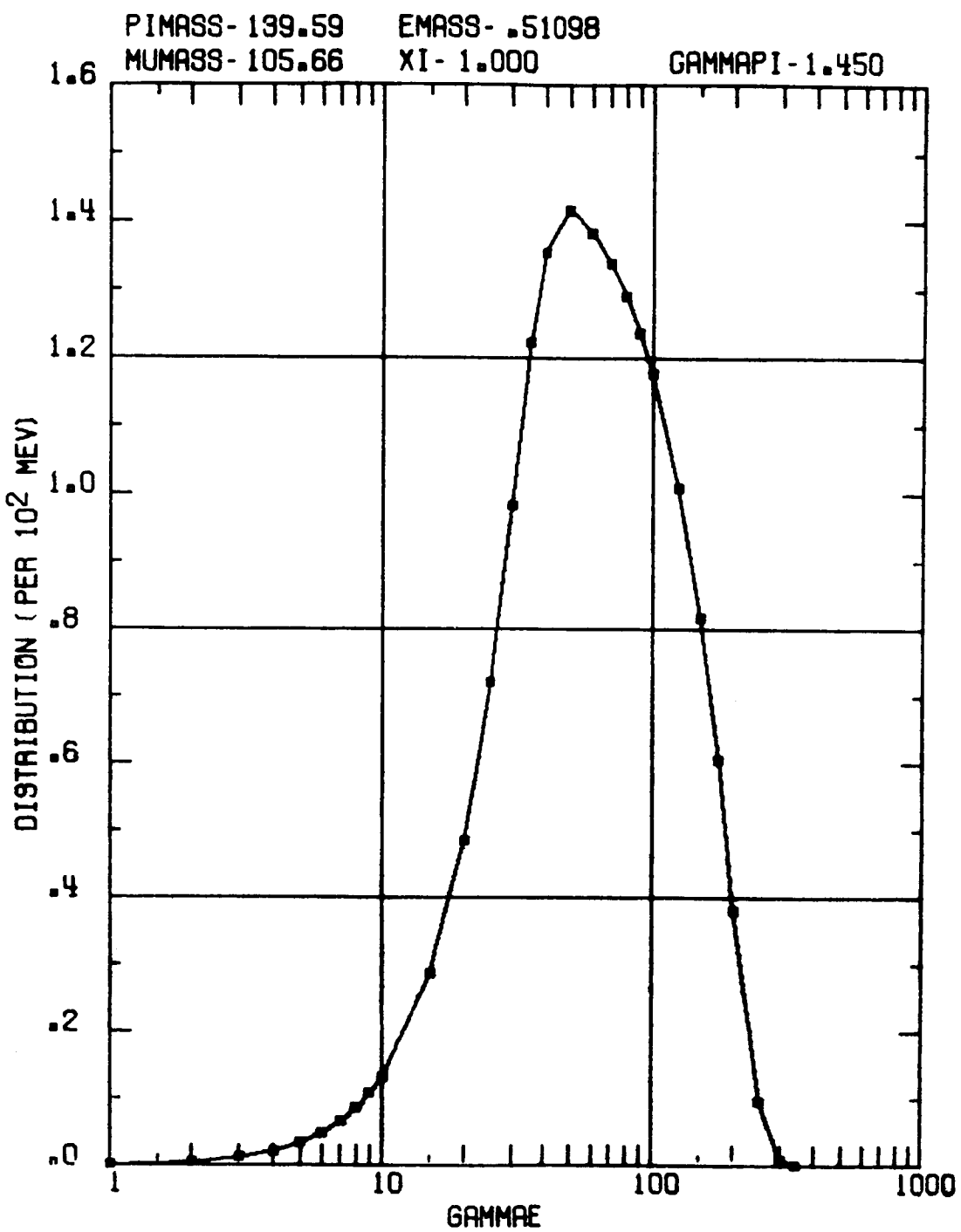
Graph 2. Electron Distribution Function ($\xi = 1$)



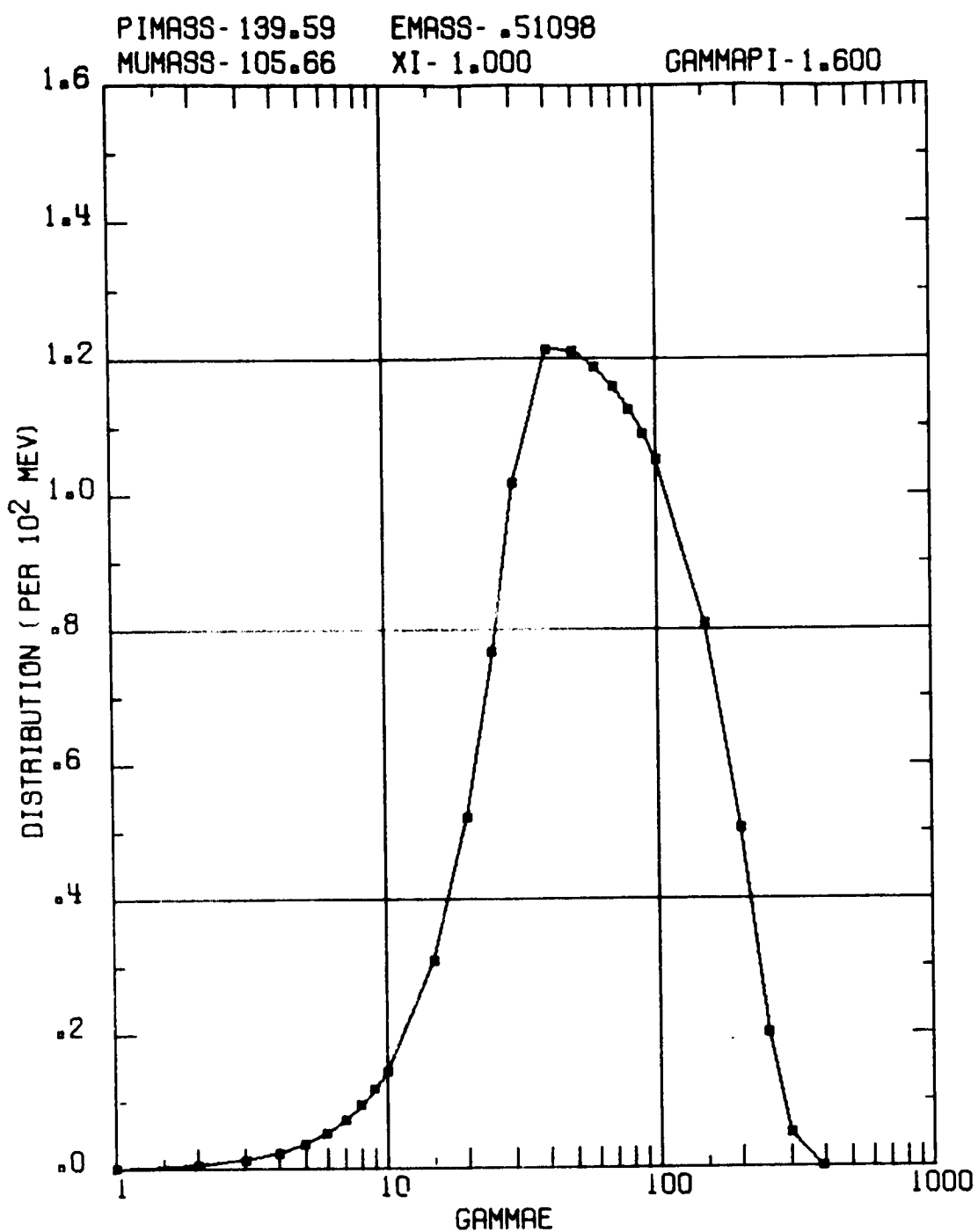
Graph 3. Electron Distribution Function ($\xi = 1$)



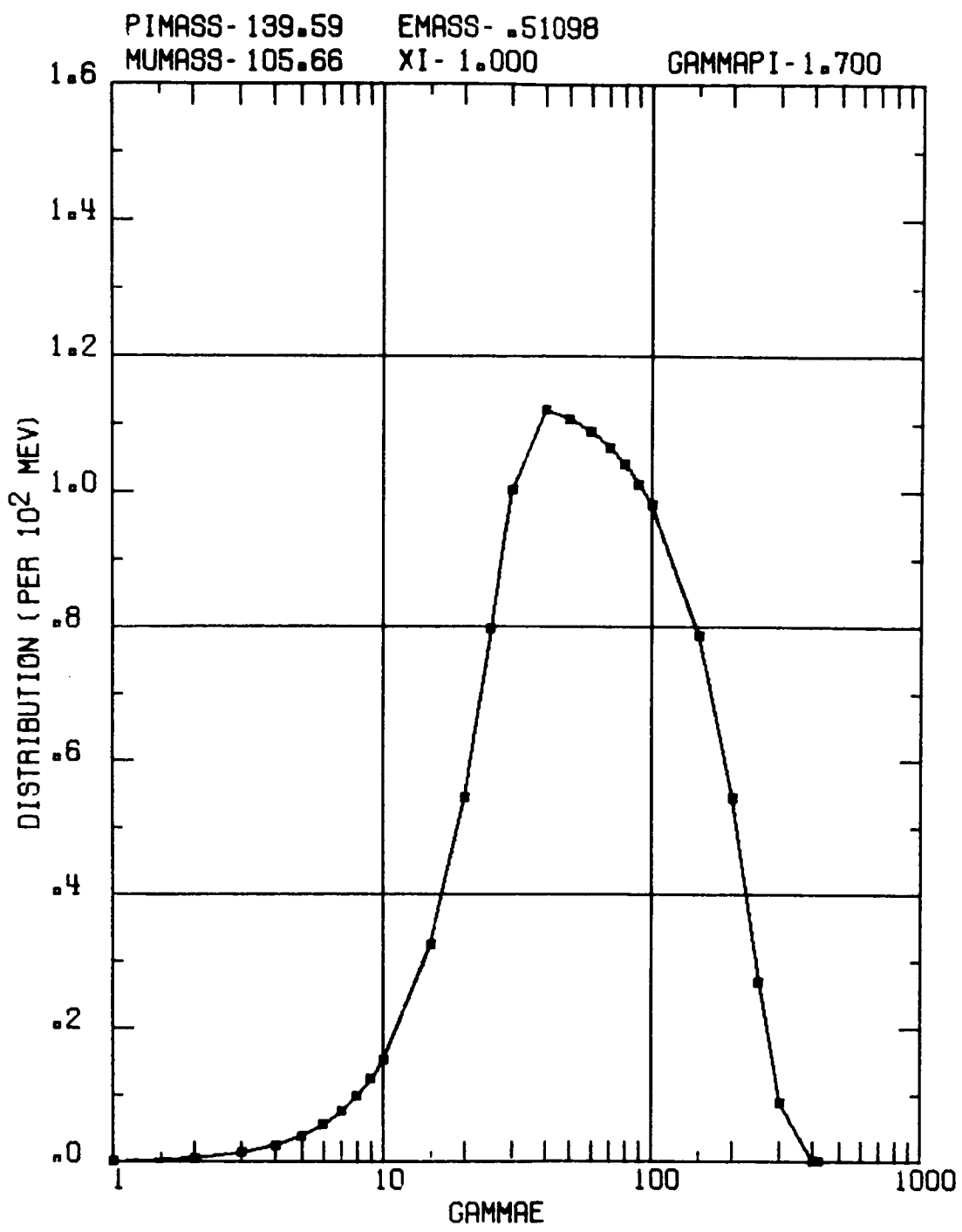
Graph 4. Electron Distribution Function ($\xi = 1$)



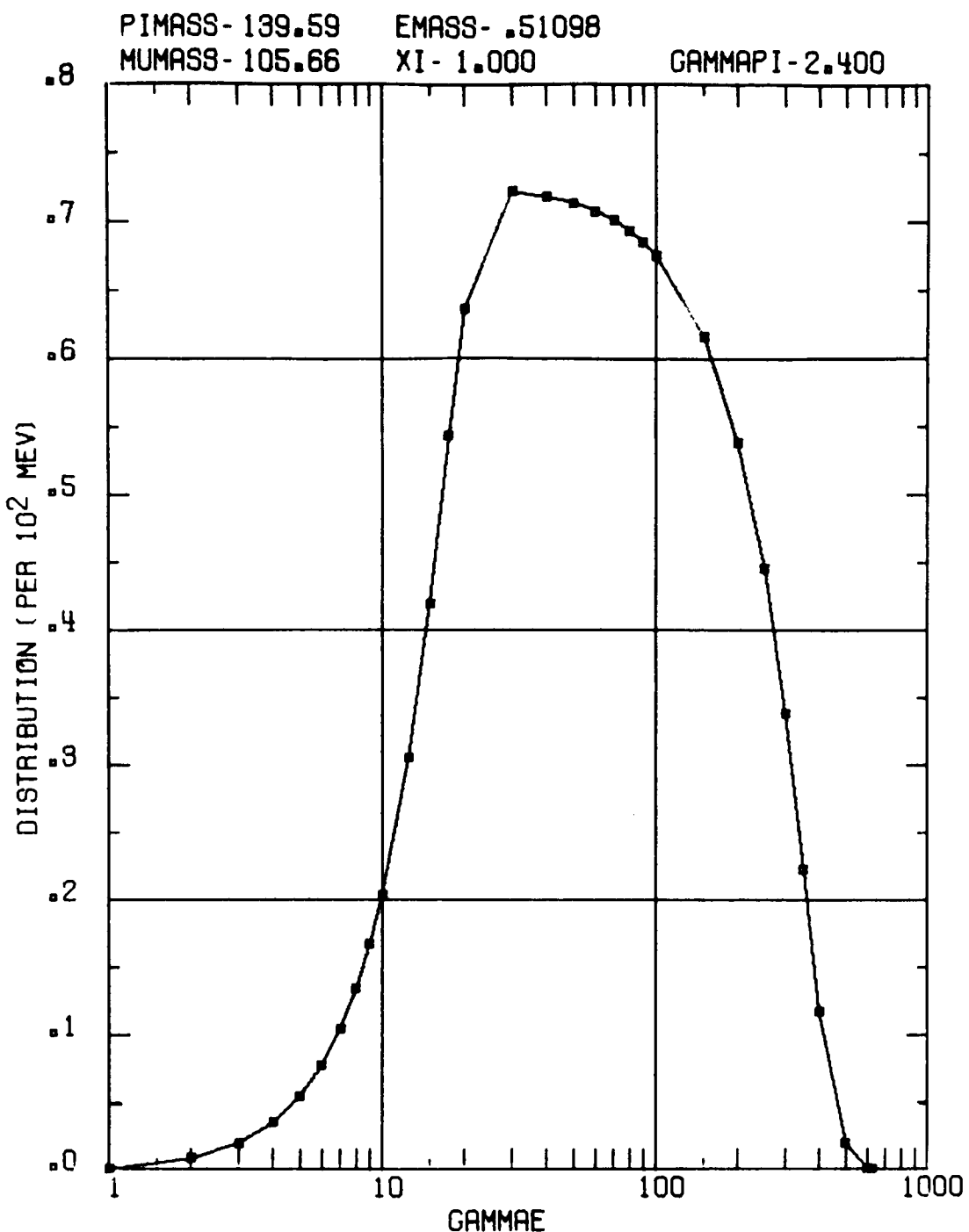
Graph 5. Electron Distribution Function ($\xi = 1$)



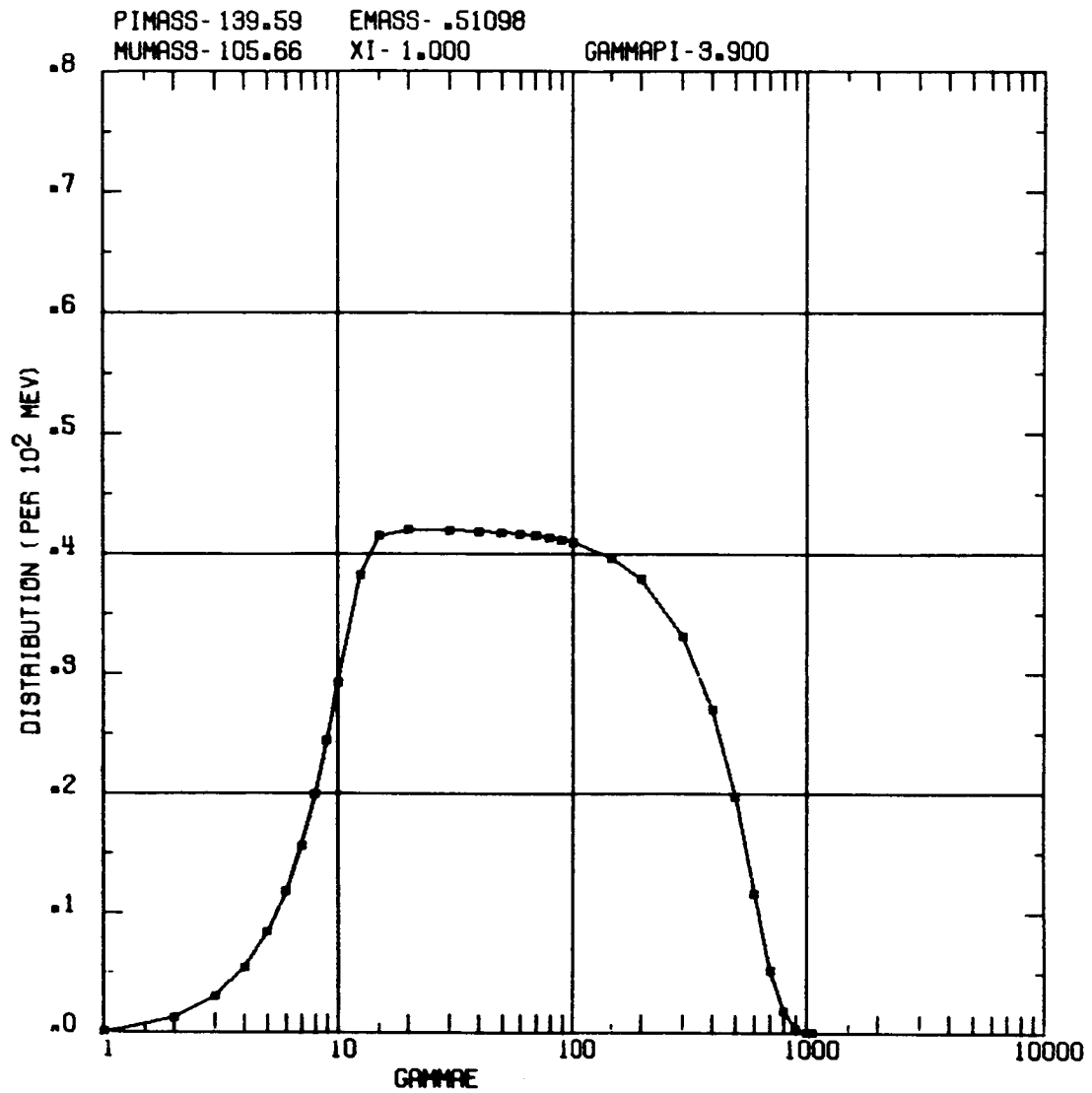
Graph 6. Electron Distribution Function ($\xi = 1$)



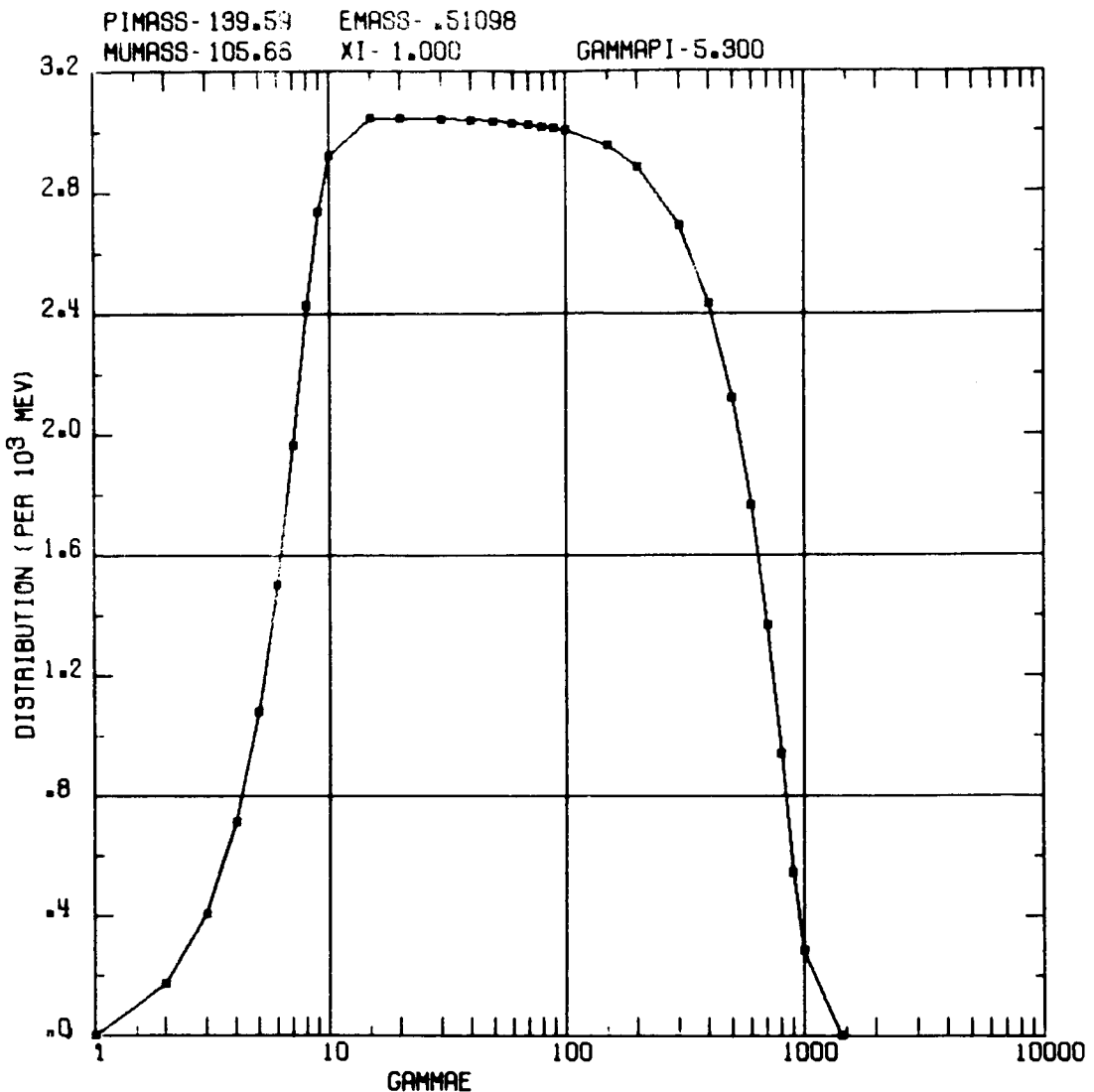
Graph 7. Electron Distribution Function ($\xi = 1$)



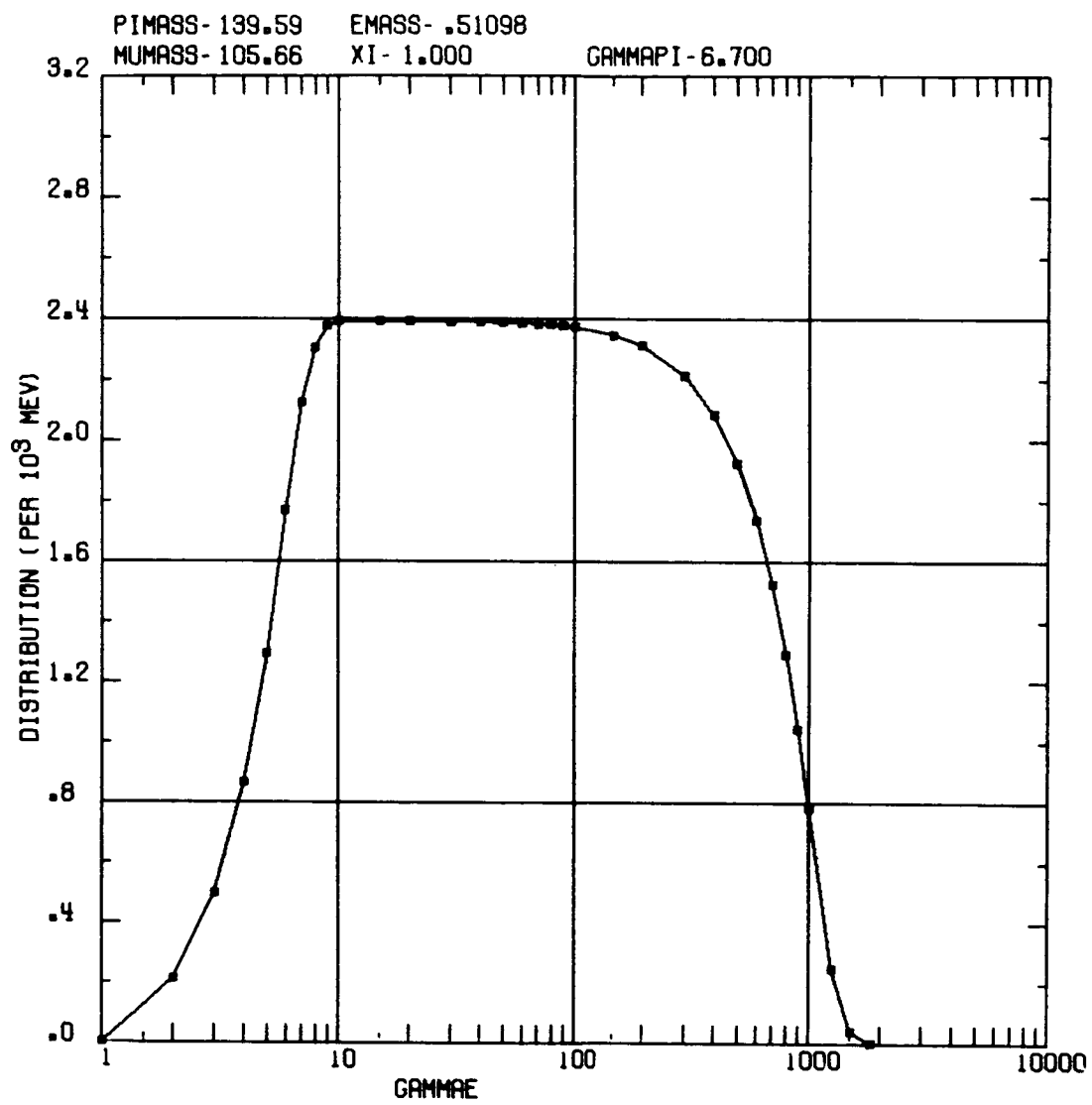
Graph 8. Electron Distribution Function ($\xi = 1$)



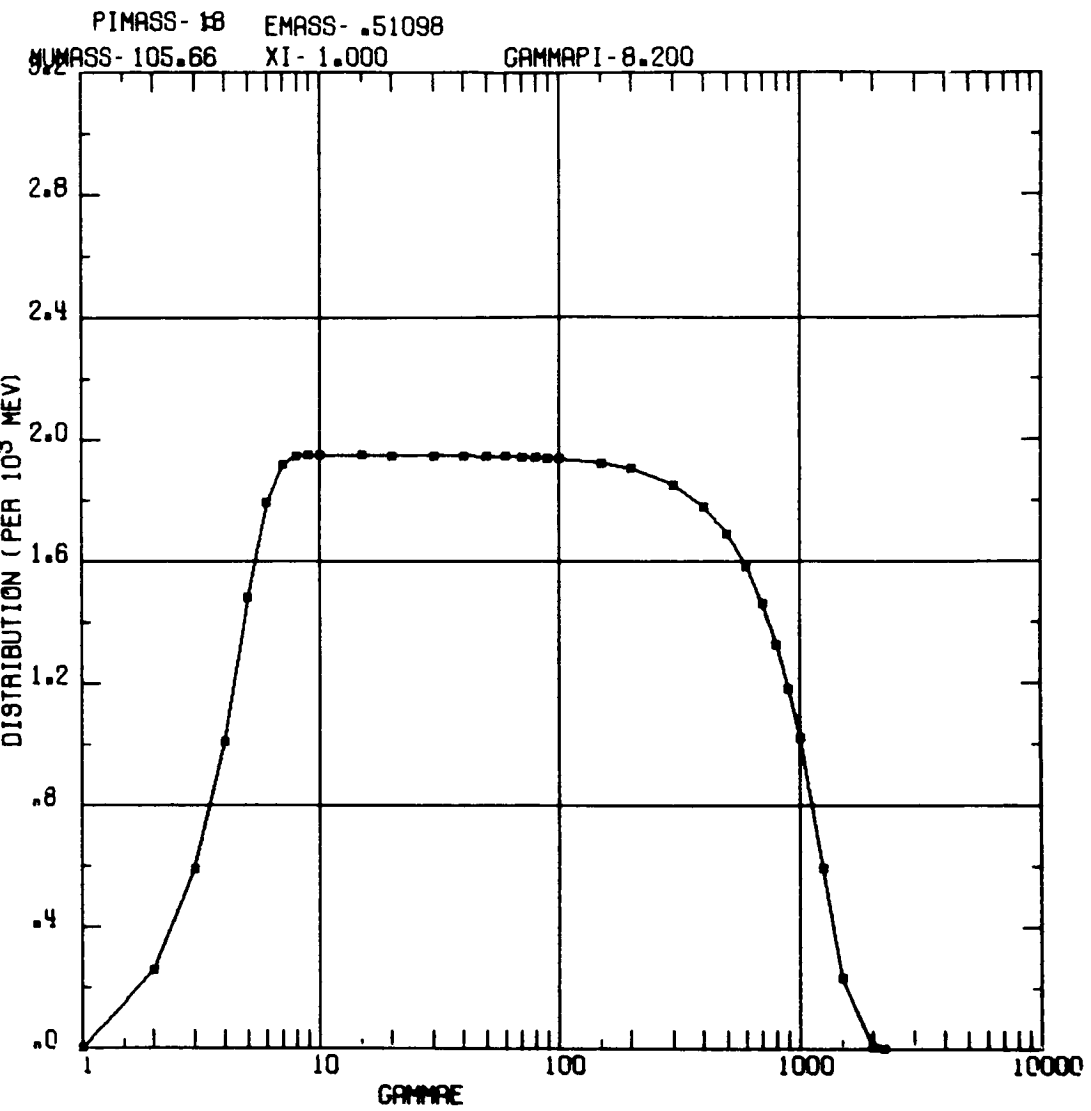
Graph 9. Electron Distribution Function ($\xi = 1$)



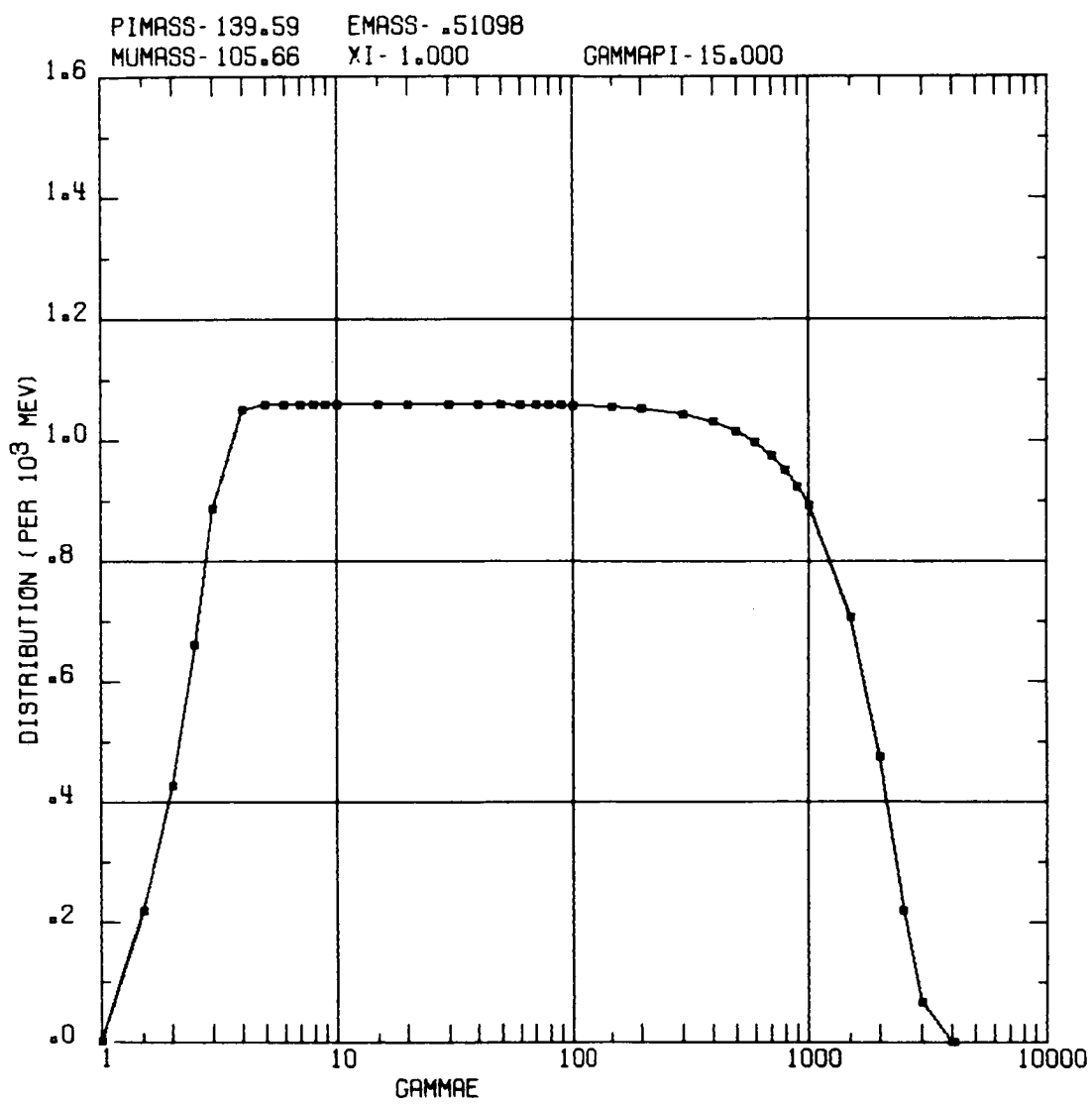
Graph 10. Electron Distribution Function ($\xi = 1$)



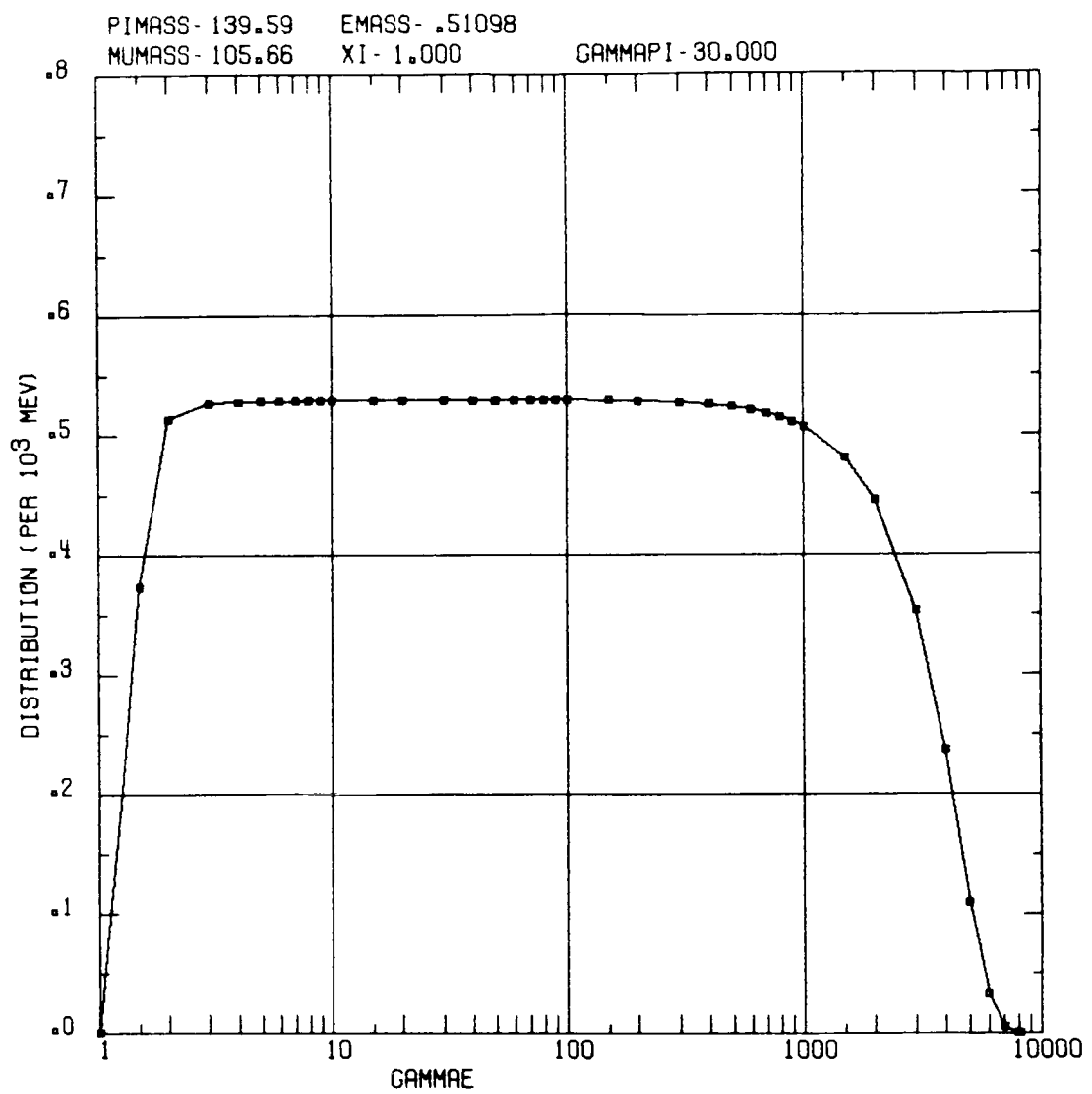
Graph 11. Electron Distribution Function ($\xi = 1$)



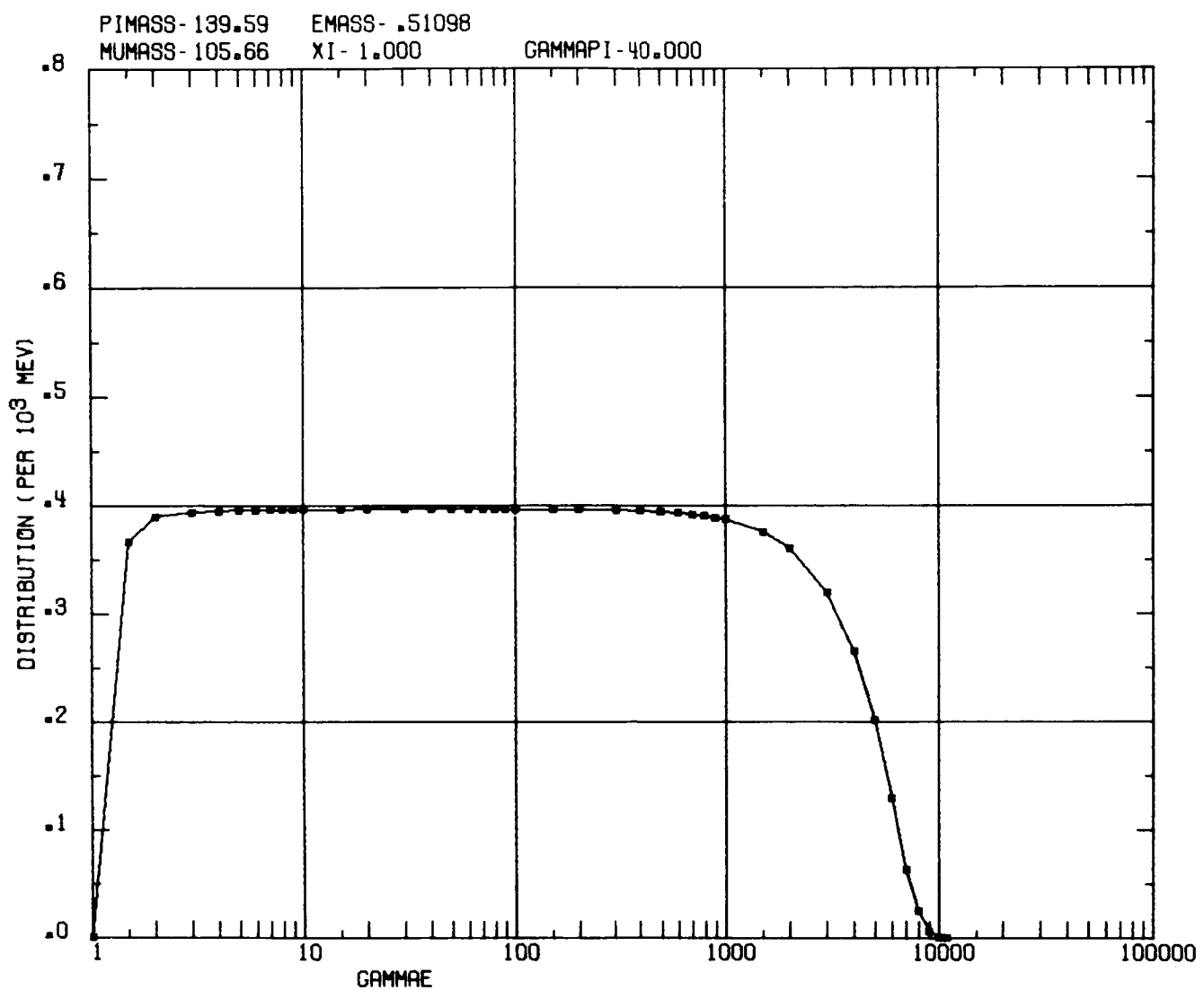
Graph 12. Electron Distribution Function ($\xi = 1$)



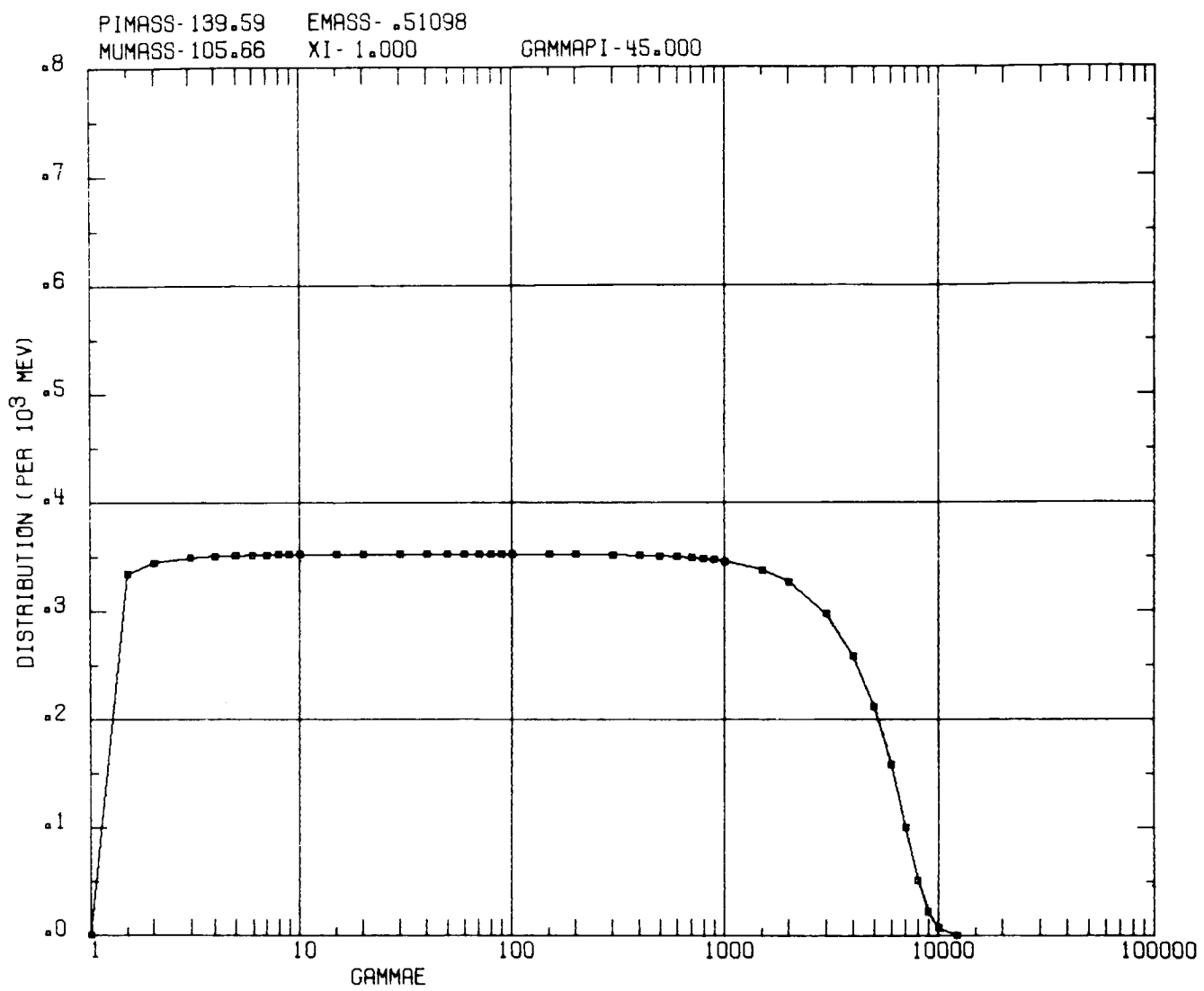
Graph 13. Electron Distribution Function ($\xi = 1$)



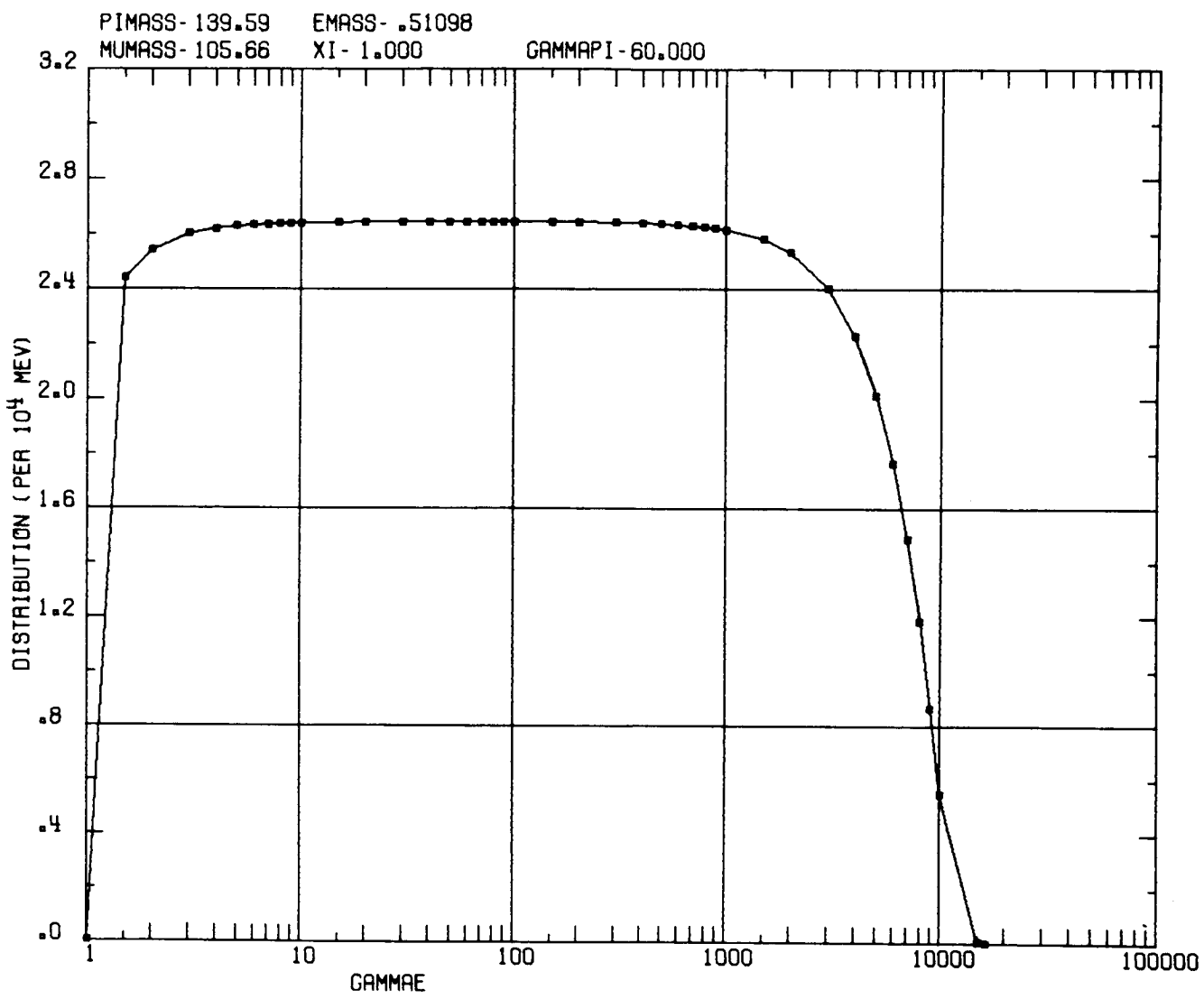
Graph 14. Electron Distribution Function ($\xi = 1$)



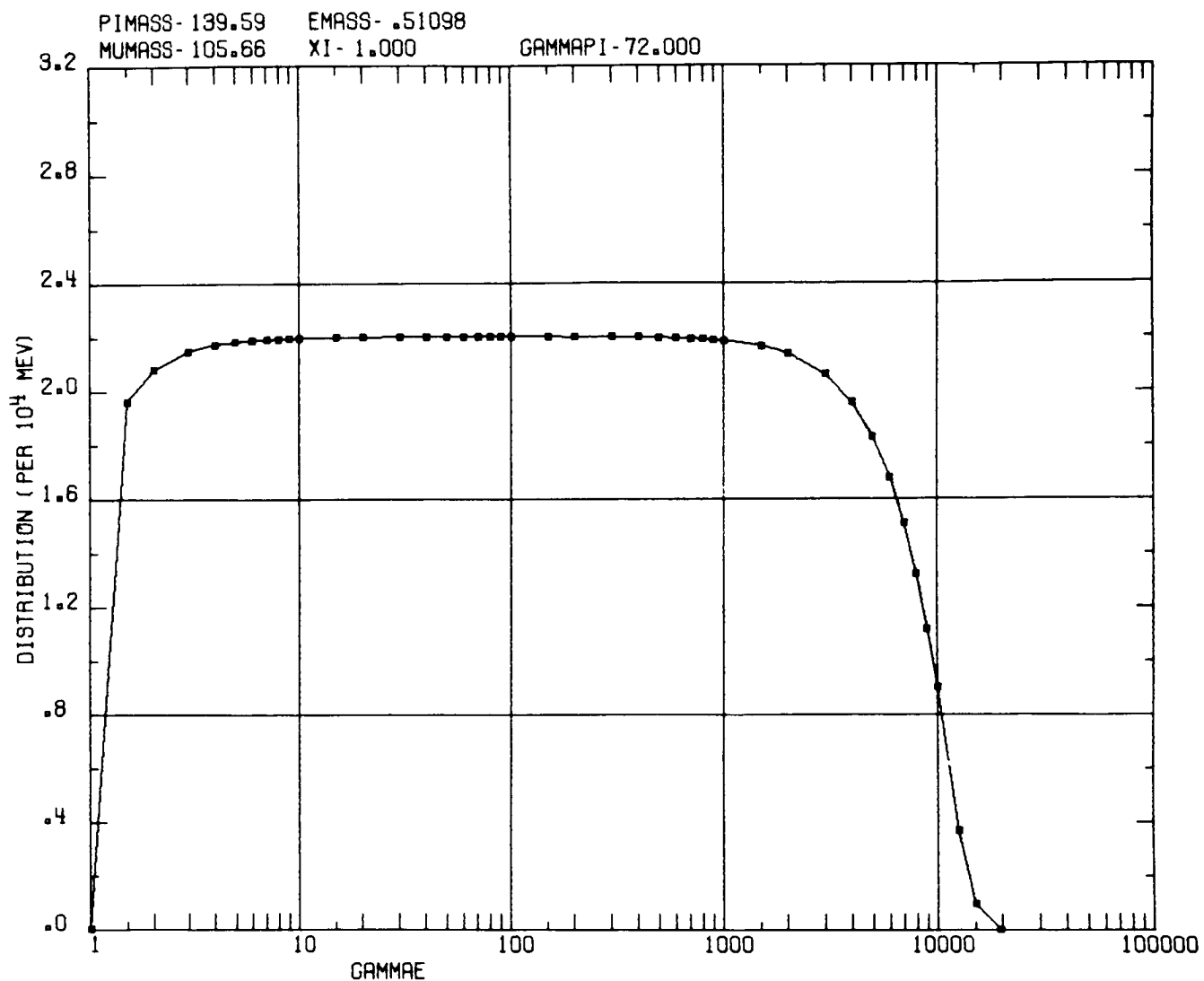
Graph 15. Electron Distribution Function ($\xi = 1$)



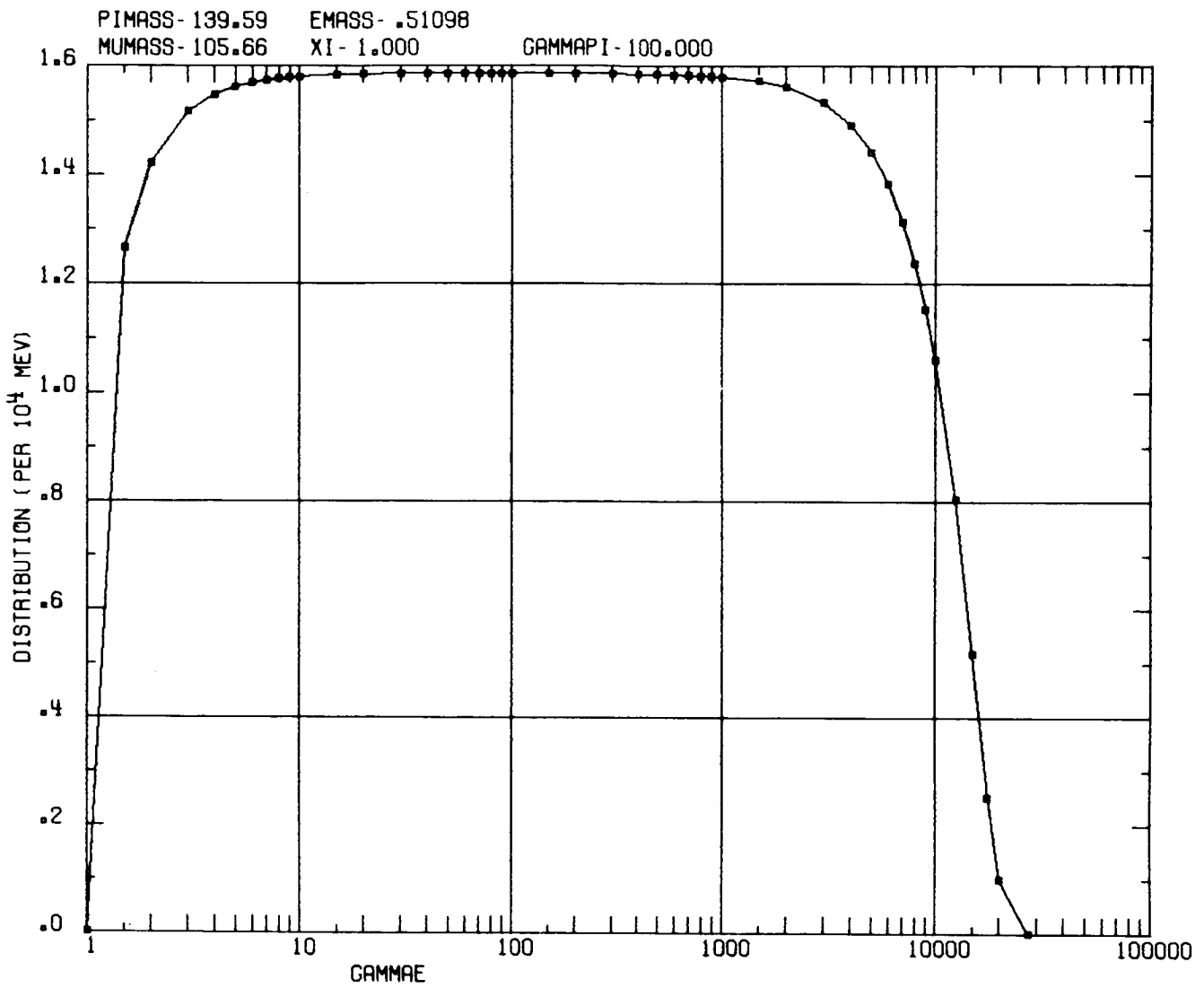
Graph 16. Electron Distribution Function ($\xi = 1$)



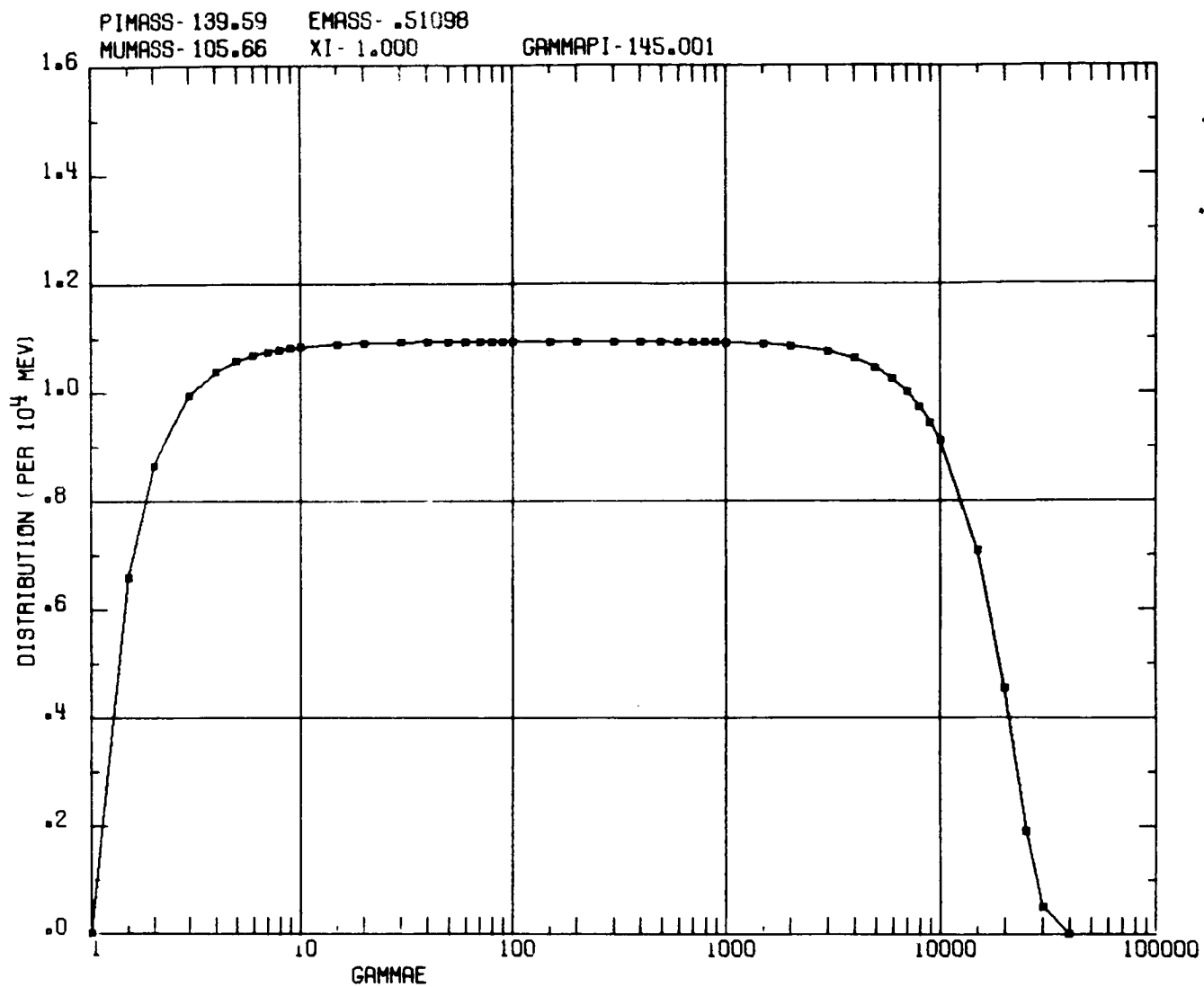
Graph 17. Electron Distribution Function ($\xi = 1$)



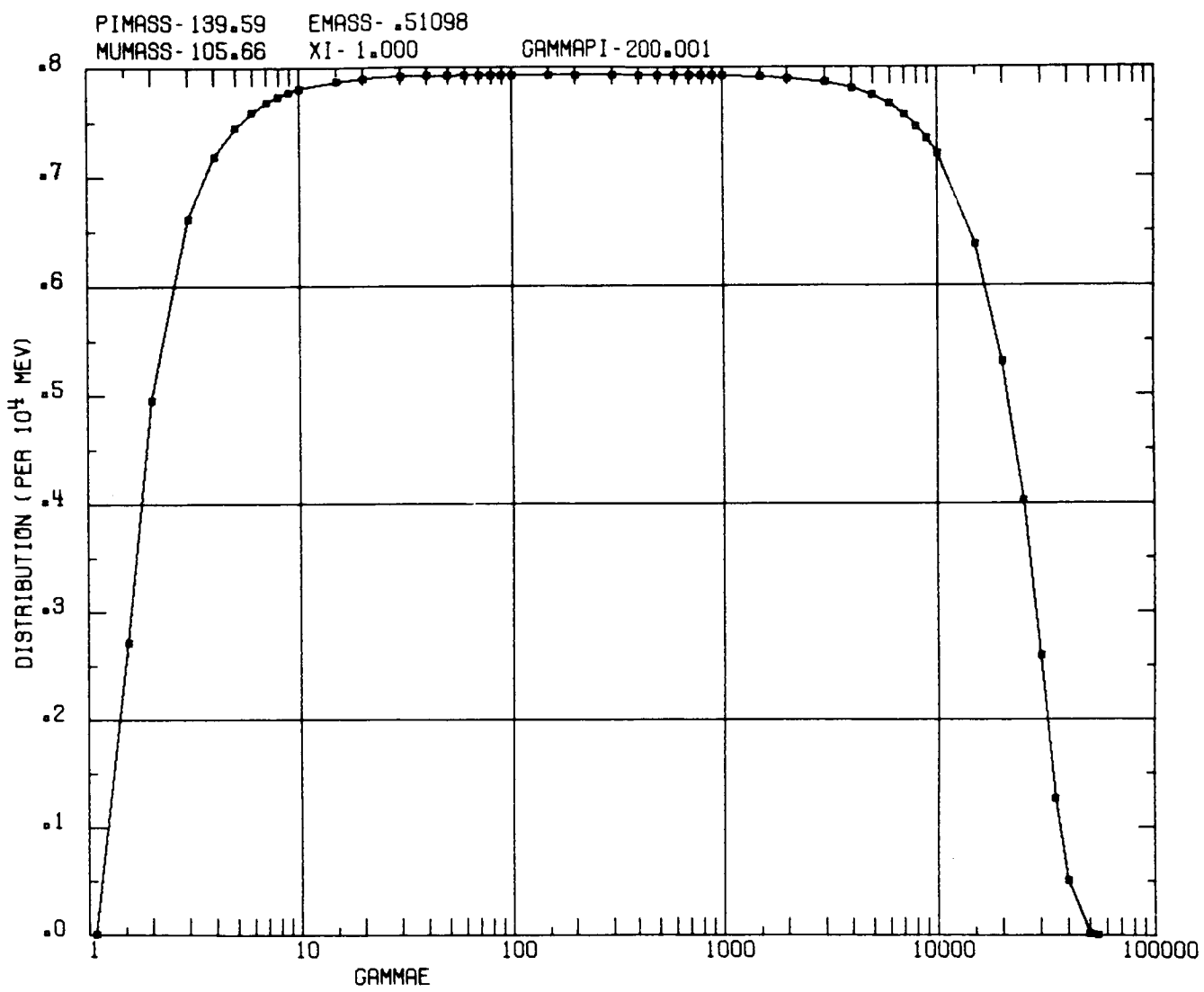
Graph 18. Electron Distribution Function ($\xi = 1$)



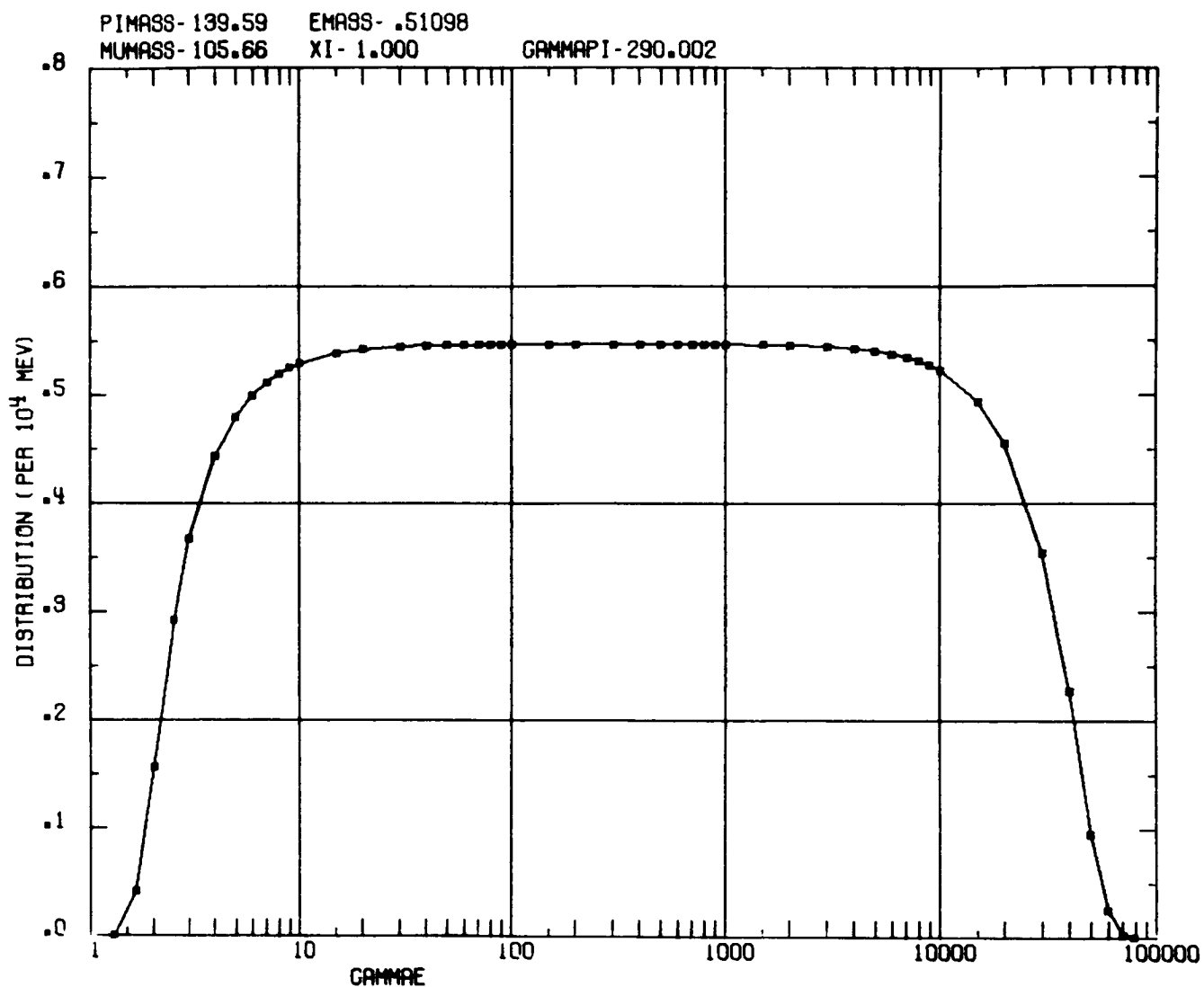
Graph 19. Electron Distribution Function ($\xi = 1$)



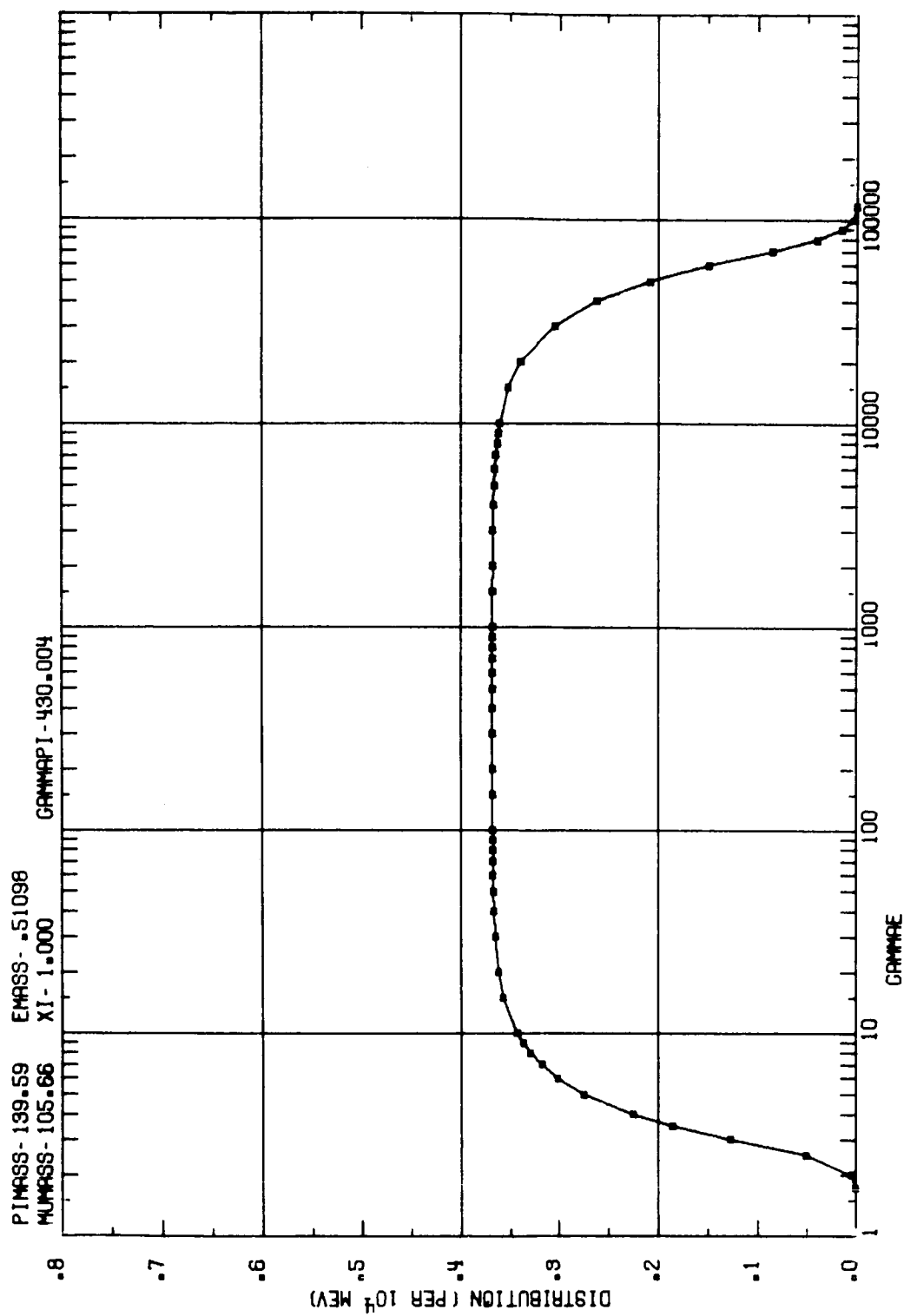
Graph 20. Electron Distribution Function ($\xi = 1$)



Graph 21. Electron Distribution Function ($\xi = 1$)

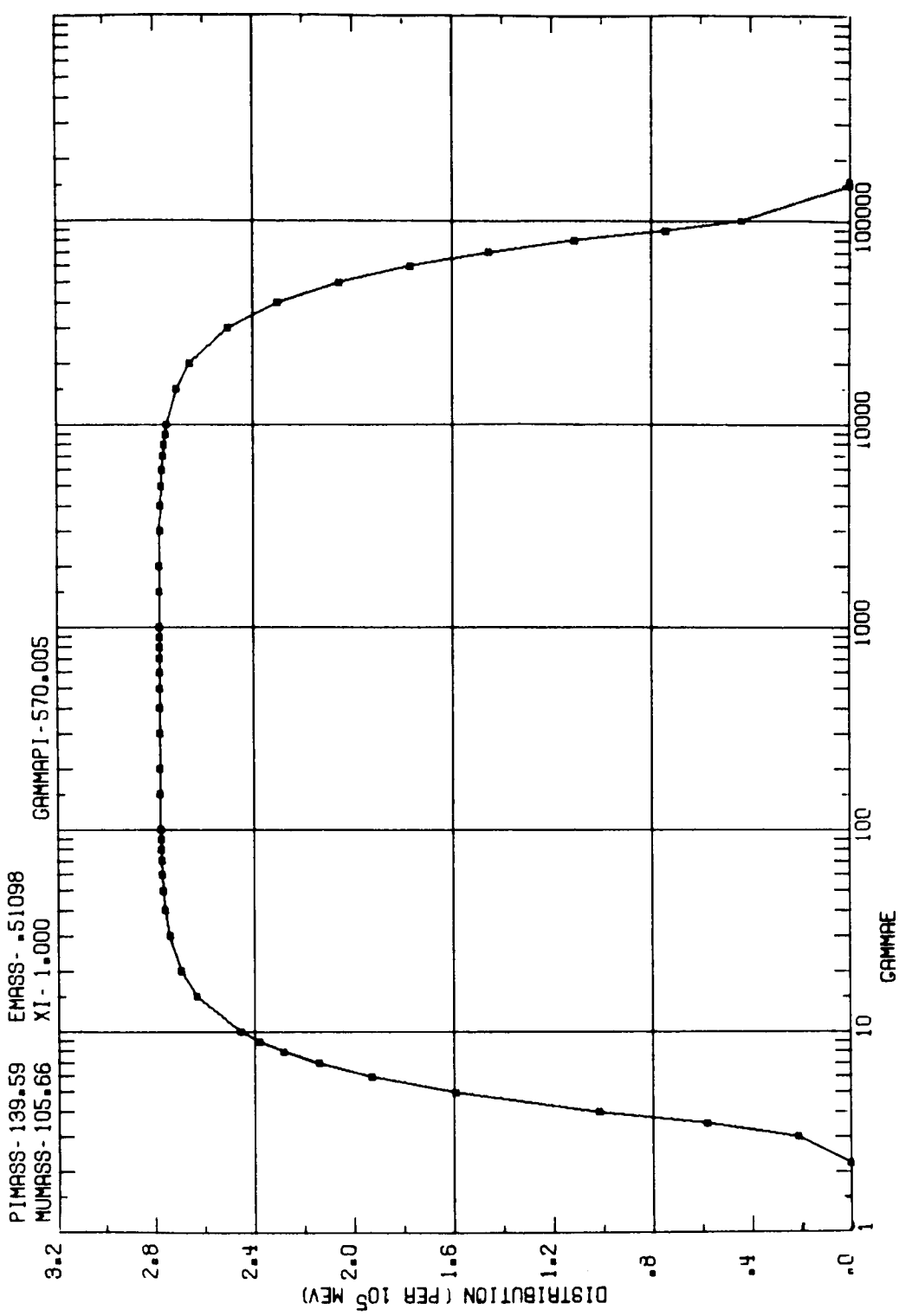


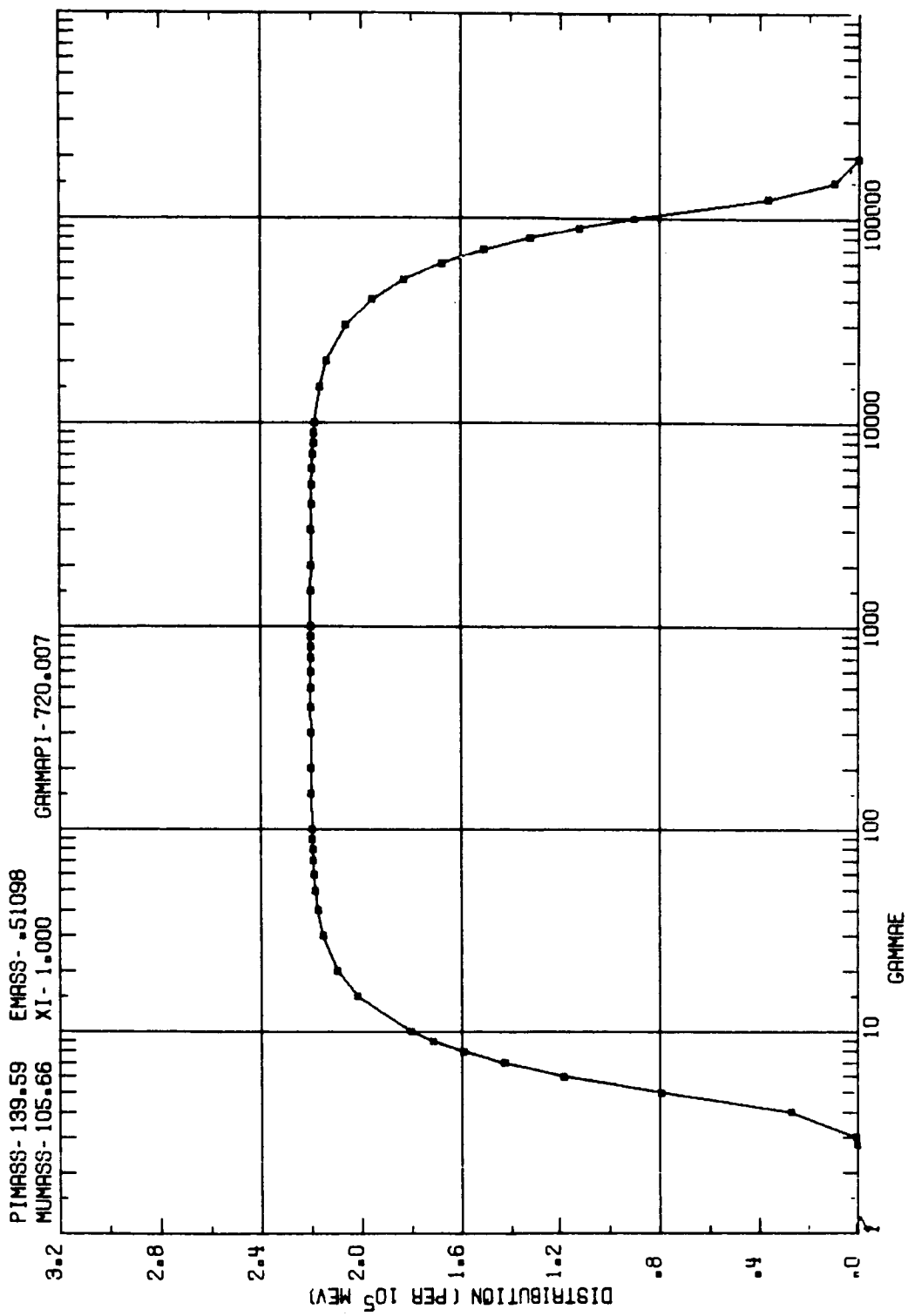
Graph 22. Electron Distribution Function ($\xi = 1$)



Graph 23. Electron Distribution Function ($\xi = 1$)

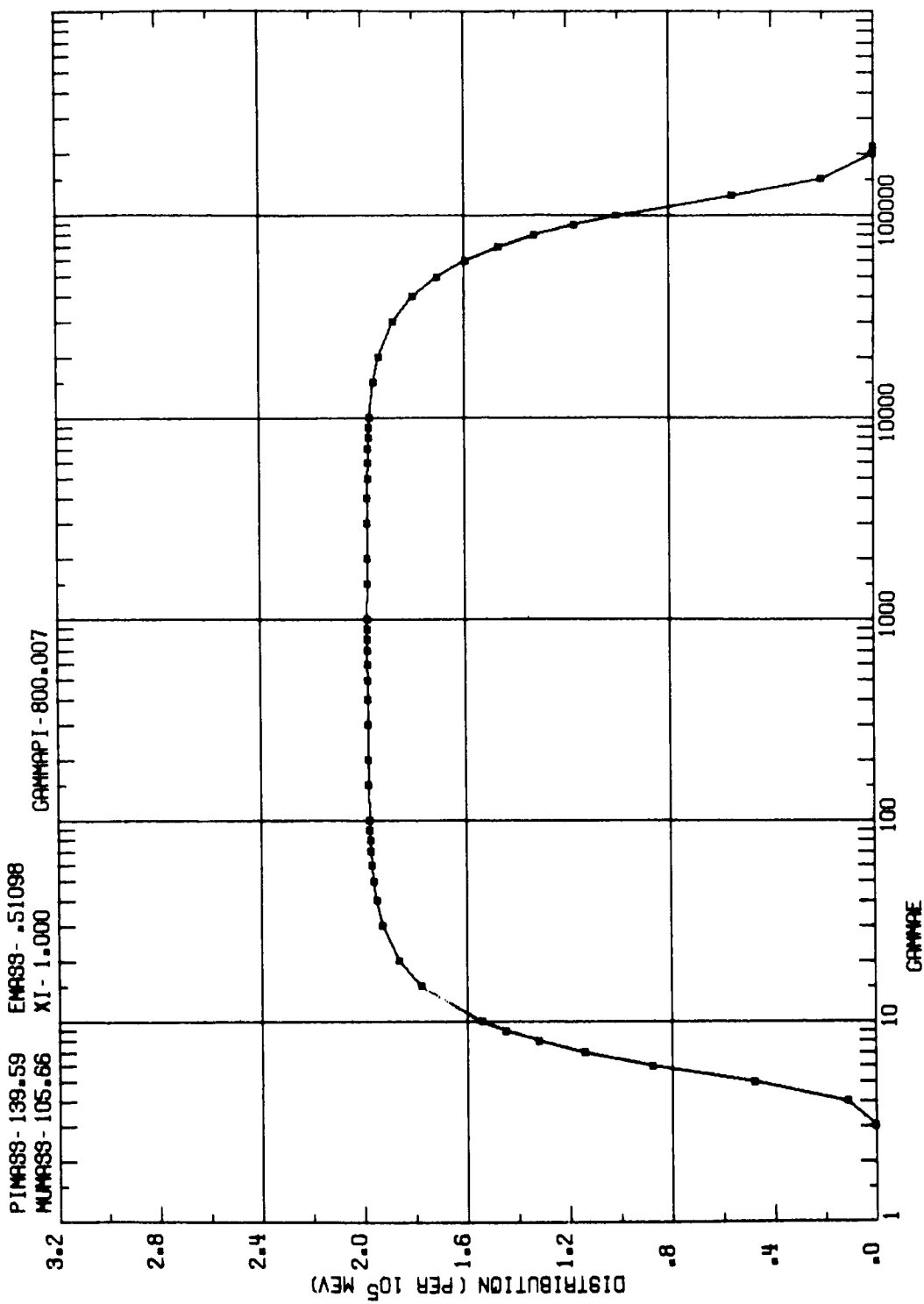
Graph 24. Electron Distribution Function ($\xi = 1$)

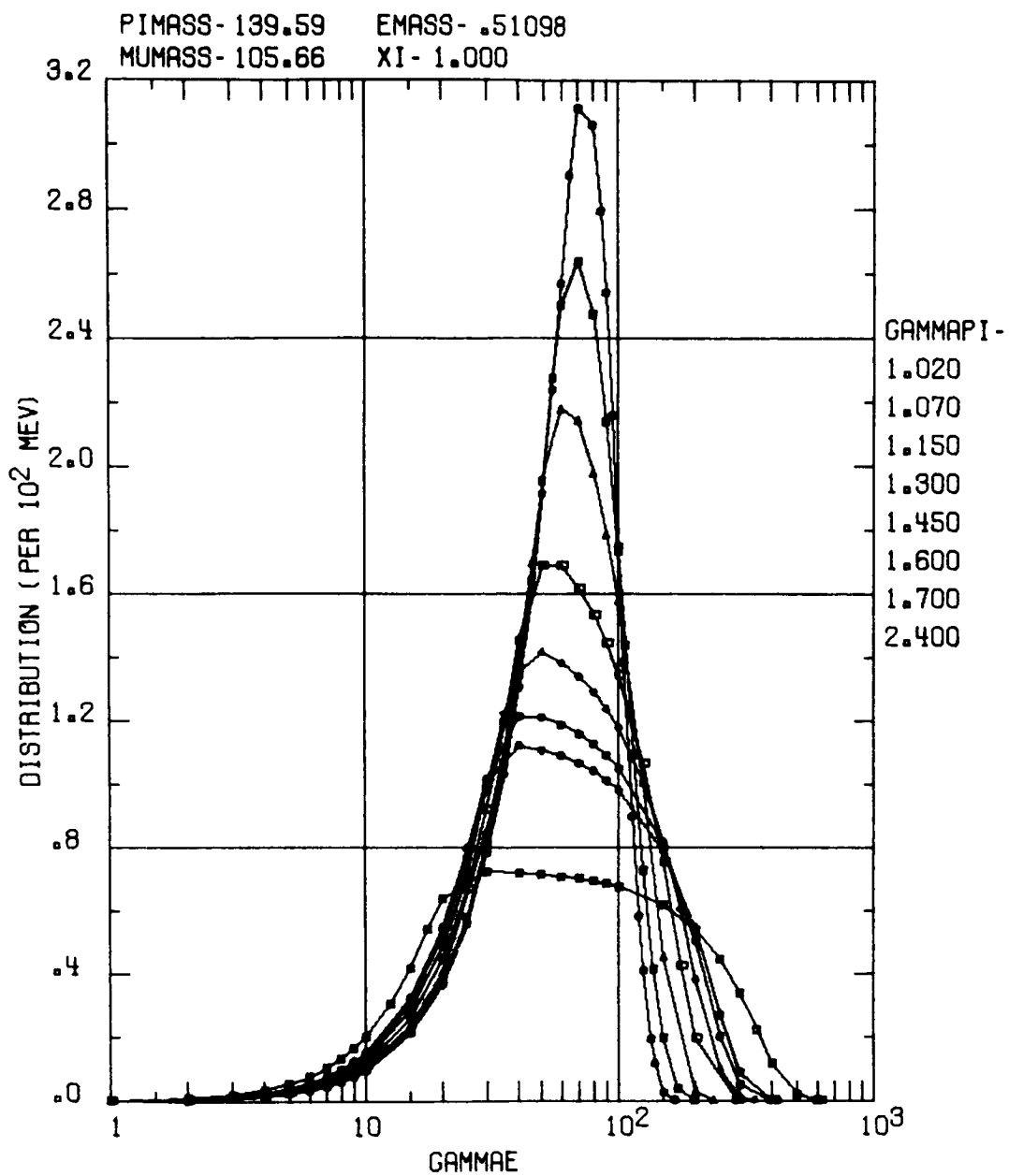




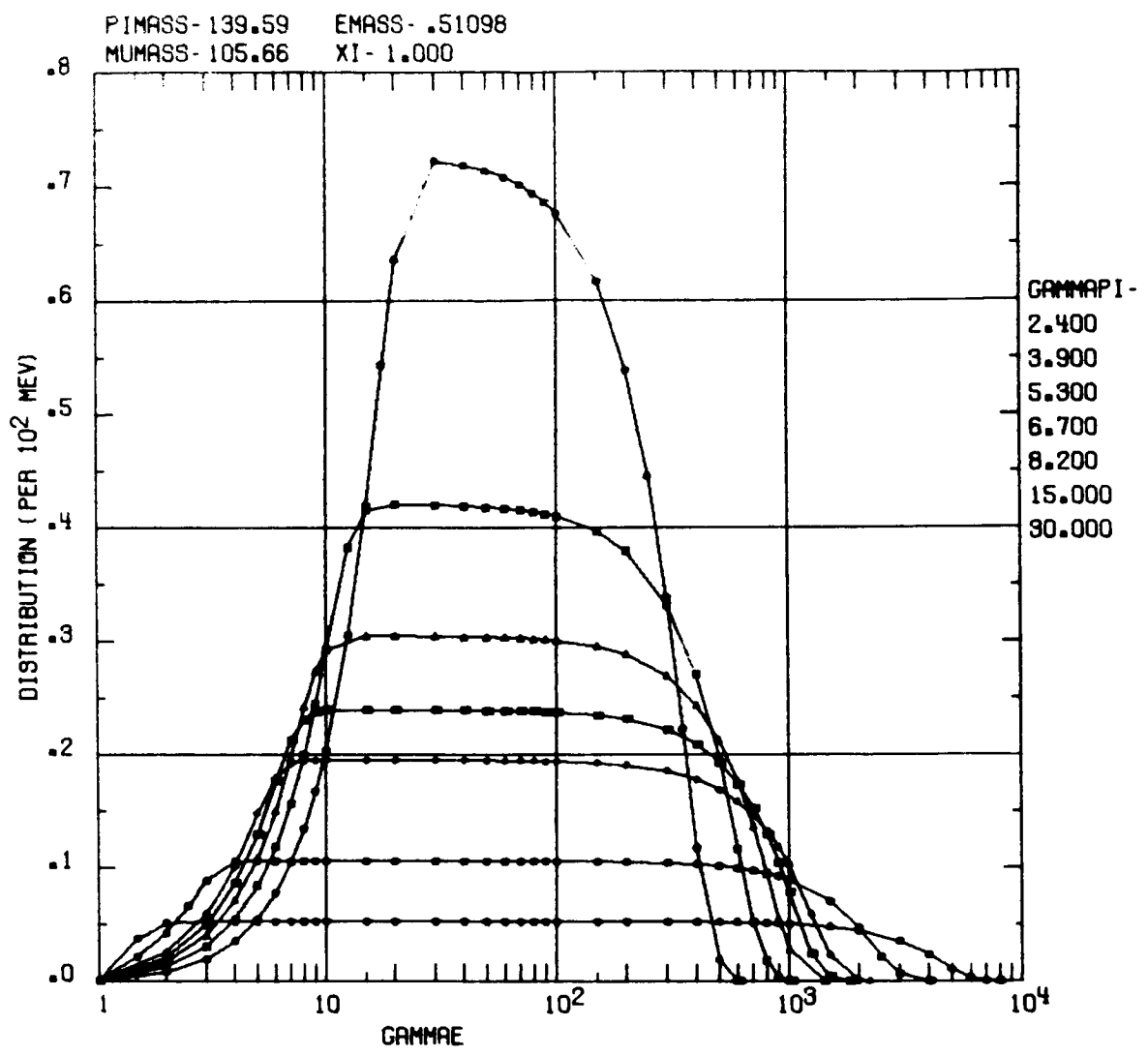
Graph 25. Electron Distribution Function ($\xi = 1$)

Graph 26. Electron Distribution Function ($\xi = 1$)

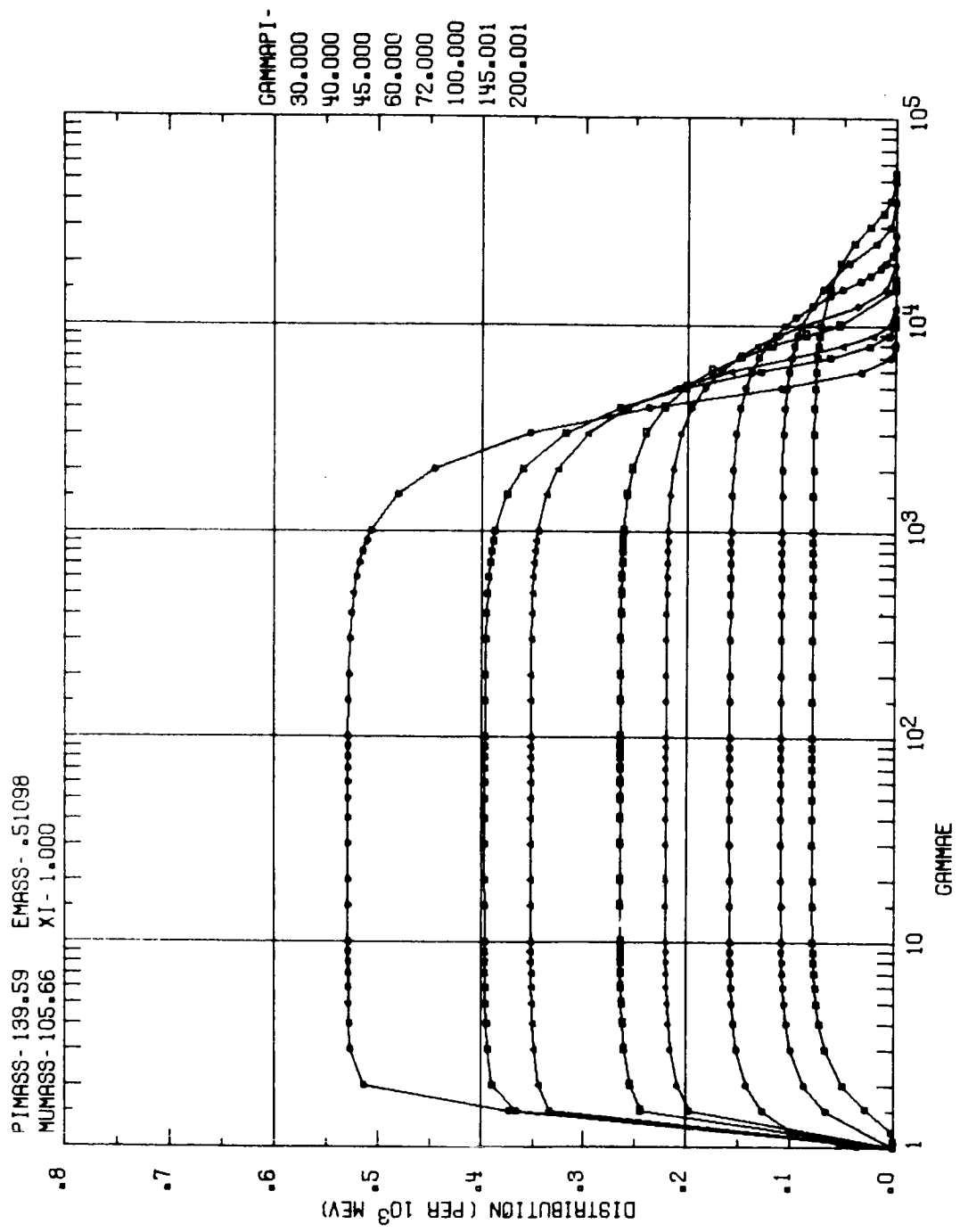




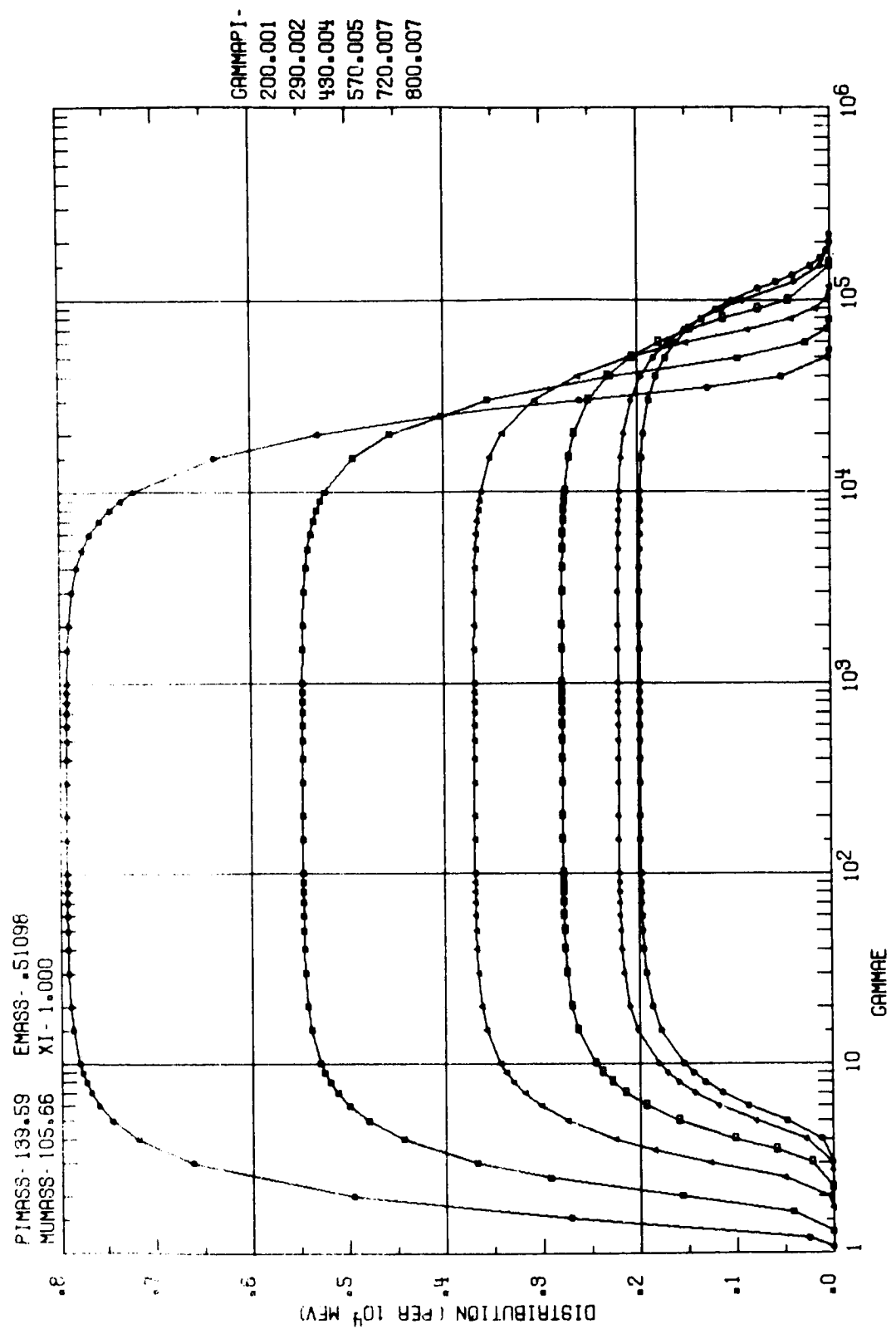
Graph 27. Electron Distribution Function ($\xi = 1$)



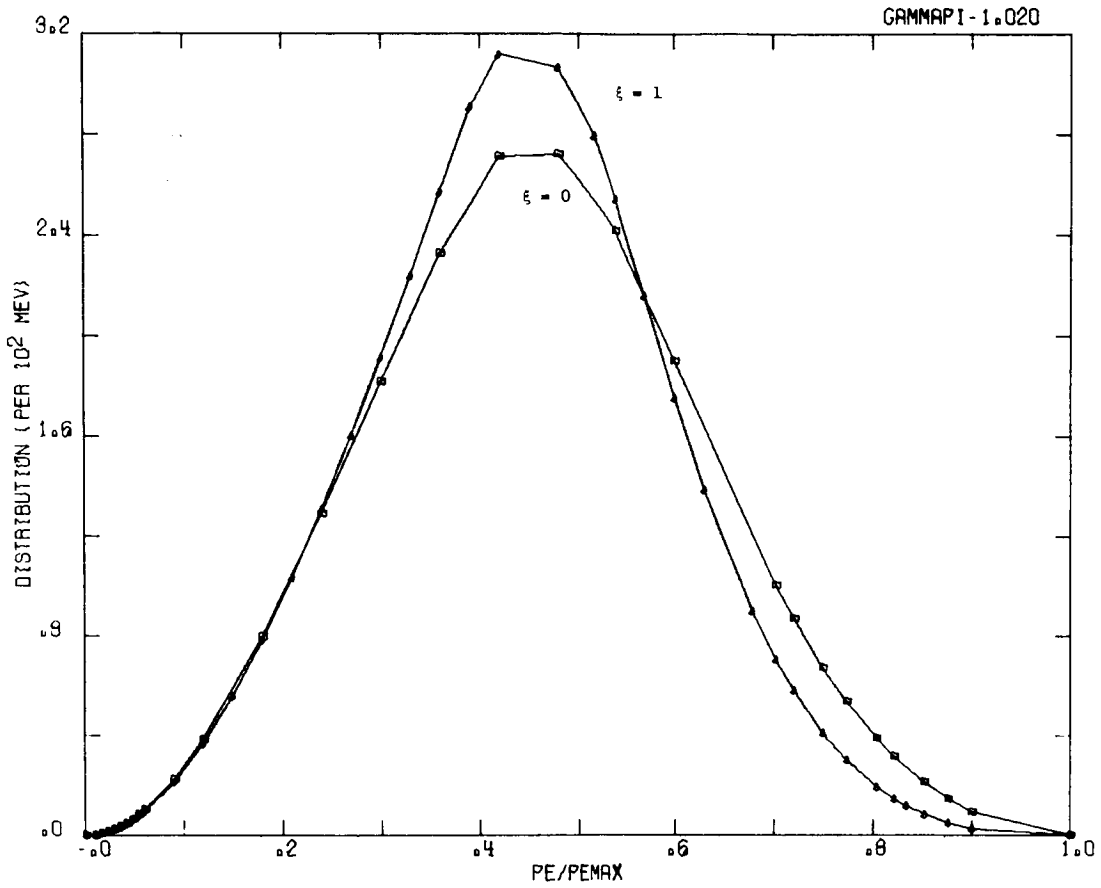
Graph 28. Electron Distribution Function ($\xi = 1$)



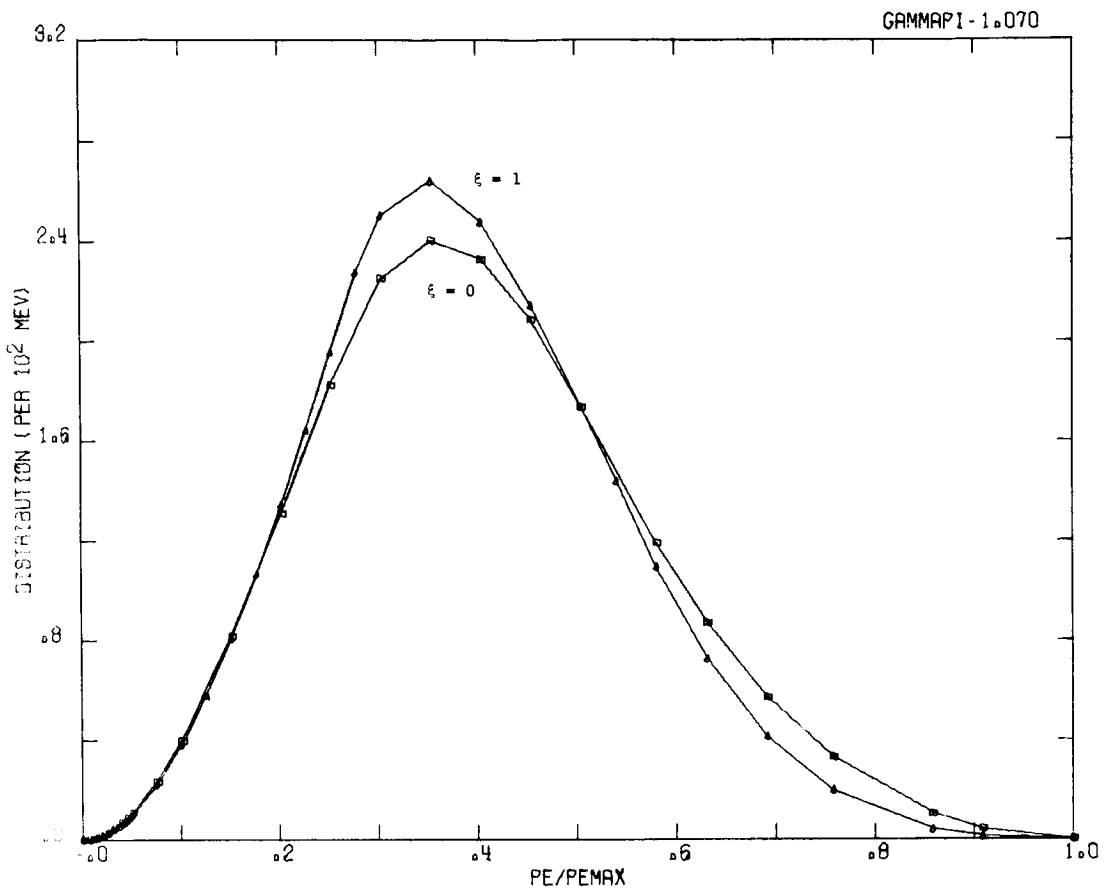
Graph 29. Electron Distribution Function ($\xi = 1$)



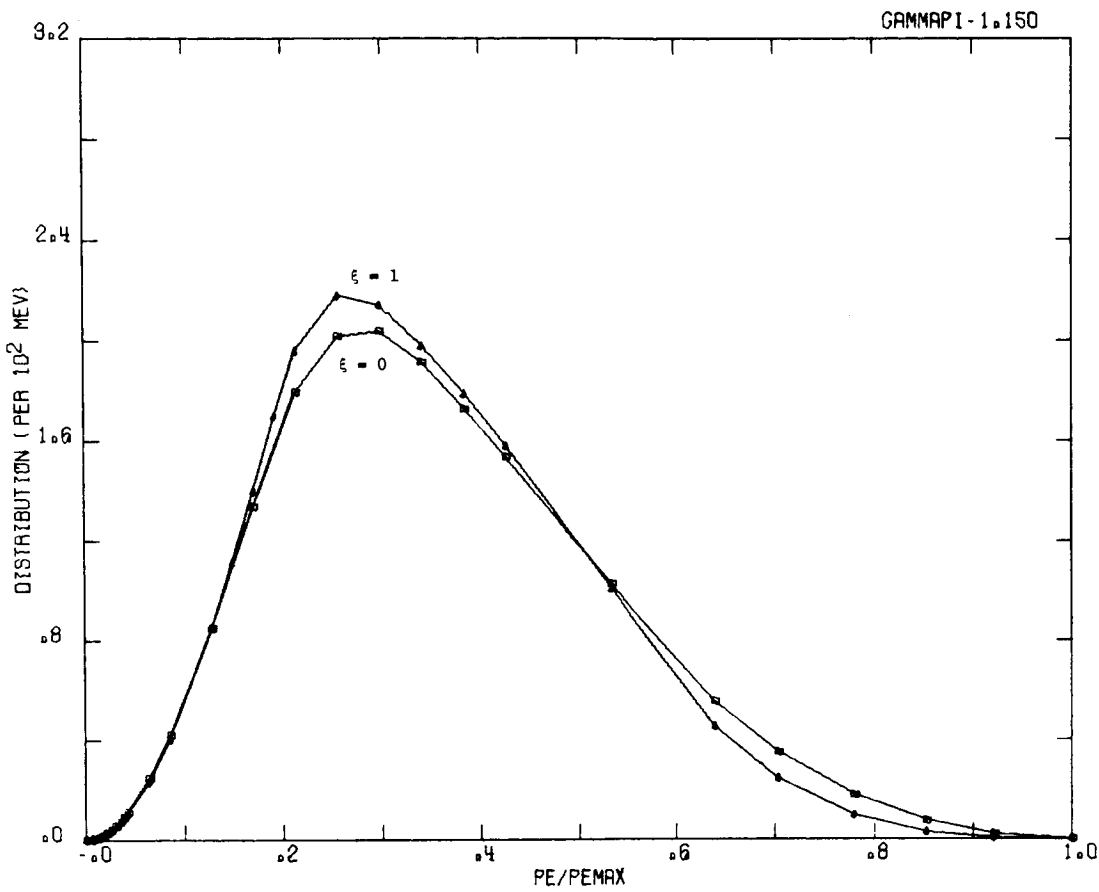
Graph 30. Electron Distribution Function ($\xi = 1$)



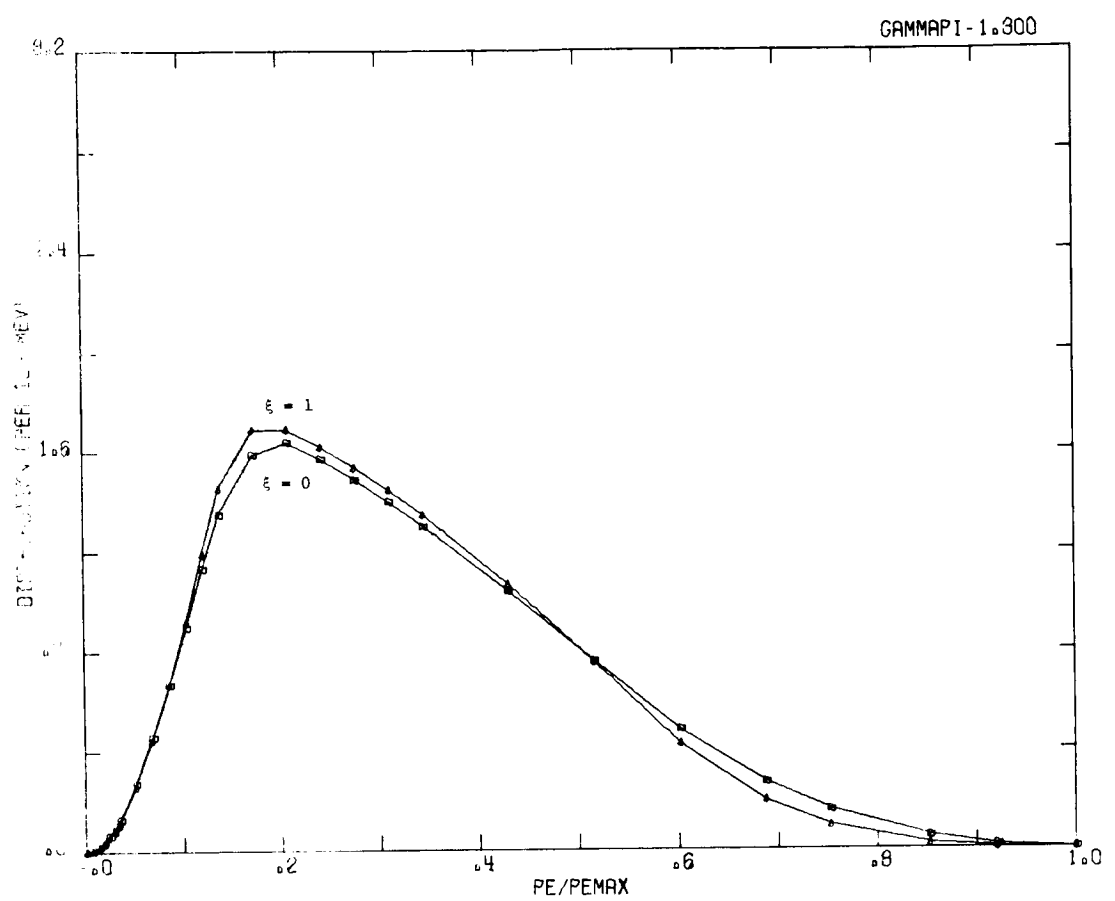
Graph 31. Electron Distribution Function ($\xi = 1, 0$)



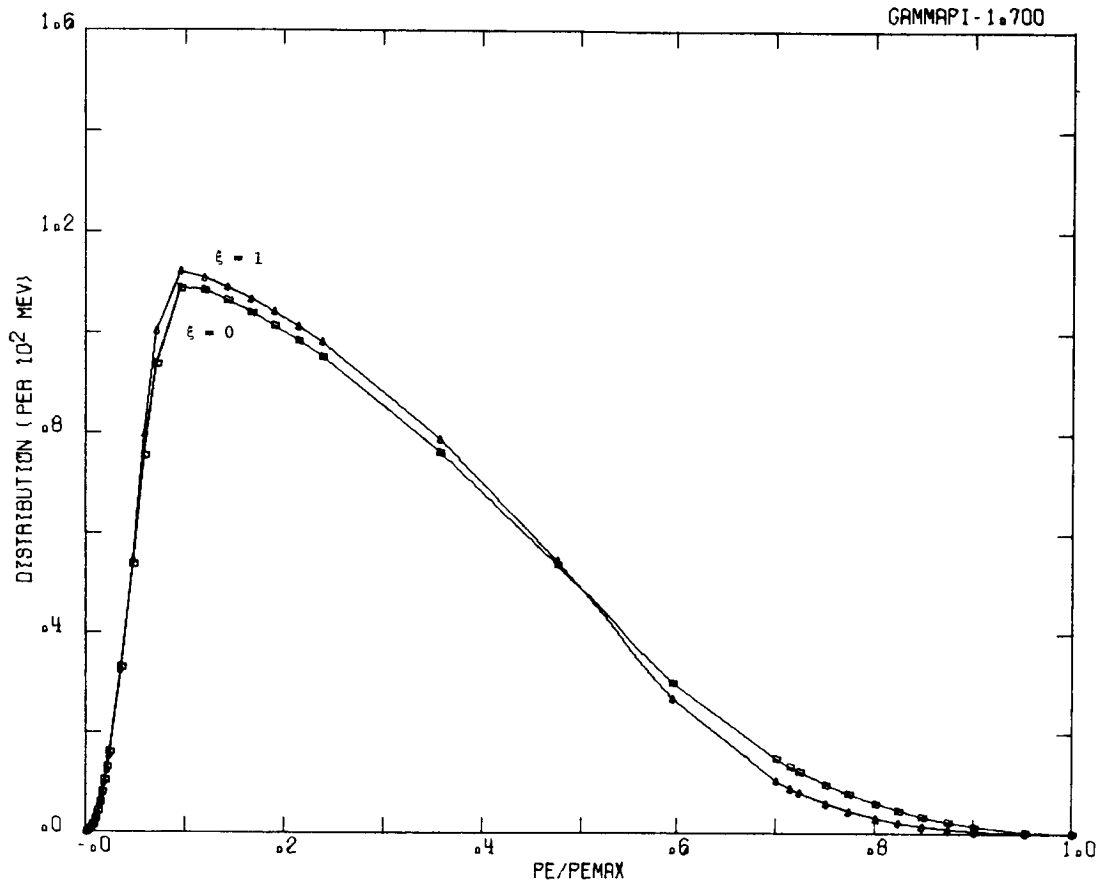
Graph 32. Electron Distribution Function ($\xi = 1, 0$)



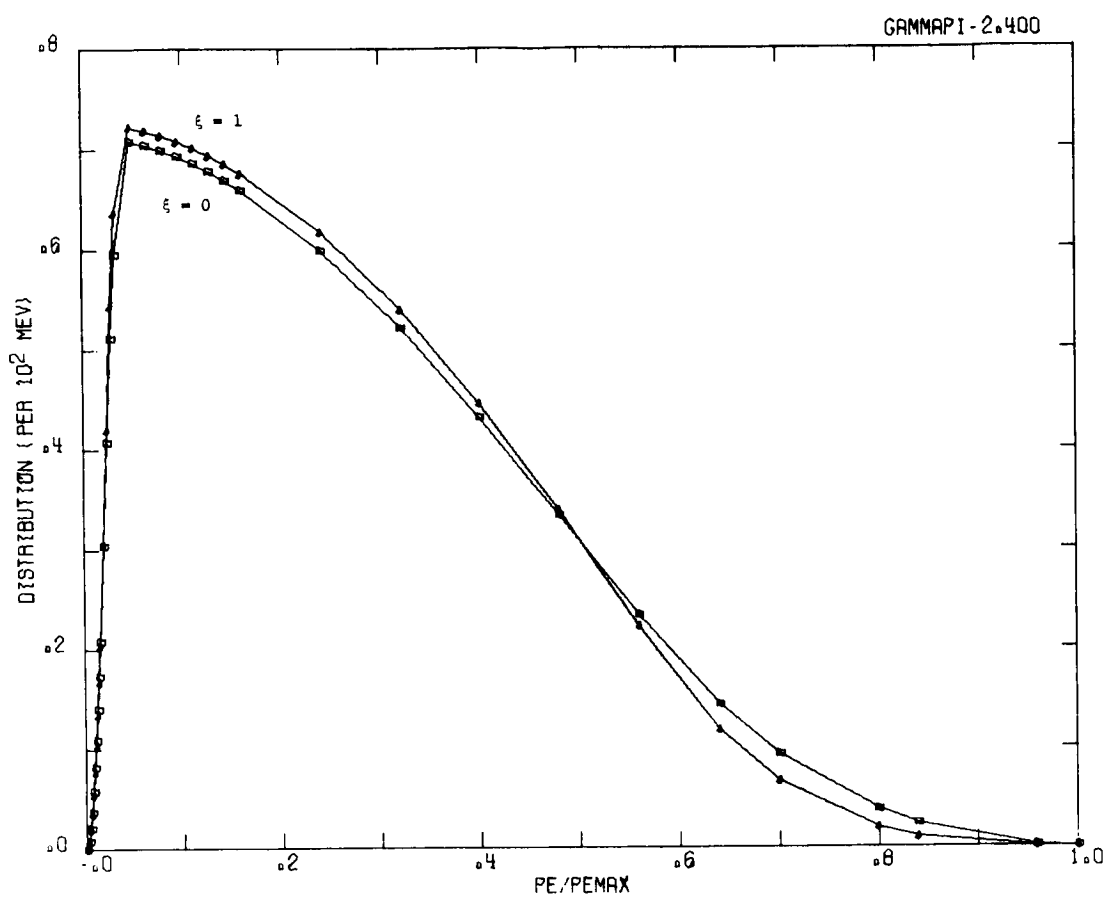
Graph 33. Electron Distribution Function ($\xi = 1, 0$)



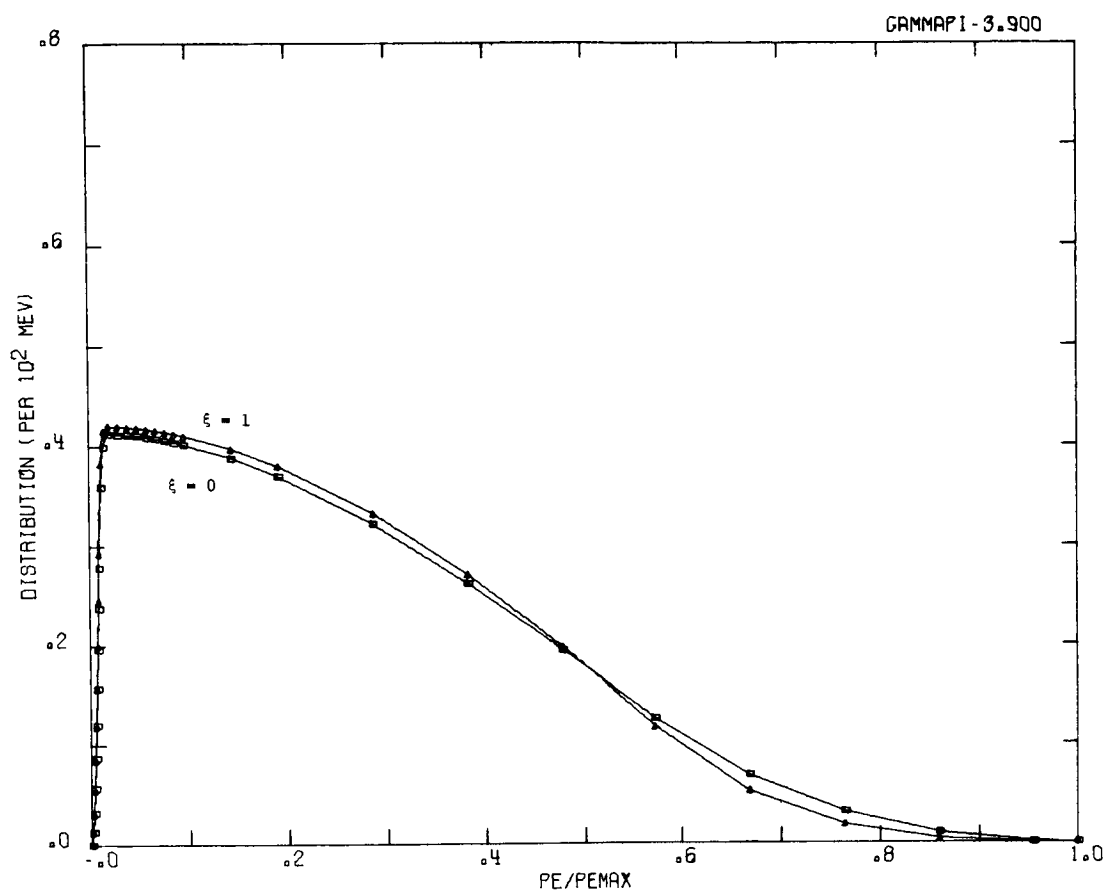
Graph 34. Electron Distribution Function ($\xi = 1, 0$)



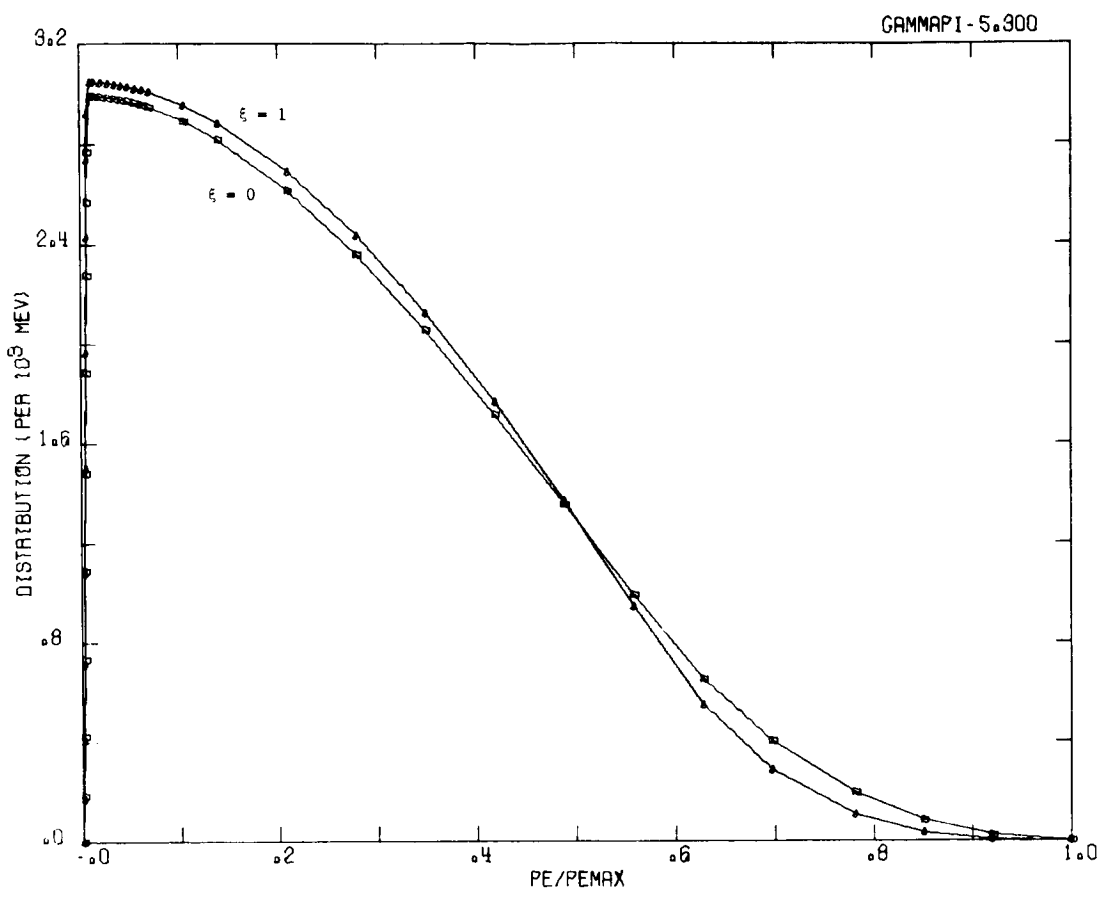
Graph 35. Electron Distribution Function ($\xi = 1, 0$)



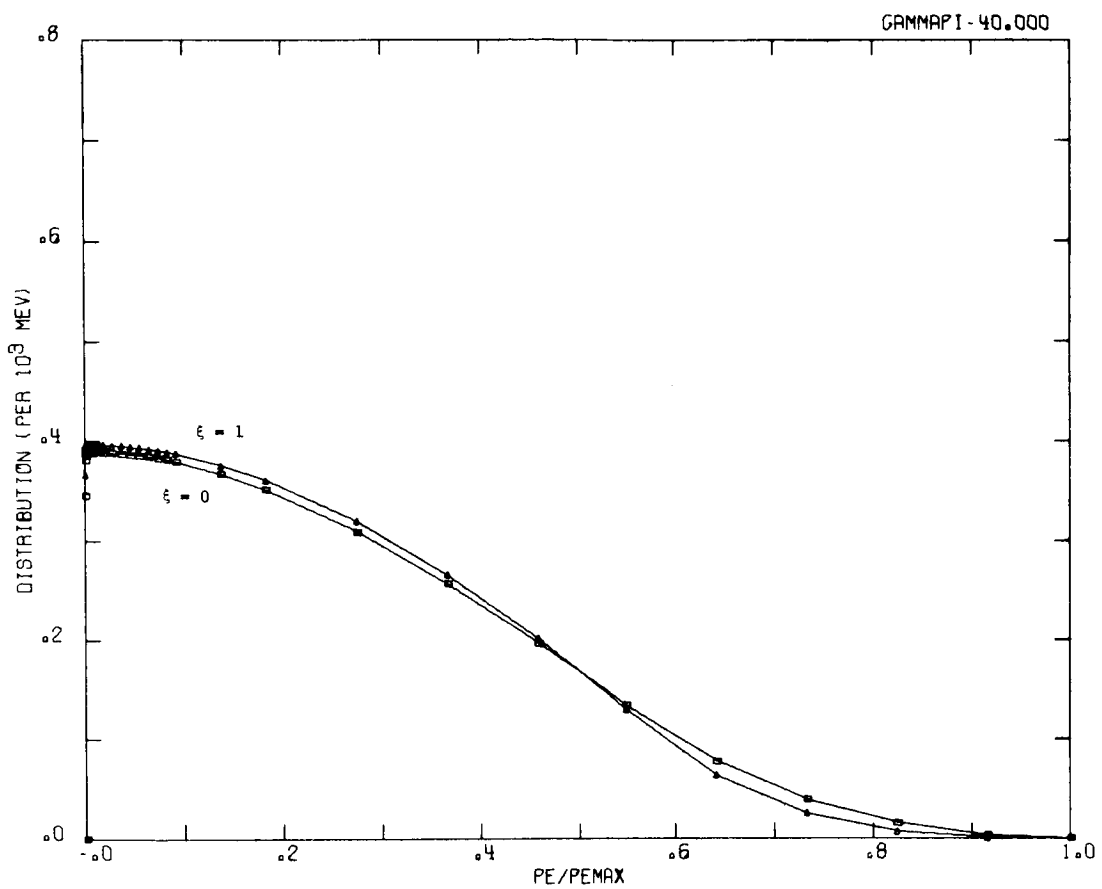
Graph 36. Electron Distribution Function ($\xi = 1, 0$)



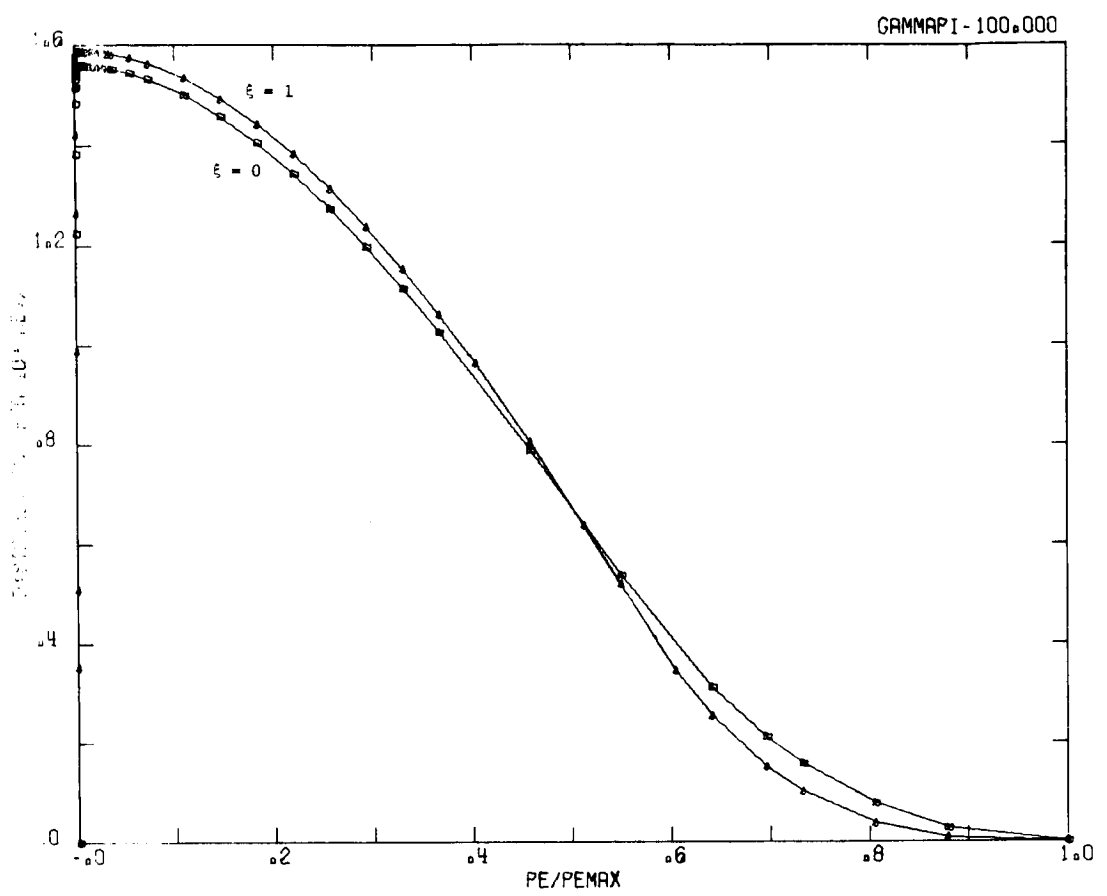
Graph 37. Electron Distribution Function ($\xi = 1, 0$)



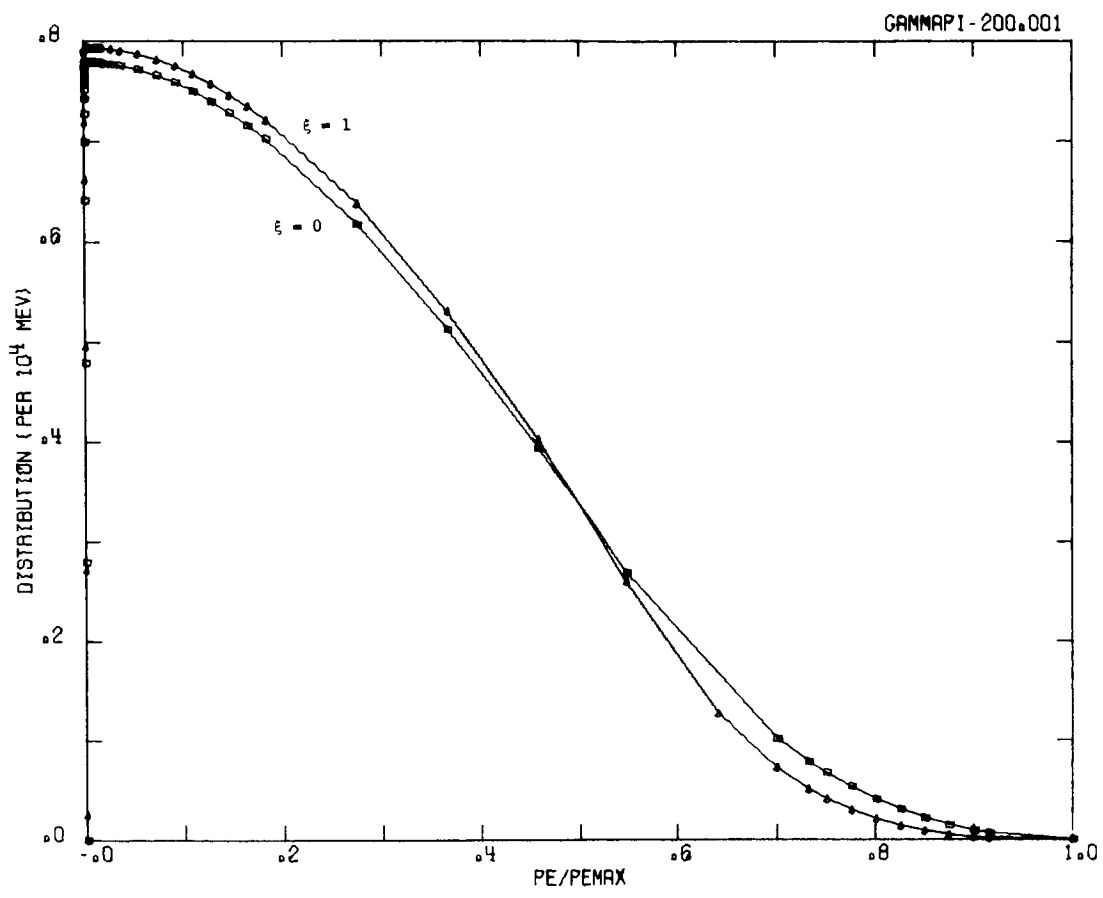
Graph 38. Electron Distribution Function ($\xi = 1, 0$)



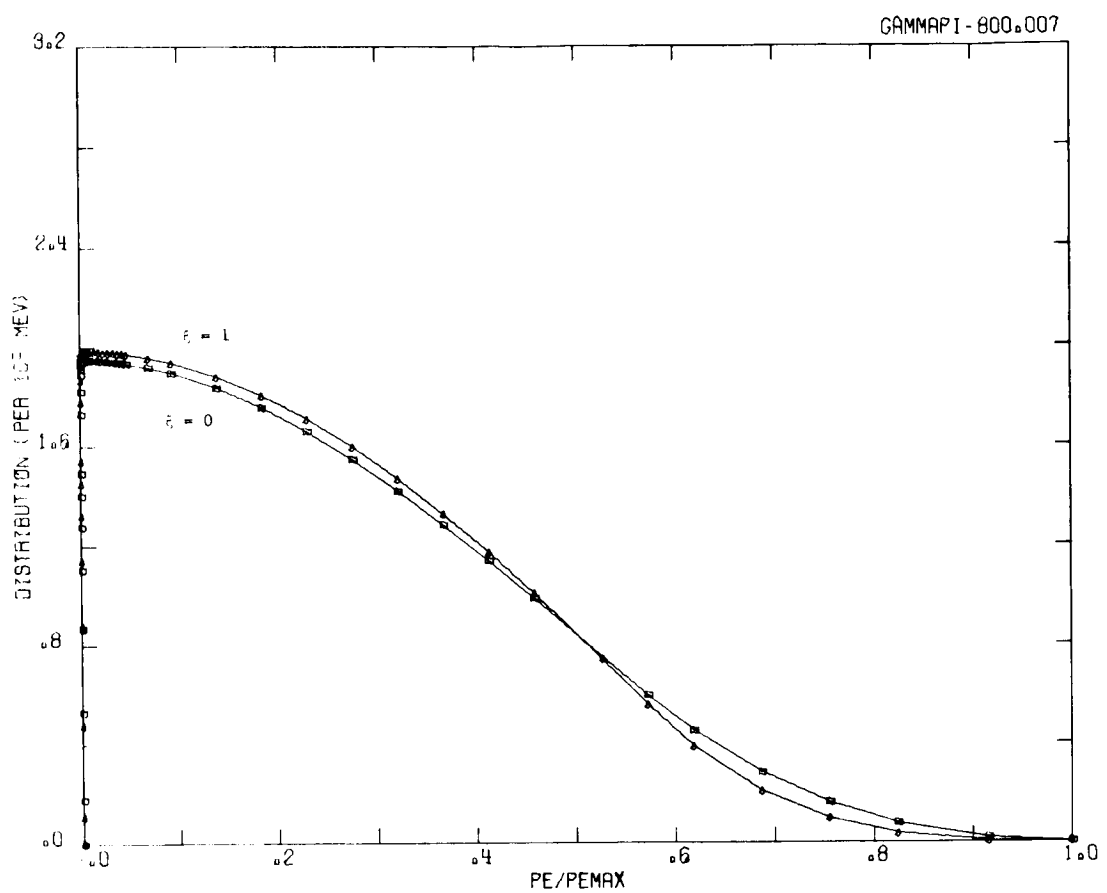
Graph 39. Electron Distribution Function ($\xi = 1, 0$)



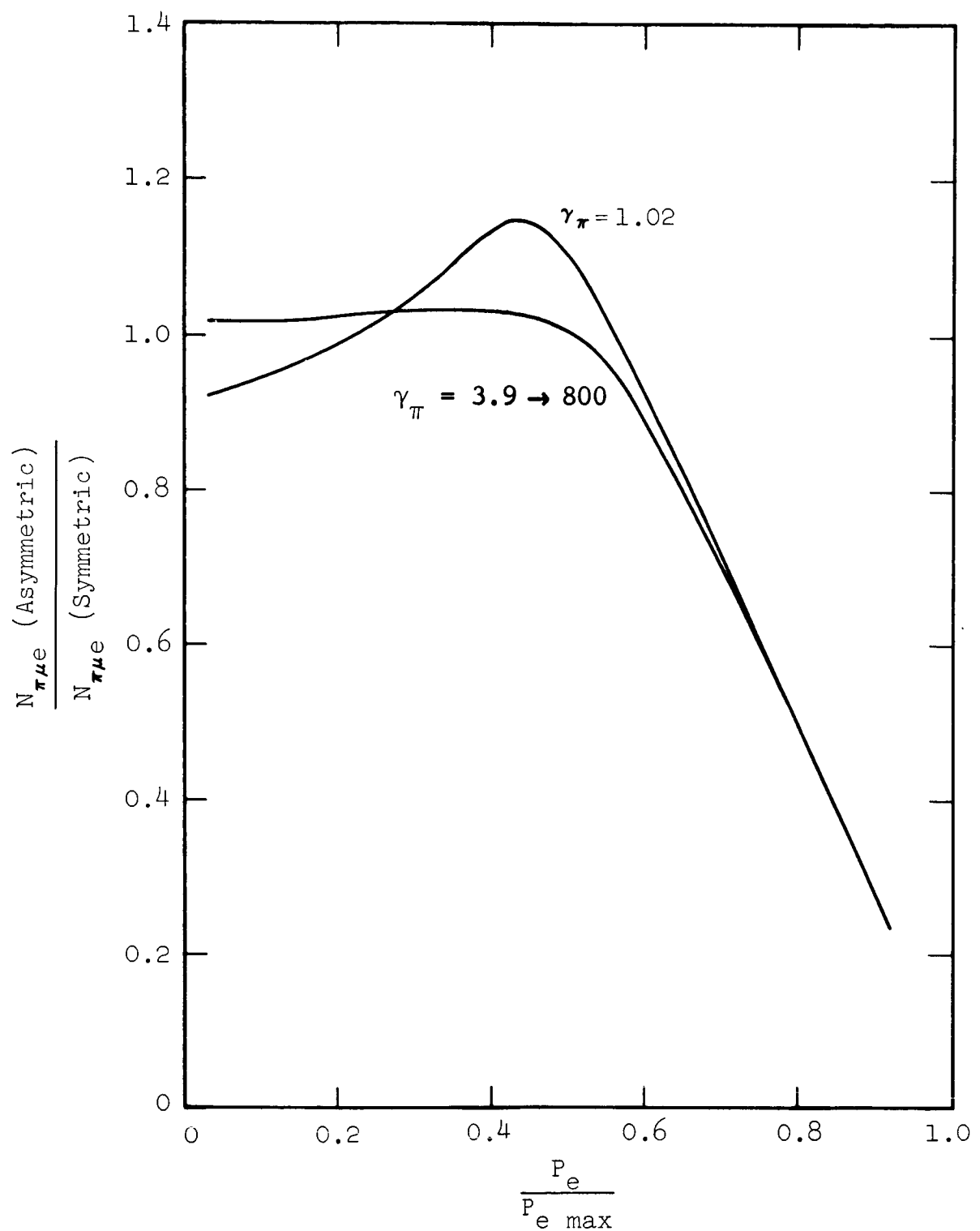
Graph 40. Electron Distribution Function ($\xi = 1, 0$)



Graph 41. Electron Distribution Function ($\xi = 1, 0$)



Graph 42. Electron Distribution Function ($\zeta = 1, 0$)



Graph 43. Effect of mu CMS Asymmetry on Electron Distribution

CHAPTER V

DISCUSSION

Numerical Results

From a comparison of Graphs 27 through 30 it is seen that as γ_{π} increases the peak of the distribution function decreases, and (on a logarithmic γ_e scale) the curve flattens. At $\gamma_{\pi} = 1.02$, $N_{\pi\mu e}$ reaches a peak value of 0.31×10^{-1} mev⁻¹. As γ_{π} approaches 800, because of the greatly enlarged electron energy range allowed, the maximum value of $N_{\pi\mu e}$ falls to 0.20×10^{-4} mev⁻¹.

The changes in $N_{\pi\mu e}$ due to the μ CMS anisotropy are shown in Graphs 31 through 42. The asymmetry causes an increase in the maximum of the distribution, which is accompanied by a lowering of the level of $N_{\pi\mu e}$ at the larger electron energies. The ratios of the asymmetric to the symmetric distributions plotted in Graph 43 show that for average electron energies the increase in $N_{\pi\mu e}$ due to anisotropy reaches about 15 per cent at the smaller pion energies, but is less than 5 per cent at a pion energy of

110 bev. At the higher electron energies, the percentage decrease in the distribution function becomes quite appreciable; for $\gamma_e \approx 0.9 \gamma_{e \text{ max}}$, it is nearly 80 per cent for all pion energies.

Previous investigators employing the $\pi\mu e$ decay to calculate the equilibrium spectrum of electrons in space have assumed, in addition to μ CMS isotropy, that the pions are sufficiently energetic to produce muons with the same speed as the pions in the lab frame. Because our analysis of the decays treats these situations exactly, possible approximation errors generated in these earlier calculations are avoided.

Our $\pi\mu e$ formulation offers the advantage that it holds for all pion energies. We are restricted neither to very small nor very large values of p_π . These results will therefore be applicable to any processes in which intermediate energy pions play a significant part.

Possible Future Uses

Calculation of the equilibrium spectrum of electrons in space is the logical extension of this research. We have the energy spectrum of electrons due to the decay of monoenergetic pions in interstellar space. The electron

spectrum at each pion energy must then be weighted over the whole range of pion energies according to the energy distribution of pions created by monoenergetic cosmic ray collisions. The resulting electron spectrum for each cosmic ray collisional energy must in turn be weighted by the estimated distribution in energy of the cosmic rays in space. The ensuing distribution is the total production spectrum of electrons in space from cosmic ray collisions. This can be combined with other input data in the particle diffusion equations to obtain the equilibrium spectrum of electrons, which may then be compared with the measurements to be made by scientific space vehicles.

Another possible related problem is the spectra of electrons from hyperon and kaon decays, because these heavier unstable particles frequently decay into pions. The kaons are presently of particular interest. When the energy of cosmic rays is sufficiently far above the threshold for production of additional particles, a certain number of charged K mesons will be created in addition to the more frequent pi mesons. It would be useful, therefore, to know the energy spectrum of electrons from K^\pm decay as well as from π^\pm decay.

The predominant mode of charged kaon decay is $K_{\mu 2}$ ($K^+ \rightarrow \mu^+ + \nu$), with a branching ratio of nearly 60 per cent (Snow and Shapiro [1961]). Since the muon from $K_{\mu 2}$ decay appears to exhibit the same decay asymmetry as the muon from pion decay (Williams [1961]), our kinematical analysis of $\pi-\mu-e$ decay is expected to apply to $K-\mu-e$ decay as well, with some modifications, if any, to allow for the $K - \pi$ mass difference.

The $K_{\pi 2}$ mode ($K^+ \rightarrow \pi^+ + \pi^0$), with a branching ratio of 26 per cent, is the second most important charged kaon mode. The distribution of pions from K decay, when combined with our $N_{\pi\mu e}$ results, would yield the distribution of electrons from $K_{\pi 2}$ decay. These two K decay modes alone should account for nearly 80 per cent of the electrons eventually resulting from charged K decay.

It will be remembered that our formulas for $N_{\pi\mu e}$ were derived in closed form. This could prove an advantage in applications of pion decay, since it offers the possibility of obtaining analytical solutions to the problems. Alternately, electron distributions could be calculated for very many γ_π values with the present program, using as small a γ_π increment as is necessary for satisfactory numerical integration.

APPENDIX A

ANGLE AND ENERGY LIMITS AFTER LORENTZ TRANSFORMATION

When a transformation is effected from one Lorentz frame to another, the permitted values of energy and direction of a particle undergo change. Consider a system in which an electron can have any momentum \tilde{P}_e between 0 and $\tilde{P}_{e\ max}$, and let its direction be unrestricted. Take this system to be moving with speed β along the polar axis of a second system in which P_e and θ_e are the electron momentum and polar angle, respectively. See Fig. A1. Consider now the effect of this transformation on the range of allowed energies.

Energy Limits

The energy transformation equation may be written

$$E_e = \gamma \tilde{E}_e + p \tilde{P}_e \cos \tilde{\theta}_e \quad (A-1)$$

in which $\tilde{\theta}_e$ is the polar angle in the \tilde{P}_e system, and where γ is the usual $1/\sqrt{1 - \beta^2}$ and $p = \gamma\beta$. If,

coincidentally, the \tilde{P}_e frame happens to be the rest frame of some decaying particle, then the kinematic parameters γ and p are simply the nondimensionalized energy and momentum of the decay particle, respectively.

It is quite easy to see that E_e reaches its maximum value at

$$E_{e \max} = \gamma \tilde{E}_{e \max} + p \tilde{P}_{e \max}. \quad (A-2)$$

This corresponds to a momentum

$$P_{e \max} = \gamma \tilde{P}_{e \max} + p \tilde{E}_{e \max}. \quad (A-3)$$

To establish expressions for the minimum energy value it is necessary to consider separately two cases, $p < \tilde{P}_{e \max}$ and $p > \tilde{P}_{e \max}$.

For $p < \tilde{P}_{e \max}$, a deductive proof may be omitted. It is easy to verify that the conditions $\tilde{\theta}_e = \pi$ and $\tilde{p}_e = p$ in the rest frame will yield

$$E_{e \min} = m_e, \quad p < \tilde{P}_{e \max} \quad (A-4)$$

in the moving frame of the decay particle. This is, of course, the absolute minimum energy permitted to the electron since

$$P_e \min = 0 , \quad p < \tilde{p}_e \max . \quad (A-5)$$

Consider $p > \tilde{p}_e \max$. For fixed γ and \tilde{E}_e , E_e in Eq.

(A-1) has a minimum when $\tilde{\theta}_e = \pi$

$$E'_e = \gamma \tilde{E}_e - p \tilde{P}_e .$$

Now $d E'_e / d \tilde{P}_e < 0$ for $p > \tilde{p}_e$, so that E'_e decreases monotonically with \tilde{P}_e . It therefore reaches its minimum at $\tilde{P}_e \max$

$$E_e \min = \gamma \tilde{E}_e \max - p \tilde{P}_e \max , \quad p > \tilde{p}_e \max \quad (A-6)$$

$$P_e \min = p \tilde{E}_e \max - \gamma \tilde{P}_e \max , \quad p > \tilde{p}_e \max . \quad (A-7)$$

Momentum Ellipses

The device of momentum ellipses provides a convenient pictorial representation of these relations. From the Lorentz transformation equations

$$P_{e_x} = \gamma \tilde{P}_{e_x} + p \tilde{E}_e \quad (A-8)$$

$$P_{e_y} = \tilde{P}_{e_y}$$

the components in the rest frame can be eliminated

$$\frac{(P_{ex} - p \tilde{E}_e)^2}{(\gamma \tilde{P}_e)^2} + \frac{P_{ey}^2}{\tilde{P}_e^2} = 1 . \quad (A-9)$$

Thus a circle $\tilde{P}_e = \text{constant}$ in the rest frame transforms in the lab system to an ellipse with center displaced a distance $h = p \tilde{E}_e$ along the positive x axis, and with semimajor axis $a = \gamma \tilde{P}_e$ and semiminor axis $b = \tilde{P}_e$. See Figs. A2 and A3.

Now

$$a + h = \gamma \tilde{P}_e + p \tilde{E}_e \quad (A-10)$$

$$a - h = \gamma \tilde{P}_e - p \tilde{E}_e . \quad (A-11)$$

From the behavior of Eqs. (A-9) - (A-11) with \tilde{P}_e , it is possible to demonstrate that momentum ellipses resulting from different \tilde{E}_e are completely nested, with the outermost corresponding to $\tilde{E}_{e \max}$. See Figs. A4 and A5.

Note that $a + h$ for $\tilde{E}_e = \tilde{E}_{e \max}$, which corresponds to point A in both figures, is just $P_{e \max}$ of Eq. (A-3). It is evident from Fig. A4 that for the case $\tilde{P}_{e \max} > p$ the ellipse $\tilde{P}_e = p$ yields $P_{e \min} = 0$, in agreement with Eq. (A-5). And $h - a$ for $\tilde{E}_e = \tilde{E}_{e \max}$,



Fig. A1 Lorentz Transformation

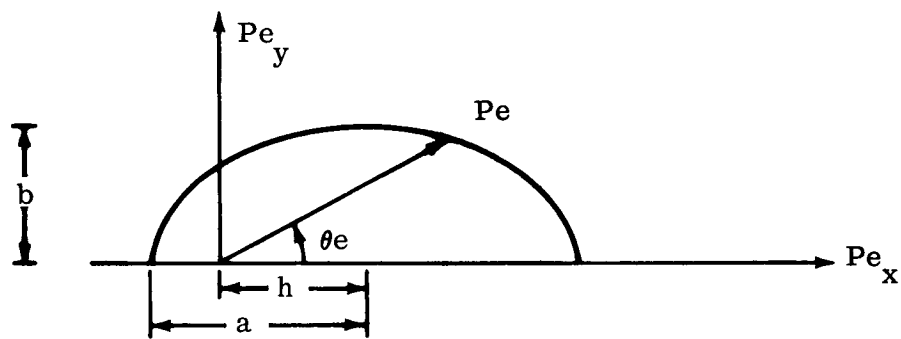


Fig. A2 Momentum Ellipse for $\tilde{p}_e > p$

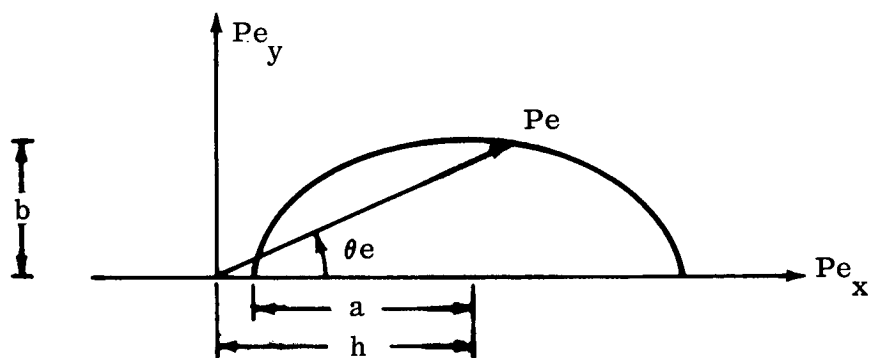


Fig. A3 Momentum Ellipse for $\tilde{p}_e < p$

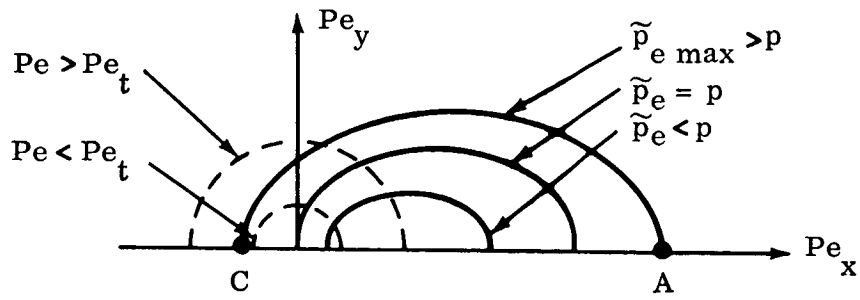


Fig. A4 Nest of Momentum Ellipses for $\tilde{p}_e \text{ max} > p$

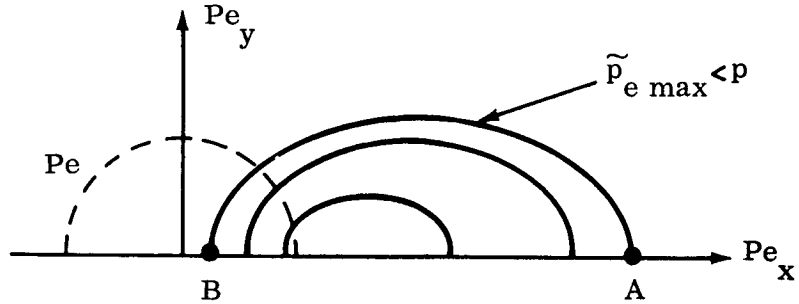


Fig. A5 Nest of Momentum Ellipses for $\tilde{p}_e \text{ max} < p$

corresponding to point B in Fig. A5, is just $P_e \min$ for the case $\tilde{P}_e \max < p$, given by Eq. (A-7).

Angle Limits

The most convenient (though not the most rigorous) method of obtaining the angular extremes in the moving system of the decay particle is to employ the momentum ellipses. From Figs. A4 and A5, one can see that, for any allowed value of P_e , the minimum angle of emission permitted is

$$\theta_e \min = 0 . \quad (A-12)$$

That is, forward emission is always possible. Define, for $\tilde{P}_e \max > p$

$$P_{e_t} = \gamma \tilde{P}_e \max - p \tilde{E}_e \max \quad (A-13)$$

corresponding to point C in Fig. A4. Then for values of P_e smaller than P_{e_t} there is some momentum ellipse for which emission at $\theta_e = \pi$ is possible. Thus

$$y_m = -1 , \quad P_e < P_{e_t}, \quad \tilde{P}_e \max > p \quad (A-14)$$

where

$$y_m = \cos \theta_{e \max} . \quad (A-15)$$

For values of P_e larger than P_{et} , however, there is an upper limit on the angle of emission permitted. From the Lorentz transformation of $\tilde{E}_{e \max}$ this is seen to be

$$y_m = y_p , \quad P_e > P_{et}, \quad \tilde{p}_{e \max} > p \quad (A-16)$$

where

$$y_p = \frac{\gamma E_e - \tilde{E}_{e \max}}{p P_e} . \quad (A-17)$$

For $\tilde{p}_{e \max} < p$, clearly θ_e is always restricted. As before

$$y_m = y_p , \quad \tilde{p}_{e \max} < p . \quad (A-18)$$

These relations for the θ_e extremes can also be derived on a more formal basis than has been done here.

It should be pointed out that the above limitations on energy and angle hold not merely for electrons but for any particle that is transformed from one frame where it has a continuum of momenta between zero and some maximum, to some other Lorentz frame of the type defined.

Although it may happen that the parameters γ and

p may be associated with the nondimensionalized energy and momentum of some decay particle, it should be remembered that this is coincidental, not necessary. For this reason, the γ and p need not characterize the particle directly causing the decay; they may represent any particle from whose rest frame the electrons are being transformed. Therefore, the above expressions for energy and angle limits will hold for transforming the electron not only from the muon rest frame to the pion rest frame with $\gamma = \gamma_{\mu}$, but also from the pion rest frame to the pion moving frame with $\gamma = \gamma_{\pi}$.

APPENDIX B

REGION OF MUON ANGULAR INTEGRATION

To determine the region over which the muon direction must be integrated, it is necessary to examine the variation of the muon polar angle λ with U for specific values of λ_e and $\bar{\theta}_e$. Expression (42) for $\sin \lambda_{\pm}$ is a convenient starting point. One can learn much about the properties of λ_{\pm} by imposing known physical and mathematical restrictions on its values.

We shall first require $\sin \lambda \geq 0$. There are eight separate cases to be considered.

(1) $s, \bar{y}, \delta_e > 0$. The ratio of the second term (without the preceding \pm) to the first term in Eq. (42) is

$$r = \frac{\delta_e}{\bar{y}} \sqrt{1 + \frac{\delta_e^2 - \bar{y}^2}{s^2}} .$$

The (+) root is not restricted. The (-) root, however, is prohibited whenever the second term is the larger, i.e., $r > 1$. This occurs when $\delta_e > \bar{y}$, or $\bar{\theta}_e > \lambda_e$.

(2) $s, \bar{y} < 0; \delta_e > 0$. Since s is now negative, r becomes

$$r = -\frac{\delta_e}{\bar{y}} \sqrt{1 + \frac{\delta_e^2 - \bar{y}^2}{s^2}}.$$

The $(-)$ root is not permitted when $\delta_e > -\bar{y}$, i.e., $\bar{\theta}_e < \pi - \lambda_e$.

(3) $s, \delta_e > 0; \bar{y} < 0$. Since the first term in Eq. (42) is negative, the $(-)$ root is always forbidden.

The $(+)$ root is also forbidden when $\bar{\theta}_e > \pi - \lambda_e$.

(4) $s < 0; \bar{y}, \delta_e > 0$. The $(-)$ root is prohibited. For $\bar{\theta}_e < \lambda_e$, the $(+)$ root also is.

(5) $s, \bar{y} > 0; \delta_e < 0$. One finds that the $(+)$ root is not allowed when $\bar{\theta}_e > \pi - \lambda_e$.

(6) $s, \bar{y}, \delta_e < 0$. The $(+)$ root in $\sin \lambda$ is prohibited if $\bar{\theta}_e < \lambda_e$.

(7) $s > 0; \bar{y}, \delta_e < 0$. The $(+)$ root is never permitted. The $(-)$ root is likewise not permitted if $\bar{\theta}_e > \lambda_e$.

(8) $s, \delta_e < 0; \bar{y} > 0$. The $(+)$ root is prohibited. The $(-)$ root is prohibited for $\bar{\theta}_e < \pi - \lambda_e$.

These results are summarized in Table B-I. The restrictions of $\bar{\theta}_{eL}$ and $\bar{\theta}_{eH}$ are discussed below.

We now require Eqs. (41) and (42) to yield real

TABLE B-I

ALLOWED SIN λ ROOTS

	$\bar{\theta}_e$	Allowed Root
$\lambda_e < \pi/2, U < \pi/2$	$\bar{\theta}_{eL} < \bar{\theta}_e < \lambda_e$	\pm
	$\lambda_e < \bar{\theta}_e < \pi - \lambda_e$	$+$
	$\pi - \lambda_e < \bar{\theta}_e$	None
$\lambda_e < \pi/2, U > \pi/2$	$\bar{\theta}_e < \lambda_e$	None
	$\lambda_e < \bar{\theta}_e < \pi - \lambda_e$	$+$
	$\pi - \lambda_e < \bar{\theta}_e < \bar{\theta}_{eH}$	\pm
$\lambda_e > \pi/2, U < \pi/2$	$\bar{\theta}_{eL} < \bar{\theta}_e < \pi - \lambda_e$	\pm
	$\pi - \lambda_e < \bar{\theta}_e < \lambda_e$	-
	$\lambda_e < \bar{\theta}_e$	None
$\lambda_e > \pi/2, U > \pi/2$	$\bar{\theta}_e < \pi - \lambda_e$	None
	$\pi - \lambda_e < \bar{\theta}_e < \lambda_e$	-
	$\lambda_e < \bar{\theta}_e < \bar{\theta}_{eH}$	\pm

roots. This means that

$$\sin \bar{\theta}_e \geq |\sin \lambda_e| \sin U \quad (B-1)$$

must be satisfied. This cuts off the $\bar{\theta}_e$ values that can contribute to a given (λ_e, U) combination. For $\bar{\theta}_e < \pi/2$, call this limiting value $\bar{\theta}_{eL}$; for $\bar{\theta}_e > \pi/2$, call it $\bar{\theta}_{eH}$.

$$\sin \bar{\theta}_{eL, H} = |\sin \lambda_e| \sin U . \quad (B-2)$$

The effect of this cutoff is seen in Table B-I.

One can make a series of sketches illustrating the various conditions in Table B-I. We have done this, and the pictures seem to verify the existence of two, one, or no solutions in the corresponding cases. Sample calculations for nineteen different combinations of λ_e , U , and $\bar{\theta}_e$, covering all the possible cases in Table B-I, have been performed. All the results are in agreement with the Table.

The conditions $\sin \lambda \leq 1$ and $\cos^2 \lambda \leq 1$ yield no new restrictions.

Some useful limiting relations for Eqs. (41) and (42) are

$$\begin{aligned} \lambda_- &= 0 \quad \text{for } \bar{\theta}_e = \lambda_e \\ \lambda_+ &= \pi \quad \text{for } \bar{\theta}_e = \pi - \lambda_e \end{aligned} \quad \left. \right\} \quad |U| < \pi/2$$

$$\begin{aligned} \lambda_- &= \pi \quad \text{for } \bar{\theta}_e = \pi - \lambda_e \\ \lambda_+ &= 0 \quad \text{for } \bar{\theta}_e = \lambda_e \end{aligned} \quad \left. \right\} |U| > \pi/2 . \quad (B-3)$$

And from Eq. (B-2)

$$\begin{aligned} \bar{\theta}_{eL} &= 0 \quad \text{for } |U| = 0 \\ &= \lambda_e \quad \text{for } |U| = \pi/2 \\ \bar{\theta}_{eH} &= \pi - \lambda_e \quad \text{for } |U| = \pi/2 \\ &= \pi \quad \text{for } |U| = \pi \end{aligned} \quad \left. \right\} \lambda_e < \pi/2 \quad (B-4)$$

$$\begin{aligned} \bar{\theta}_{eL} &= 0 \quad \text{for } |U| = 0 \\ &= \pi - \lambda_e \quad \text{for } |U| = \pi/2 \\ \bar{\theta}_{eH} &= \lambda_e \quad \text{for } |U| = \pi/2 \\ &= \pi \quad \text{for } |U| = \pi \end{aligned} \quad \left. \right\} \lambda_e > \pi/2 . \quad (B-5)$$

Before drawing diagrams of the variation of λ vs. U with $\bar{\theta}_e$ as parameter, we wish to prove that z_+ (z_-) increases (decreases) monotonically with \bar{y} for fixed U . This will assure us that no intersection of curves corresponding to different $\bar{\theta}_e$ values occurs.

The derivative of z_+ with respect to \bar{y} is given by

$$\frac{A^2 \partial z_{\pm}}{\partial \bar{y}} = \delta_e \pm s \cot C \quad (B-6)$$

where

$$\cot C = \frac{\bar{y}}{\sqrt{A^2 - \bar{y}^2}} . \quad (B-7)$$

This may also be written as

$$\frac{A^2}{\bar{y}} \frac{\partial z_{\pm}}{\partial \bar{y}} = \pm \frac{\sin \lambda_{\pm}}{\sqrt{A^2 - \bar{y}^2}} . \quad (B-8)$$

Thus the derivative of z goes to zero when $\sin \lambda = 0$.
(Cf. Eqs. [B-3]).

It is necessary to consider separately the four cases in Table B-I. Consider the first case, for which s and δ_e are positive. In the second term of Eq. (B-6), multiplying $\cot C$ by s merely alters the level of the points a bit but not the general shape of the curve. See Figs. B1 and B2. For z_+ , the addition of the first term translates the whole curve upward so that $\partial z_+ / \partial \bar{y}$ goes to zero for some value of $\bar{\theta}_e > \pi/2$. See Fig. B3. From Eqs. (B-3) and (B-8) together with Table B-I it is seen that this point corresponds to $\pi - \lambda_e$, the largest possible $\bar{\theta}_e$ value. The change of z_+ with \bar{y} is always positive, therefore, for given values of λ_e and U .

In similar fashion one can treat z_- for this case. The behavior pictured in Fig. B4 is found. Since

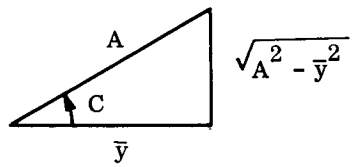


Fig. B1 Definition of C

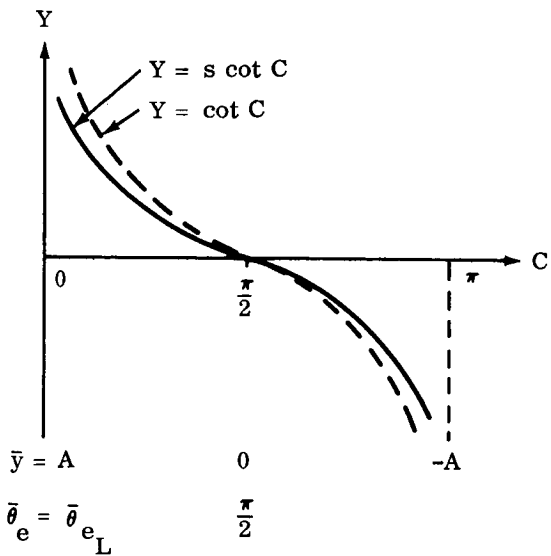


Fig. B2 $s \cot C$ for $s > 0$

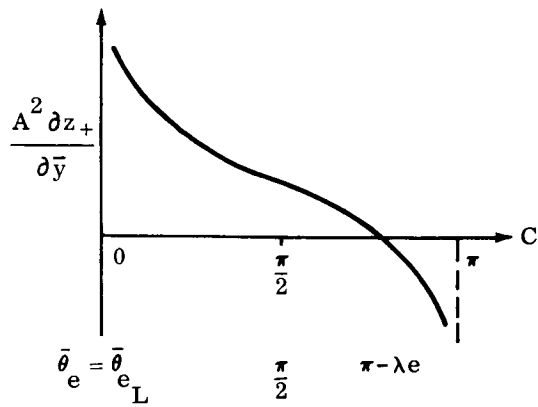


Fig. B3 Z_+ Derivative for $s, \delta e > 0$

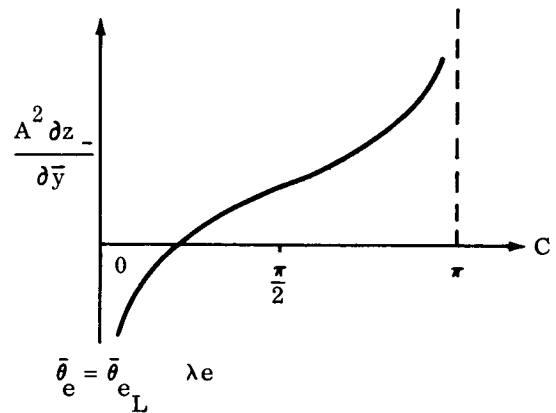


Fig B4 Z_- Derivative for $s, \delta e > 0$

λ_e is the maximum $\bar{\theta}_e$ value allowed for the negative root, this means that $\partial z_- / \partial \bar{y}$ is always negative.

In much the same manner one can show for all cases that z_+ (z_-) increases (decreases) monotonically with \bar{y} for fixed λ_e and U . No λ vs. U curves corresponding to different $\bar{\theta}_e$ values can therefore intersect.

With all the above facts at hand it is possible to construct diagrams illustrating the variation of λ vs. U . These are given as Figs. 9 and 10.

APPENDIX C

SOLUTION OF L_i INTEGRALS

To evaluate the L_i integrals given by Eqs. (40), for the six different cases, it is helpful to introduce certain families of integrals in terms of which the L_i can eventually be expressed.

Define

$$I_n(\alpha) = \int_{1 - \sin \alpha}^{1 + \sin \alpha} dr \frac{1}{r^n \sqrt{\varphi}} \quad (C-1)$$

$$I^n(\alpha) = \int_{1 - \sin \alpha}^{1 + \sin \alpha} dr \frac{\sqrt{\varphi}}{r^n} \quad (C-2)$$

where

$$\varphi(\alpha) = -r^2 + 2r - Y^2 = \sin^2 \alpha - (r - 1)^2 \quad (C-3)$$

$$Y = \cos \alpha . \quad (C-4)$$

The I^n and I_n are related by

$$I^n = - I_{n-2} + 2 I_{n-1} - Y^2 I_n . \quad (C-5)$$

Introduce also

$$J_n (\alpha) = \int_0^{\sin \alpha} dv \frac{1}{(1-v^2)^n \sqrt{\psi}} \quad (C-6)$$

$$J^n (\alpha) = \int_0^{\sin \alpha} dv \frac{\sqrt{\psi}}{(1-v^2)^n} \quad (C-7)$$

where

$$\psi (\alpha) = \sin^2 \alpha - v^2 . \quad (C-8)$$

The J^n and J_n satisfy the relation

$$Y^2 J_n (\alpha) = J_{n-1} (\alpha) - J^n (\alpha) . \quad (C-9)$$

By appropriate substitutions and with the aid of partial fractions it is possible to show that

$$J^1 = \frac{1}{2} I^1 \quad (C-10)$$

$$J^2 = \frac{1}{4} I^2 + \frac{1}{2} J^1 \quad (C-11)$$

$$J^3 = \frac{1}{8} I^3 + \frac{3}{4} J^2 . \quad (C-12)$$

To this point the relations are all independent of the magnitude of the angle α .

It will be noted that the J_n integrals are expressible in terms of the J^n . The J^n integrals are related to the I^n , which in turn may be written in terms of the I_n . This provides a convenient chain for the evaluation of the L_i .

Having established the basic integral families, we proceed now to the solution of the L_i for the six cases corresponding to the different regions of integration. Consider first $\bar{\theta}_{e \max} < \lambda_e < \pi/2$.

From Fig. 9 one can see that the L_i are of the general form

$$L_i = 2 \int_0^{U_m} dU \left[z_{-}(U, \bar{y}_m) f_i(U, z) dz - z_{+}(U, \bar{y}_m) \right] , \quad (C-13)$$

where

$$\sin \lambda_e \sin U_m = \sin \bar{\theta}_{e \max} . \quad (C-14)$$

Now $f_i = 1$, so that

$$L_i = 2 \int_0^{U_m} [z_{-}(U, \bar{y}_m) - z_{+}(U, \bar{y}_m)] dU$$

$$L_1 = 4 \int_0^{U_m} \frac{s \sqrt{A^2 - \bar{y}_m^2}}{A^2} dU . \quad (C-15)$$

The substitution

$$v = \sin \lambda_e \sin U \quad (C-16)$$

yields directly

$$L_1 = 4 J^1 (\bar{\theta}_{e \max}) . \quad (C-17)$$

L_2 requires a bit of manipulation.

$$L_2 = 2 \int_0^{U_m} \cos U dU \left[\int_{\lambda_- (U, \bar{y}_m)}^{\lambda_+ (U, \bar{y}_m)} \sin^2 \lambda d\lambda \right]$$

$$= \int_0^{U_m} [\lambda_+ - \lambda_- + \sin \lambda_- \cos \lambda_- - \sin \lambda_+ \cos \lambda_+] \cos U dU . \quad (C-18)$$

Consider the integration in two parts

$$L_2 = L_2' + L_2'' \quad (C-19)$$

$$L_2' = 2 \int_0^{U_m} \omega \cos U dU \quad (C-20)$$

$$L_2'' = \int_0^{U_m} [\sin \lambda_- \cos \lambda_- - \sin \lambda_+ \cos \lambda_+] ccs U dU \quad (C-21)$$

where

$$\omega = \frac{1}{2} (\lambda_+ - \lambda_-) . \quad (C-22)$$

By expanding $\sin(\lambda_- - \lambda_+)$ one can show with the aid of Eqs. (41) and (42) that

$$\omega = \cos^{-1} (\bar{y}_m/A) . \quad (C-23)$$

Change the integration variable to ω in L_2' . One obtains

$$L_2' = \frac{2 \bar{y}_m^2}{\sin \lambda_e} \int_0^{\theta_{e \max}} \frac{\omega \tan \omega \sec^2 \omega d\omega}{\sqrt{1 - \bar{y}_m^2 \sec^2 \omega}} .$$

With a second change of variable $v = \bar{y}_m \sec \omega$ and integration by parts it can be shown that this integral reduces nicely to

$$L_2' = \frac{2}{\sin \lambda_e} J^1(\bar{\theta}_{e \max}) . \quad (C-24)$$

Eq. (C-21) may be rewritten as

$$L_2'' = 2 \bar{y}_m \int_0^{U_m} \frac{(A^2 - 2\delta_e^2) \sqrt{A^2 - y_m^2}}{A^4} \cos U dU .$$

With the substitution (C-16) this will take the form

$$L_2'' = \frac{2 \bar{y}_m}{\sin \lambda_e} [J^1(\bar{\theta}_{e \max}) - 2 \delta_e^2 J^2(\bar{\theta}_{e \max})] . \quad (C-25)$$

Thus

$$L_2 = \frac{2}{\sin \lambda_e} [(1 + \bar{y}_m) J^1(\bar{\theta}_{e \max}) - 2 \delta_e^2 \bar{y}_m J^2(\bar{\theta}_{e \max})] . \quad (C-26)$$

Proceed to the next integral.

$$\begin{aligned} L_3 &= 2 \int_0^{U_m} dU \int_{z_+(U, \bar{y}_m)}^{z_-(U, \bar{y}_m)} z dz \\ &= \int_0^{U_m} [z_-^2(U, \bar{y}_m) - z_+^2(U, \bar{y}_m)] dU . \end{aligned} \quad (C-27)$$

The definition of z_{\pm} and the convenient change of variable (C-16) enable one to prove that

$$L_3 = 4 \bar{y}_m \delta_e J^2(\bar{\theta}_{e \max}) . \quad (C-28)$$

Consider L_4

$$L_4 = 2 \int_0^{U_m} \cos^2 U dU \int_{z_+(U, \bar{y}_m)}^{z_-(U, \bar{y}_m)} (1-z^2) dz . \quad (C-29)$$

After z integration, one can rearrange L_4 in the form

$$L_4 = L_1 - L_5 - L'_4 + L''_4 \quad (C-30)$$

where

$$L'_4 = 2 \int_0^{U_m} [z_-(U, \bar{y}_m) - z_+(U, \bar{y}_m)] \sin^2 U dU \quad (C-31)$$

$$L''_4 = \frac{2}{3} \int_0^{U_m} [z_-(U, \bar{y}_m)^3 - z_+(U, \bar{y}_m)^3] \sin^2 U dU . \quad (C-32)$$

With the usual substitution one finds that

$$L'_4 = \frac{4}{\sin^2 \lambda_e} [J^1(\bar{\theta}_{e \max}) - J^0(\bar{\theta}_{e \max})] . \quad (C-33)$$

The terms of the last integral in L_4 can be shown to reduce eventually to

$$\begin{aligned}
 L_4'' &= \frac{4}{3} \frac{1}{\sin^2 \lambda_e} [45 \delta_e^2 \bar{y}_m^2 J^3 (\bar{\theta}_{e \max}) \\
 &\quad - (\delta_e^2 + \bar{y}_m^2 + 45 \delta_e^2 \bar{y}_m^2) J^2 (\bar{\theta}_{e \max}) \\
 &\quad + (\delta_e^2 + \bar{y}_m^2 + 1) J^1 (\bar{\theta}_{e \max}) - J^0 (\bar{\theta}_{e \max})].
 \end{aligned} \tag{C-34}$$

For the solution of L_5

$$\begin{aligned}
 L_5 &= 2 \int_0^{U_m} dU \int_{z_+(U, \bar{y}_m)}^{z_-(U, \bar{y}_m)} z^2 dz \\
 &= \frac{2}{3} \int_0^{U_m} [z_-^3(U, \bar{y}_m) - z_+^3(U, \bar{y}_m)] dU
 \end{aligned} \tag{C-35}$$

the terms in $z_-^3 - z_+^3$ suggest a division into two integrals

$$L_5 = L_5' + L_5'' \tag{C-36}$$

$$L_5' = 4 \delta_e^2 \bar{y}_m^2 \int_0^{U_m} \frac{s \sqrt{A^2 - \bar{y}_m^2}}{A^6} dU \tag{C-37}$$

$$L_5'' = \frac{4}{3} \int_0^{U_m} \frac{s^3 (A^2 - \bar{y}_m^2)^{3/2}}{A^6} dU . \quad (C-38)$$

The first may be recognized as

$$L_5' = 4 \delta_e^2 \bar{y}_m^2 J^3 (\bar{\theta}_{e \max}) . \quad (C-39)$$

With some shuffling of terms the second can be recombined into

$$\begin{aligned} L_5'' = \frac{4}{3} [& \delta_e^2 \bar{y}_m^2 J^3 (\bar{\theta}_{e \max}) - (\delta_e^2 + \bar{y}_m^2) J^2 (\bar{\theta}_{e \max}) \\ & + J^1 (\bar{\theta}_{e \max})] \end{aligned} \quad (C-40)$$

with the result that

$$\begin{aligned} L_5 = \frac{4}{3} [& 4 \delta_e^2 \bar{y}_m^2 J^3 (\bar{\theta}_{e \max}) - (\delta_e^2 + \bar{y}_m^2) J^2 (\bar{\theta}_{e \max}) \\ & - J^1 (\bar{\theta}_{e \max})] . \end{aligned} \quad (C-41)$$

The last integral for this case is

$$L_6 = 2 \int_0^{U_m} \cos U dU \int_{x_-(U, \bar{y}_m)}^{x_+(U, \bar{y}_m)} x^2 dx$$

$$L_6 = \frac{2}{3} \int_0^{U_m} [x_+ (U, \bar{y}_m)^3 - x_- (U, \bar{y}_m)^3] \cos U dU . \quad (C-42)$$

In the usual manner the terms in $x_+^3 - x_-^3$ may be combined to give

$$L_6 = \frac{4}{3} \frac{1}{\sin \lambda_e} [(\delta_e^3 + 3\delta_e \bar{y}_m^2) J^2 (\bar{\theta}_{e \max}) - 4\delta_e^3 \bar{y}_m^2 J^3 (\bar{\theta}_{e \max})]. \quad (C-43)$$

All the L_i integrals for the case $\bar{\theta}_{e \max} < \lambda_e < \pi/2$, therefore, may be expressed in terms of the basic family of J^n . The I_n are all known integration forms. With the aid of the condition $\bar{y}_m > 0$ for this case, one finds that

$$I_{-1}(\bar{\theta}_{e \max}) = I_0(\bar{\theta}_{e \max}) = \pi$$

$$I_1(\bar{\theta}_{e \max}) = \pi / \bar{y}_m \quad (C-44)$$

$$I_2(\bar{\theta}_{e \max}) = \pi / \bar{y}_m^3$$

$$I_3(\bar{\theta}_{e \max}) = \frac{\pi}{2 \bar{y}_m^5} (3 - \bar{y}_m^2) .$$

Consequently it follows that

$$\begin{aligned}
 J^0(\bar{\theta}_{e \max}) &= \frac{\pi}{4} (1 - \bar{y}_m^2) \\
 J^1(\bar{\theta}_{e \max}) &= \frac{\pi}{2} (1 - \bar{y}_m) \\
 J^2(\bar{\theta}_{e \max}) &= \frac{\pi}{4} \frac{(1 - \bar{y}_m^2)}{\bar{y}_m} \\
 J^3(\bar{\theta}_{e \max}) &= \frac{\pi}{16\bar{y}_m^3} (1 - \bar{y}_m^2)(1 + 3\bar{y}_m^2).
 \end{aligned} \tag{C-45}$$

Substitution of these J^n values into the derived expressions for L_i yields Eqs. (47).

In the limit $\bar{\theta}_{e \max} = 0$, the L_i are all zero and, hence, so is the distribution function. This, of course, must be true from a physical viewpoint. Eqs. (47) in the limit $\bar{\theta}_{e \max} = \lambda_e = \pi/2$ agree with the results obtained from integrating directly over the right hand rectangle in Fig. 9.

The procedure for evaluating the L_i in the remaining five cases is generally the same as that outlined above. However, it must be admitted that, as the regions of integration grow larger, the number of terms and the complication of the integrals increase.

It should be remarked that there exist symmetry relations between the various cases, which one can sometimes

conveniently employ to shorten the solution of the integrals.

In the remaining five cases, as above, one finds that the L_i are given by Eqs. (47).

APPENDIX D

ANGULAR LIMITS IN PION LABORATORY FRAME

Corresponding to $\bar{y}_m = -1$ and $\bar{y}_m = \bar{y}_p$ in the pion rest frame there are restrictions on the electron direction in the pion moving frame. To derive these conditions, it will be convenient to employ the momentum ellipses again. One must distinguish several cases.

Consider first $\gamma_\pi \geq \bar{w}$. It is important to keep in mind that $\bar{y}_m = -1$ for $\bar{p}_e < \bar{p}_{et}$ corresponds to N^1 and $\bar{y}_m = \bar{y}_p$ for $\bar{p}_e > \bar{p}_{et}$ corresponds to N^2 . Define

$$\gamma_{er} = \gamma_\pi \bar{\gamma}_{et} + p_\pi \bar{p}_{et} \quad (D-1)$$

$$p_{er} = p_\pi \bar{\gamma}_{et} + \gamma_\pi \bar{p}_{et}$$

where p_{er} corresponds in Fig. D1 to the momentum at point R, and

$$\gamma_{es} = \gamma_\pi \bar{\gamma}_{et} - p_\pi \bar{p}_{et} \quad (D-2a)$$

$$p_{es} = p_\pi \bar{\gamma}_{et} - \gamma_\pi \bar{p}_{et}, \quad \gamma_\pi \geq \bar{\gamma}_{et}$$

where p_{e_s} corresponds to the momentum at point S. Note that $\gamma_{e_r} \geq \gamma_{e_s}$.

For $p_e \text{ min} \leq p_e \leq p_{e_s}$, it is seen from Fig. D1 that only values of \bar{P}_e contribute for which $\bar{P}_e \geq \bar{P}_{e_t}$. Therefore $N = N^2$. Notice that the y values span the range y_x to 1, where

$$y_x = \frac{\gamma_\pi \gamma_e - \bar{w}}{p_\pi p_e} \quad (D-3)$$

which is found in the usual way from the relativistic transformation equations.

For $p_{e_s} \leq p_e \leq p_{e_r}$, both $\bar{P}_e \leq \bar{P}_{e_t}$ and $\bar{P}_e \geq \bar{P}_{e_t}$ contribute. For $\bar{P}_e \leq \bar{P}_{e_t}$, $N = N^1$ with y values between y_t and 1 allowed, where

$$y_t = \frac{\gamma_\pi \gamma_e - \bar{\gamma}_{e_t}}{p_\pi p_e} \quad (D-4)$$

For $\bar{P}_e \geq \bar{P}_{e_t}$, $N = N^2$ and y such that $y_x \leq y \leq y_t$ are allowed.

For $p_{e_r} \leq p_e \leq p_{e \text{ max}}$, again $N = N^2$ and y is limited to $y_x \leq y \leq 1$.

Consider now $\bar{w} \geq \gamma_\pi \geq \bar{\gamma}_{e_t}$. Define

$$\gamma_{e_t} = \gamma_\pi \bar{w} - p_\pi \bar{v}$$

(D-5)

$$p_{e_t} = \gamma_\pi \bar{v} - p_\pi \bar{w}$$

where p_{e_t} has meaning only for $\bar{w} \geq \gamma_\pi$. It is seen that p_{e_t} corresponds to the point T in Fig. D2. It can be proved that $\gamma_{e_t} \geq \gamma_{e_s}$ for $\bar{w} \geq \gamma_\pi$. It can also be shown that $\gamma_{e_r} \geq \gamma_{e_t}$ if $\gamma_\pi \geq \gamma_\mu$ (which is true for this case) and $\gamma_{e_r} \leq \gamma_{e_t}$ if $\gamma_\pi \leq \gamma_\mu$. The conditions under which N¹ or N² are used can be derived in much the same way for the case $\bar{w} \geq \gamma_\pi \geq \bar{\gamma}_{e_t}$ as for the previous case.

For $\pi\mu-e$ decay simple calculation shows that $\bar{\gamma}_{e_t} > \gamma_\mu$. There will, therefore, be two more cases to consider, $\bar{\gamma}_{e_t} \geq \gamma_\pi \geq \gamma_\mu$ and $\gamma_\mu \geq \gamma_\pi$. Their momentum ellipses are illustrated in Figs. D3 and D4. They are likewise handled in the same manner as in the first case.

For these latter two cases note that

$$p_{e_s} = \gamma_\pi \bar{p}_{e_t} - p_\pi \bar{\gamma}_{e_t}, \quad \gamma_\pi \leq \bar{\gamma}_{e_t}. \quad (D-2b)$$

A complete summary of the range of permissible electron directions in the pion lab system is given in Table I.

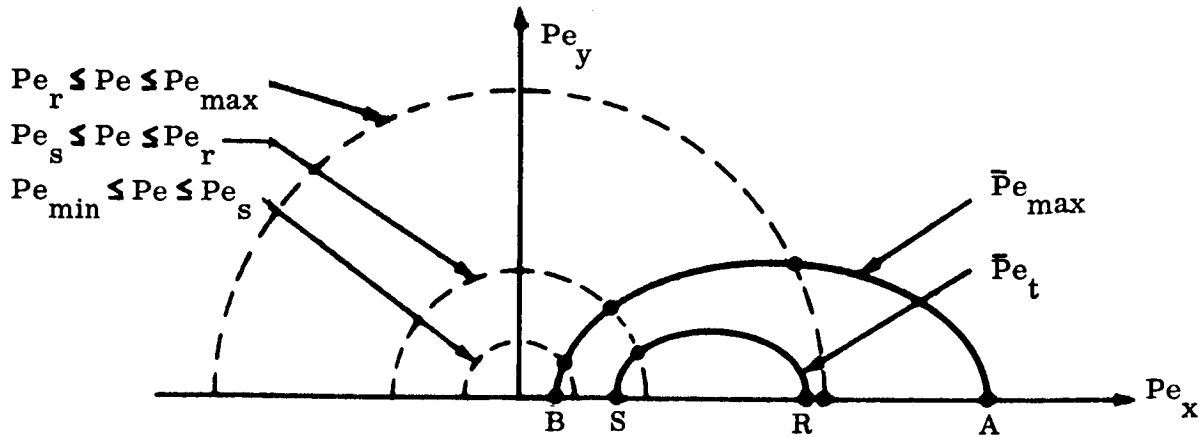


Fig. D1 Momentum Ellipses for $\gamma_\pi \geq \bar{w}$

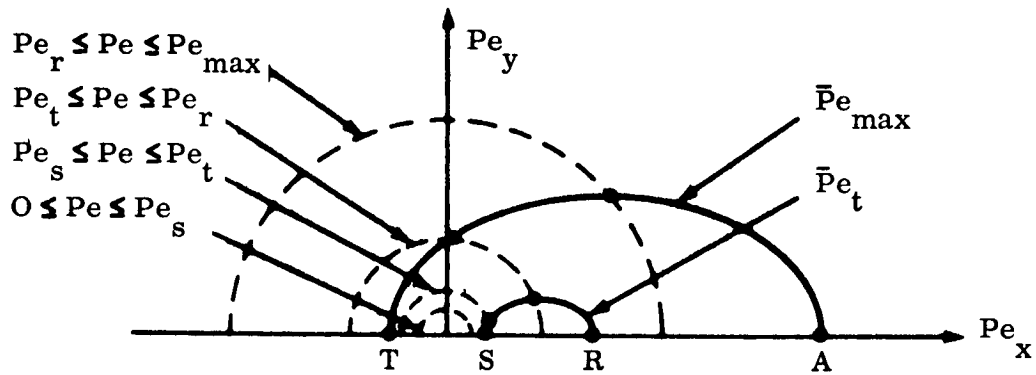


Fig. D2 Momentum Ellipses for $\bar{w} \geq \gamma_\pi \geq \bar{\gamma}_{et}$

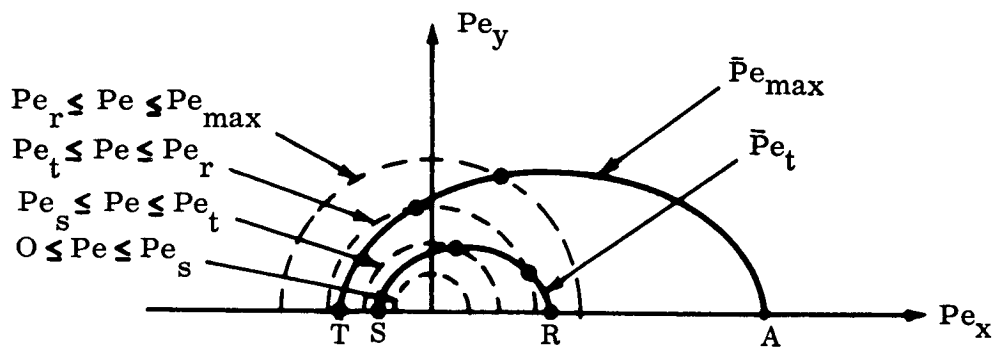


Fig. D3 Momentum Ellipses for $\bar{\gamma}_{e_t} \geq \gamma_\pi \geq \gamma_\mu$

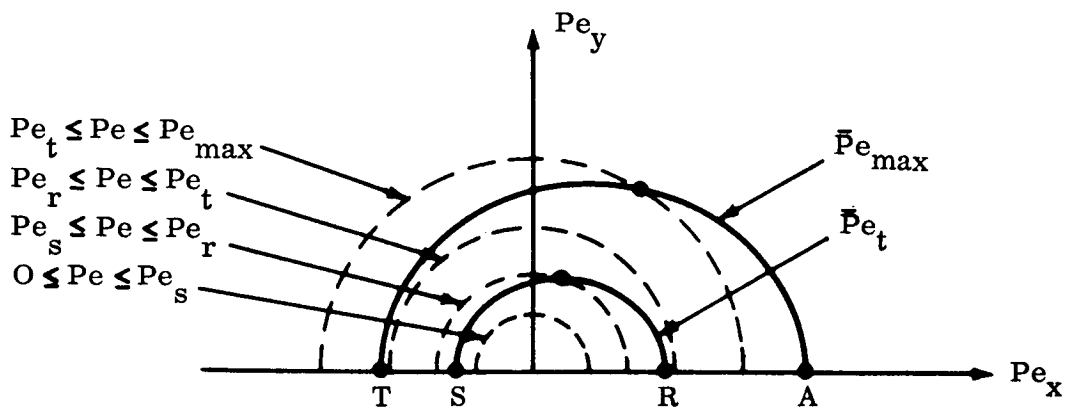


Fig. D4 Momentum Ellipses for $\gamma_\mu \geq \gamma_\pi$

BIBLIOGRAPHY

- Ascoli, Giulio, "Transformation of 'Spin Direction' by Ordinary Lorentz Transformation," Z. Physik, Vol. 150 (1958), pp. 407-408.
- Ali-Zade, S. A., Gurevich, I. I., and Nikol'skii, B. A., "Asymmetry in the Angular Distribution of Electrons from μ -e Decay in Magnetic Fields up to 35 000 Oersted," Soviet Phys.-JETP, Vol. 13 (1961), pp. 313-316.
- Backenstoss, G., Hyams, B. D., Knop, G., Marin, P. C., and Stierlin, U., "Helicity of μ^- Mesons from π -Meson Decay," Phys. Rev. Letters, Vol. 6 (1961), pp. 415-416.
- Baldin, Aleksandr Mikhailovich, Gol'danskii, V. I., and Rozenthal I. L., Kinematics of Nuclear Reactions, pp. 16, 28, 79, New York, 1961.
- Bardon, Marcel, Berley, D., and Lederman, Leon M., "Asymmetry Parameter in Muon Decay," Phys. Rev. Letters, Vol. 2 (1959), pp. 56-57.
- Bardon, Marcel, Franzini, Paolo, and Lee, Juliet, "Mott Scattering of Polarized Muons," Phys. Rev., Vol. 126 (1962), pp. 1826-1835.
- Berman, S. M., "Radiative Corrections to Muon and Neutron Decay," Phys. Rev., Vol. 112 (1958), pp. 267-270.
- Block, M. M., Fiorini, E., Kikuchi, T., Giacomelli, G., and Ratti, S., "The ρ -Value for the β -Decay of the Negative Muon," Nuovo Cimento, Vol. 23 (1964), pp. 1114-1125.
- Bouchiat, Claude, and Michel, Louis, "Theory of μ -Meson Decay with the Hypothesis of Nonconservation of Parity," Phys. Rev., Vol. 106 (1957), pp. 170-172.

Feinberg, Gerald, and Lederman, Leon M., "The Physics of Muons and Muon Neutrinos," Ann. Rev. Nuclear Sci., Vol. 13 (1963), pp. 431-504.

Friedman, Jerome I., and Telegdi, V. L., "Nuclear Emulsion Evidence for Parity Nonconservation in the Decay Chain $\pi^+ - \mu^+ - e^+$," Phys. Rev., Vol. 105 (1957), pp. 1681-1682.

Garwin, Richard L., Lederman, Leon M., and Weinrich, Marcel, "Observations of the Failure of Conservation of Parity and Charge Conjugation in Meson Decays: the Magnetic Moment of the Free Muon," Phys. Rev., Vol. 105 (1957), pp. 1415-1417.

Ginzburg, V. L., and Syrovat-skii, S. I., "Gamma Rays and Cyclotron Radiation X-Rays of Galactic and Metagalactic Origin," Soviet Phys. - JETP, Vol. 18 (1964), pp. 245-252.

Hayakawa, Satio, and Okuda, Haruyuki, "Electronic Components in Galactic Cosmic Rays," Progr. Theor. Phys., Vol. 28 (1962), pp. 517-528.

Jones, Frank C., "The Energy Spectrum of Galactic Electrons Produced by Cosmic Rays," J. Geophys. Res., Vol. 68 (1963), pp. 4399-4407.

Kadyk, John A., "Generation of Three-Body Production and Decay Processes Following Phase Space Distribution by Monte Carlo Method," Lawrence Radiation Laboratory Report UCRL-9614, 1961.

Kinoshita, Toichiro, and Sirlin, Alberto, "Polarization of Electrons in Muon Decay and the Two-Component Theory of the Neutrino," Phys. Rev., Vol. 106 (1957a), pp. 1110-1111.

_____, "Muon Decay with Parity Nonconserving Interactions and Radiative Corrections in the Two-Component Theory," Phys. Rev., Vol. 107 (1957b), pp. 593-599.

Konopinski, E. J., "The Experimental Clarification of the Laws of β -Radioactivity," Ann. Rev. Nuclear Sci., Vol. 9 (1959), pp. 99-158.

Lee, T. D., and Yang, C. N., "Parity Nonconservation and a Two-Component Theory of the Neutrino," Phys. Rev., Vol. 105 (1957a), pp. 1671-1675.

_____, "Possible Nonlocal Effects in μ Decay," Phys. Rev., Vol. 108 (1957b), pp. 1611-1614.

Milford, Nevil, Ferentz, Melvin, Lieber, Michael, McCoyd, Gerard, Scanlon, Joseph, and Spergel, Martin, "Cosmic Ray Collisions in Space," Grumman Aircraft Engineering Corporation Research Department Memorandum RM-226, 1964.

Monahan, J., "Kinematics of Neutron-Producing Reactions," Fast Neutron Physics, Part I, (ed. by Jerry B. Marion and Joseph L. Fowler), pp. 49-72, New York, 1960.

Okun', L., "Strange Particles: Decays," Ann. Rev. Nuclear Sci., Vol. 9 (1959), pp. 61-98.

Plano, Richard J., "Momentum and Asymmetry Spectrum of μ -Meson Decay," Phys. Rev., Vol. 119 (1960), pp. 1400-1408.

Rainwater, J., "Mu-Meson Physics," Ann. Rev. Nuclear Sci., Vol. 7 (1957), pp. 1-30.

Snow, G.A., and Shapiro, M. M., "Mesons and Hyperons," Revs. Modern Phys., Vol. 33 (1961), pp. 231-238.

Vaisenberg, A. O., "New Experimental Data on π^- and μ -Meson Decays," Soviet Phys.-Uspekhi, Vol. 3 (1960), pp. 195-229.

Vaisenberg, A. O., Kolganova, E. D., and Minervina, Z. V., "Angular Distribution of μ Mesons from π^- - μ Decay," Soviet Phys.-JETP, Vol. 14 (1962), pp. 79-80.

Wigner, Eugene P., "Relativistic Invariance and Quantum Phenomena," Revs. Modern Phys., Vol. 29 (1957), pp. 255-268.

Williams, William S. C., An Introduction to Elementary Particles, pp. 301, 364, New York, 1961.